Passive Radio Sensor Systems

HABILITATIONSSCHRIFT

eingereicht an der

Technischen Universität Wien

Fakultät für Elektrotechnik

von

Alfred Pohl
Hochgasse 4
2130 Mistelbach

Wien, im März 2000

Contents

Die Habilitationsschrift besteht aus einer unveröffentlichten Einführung in die Funksensorik und dem zum Druck in *IEEE Transactions on Ultrasonics Ferroelectrics and Frequency Control* erschienenen Übersichtsartikel, *A. Pohl, "A Review of Wireless SAW Sensors",* [1]. Weitere Teile der Arbeit sind ausgewählte Publikationen zum Thema. Die in [1] in den Abschnitten 7 (Discussion) und 8 (Conclusion) erzielten Ergebnisse gelten auch für die Gesamtheit der vorliegenden Arbeit.

Vorwort

Durch die hohe Verfügbarkeit elektronischer Regelschaltungen in der Industrie gewinnt die Sensortechnik immer mehr an Bedeutung. Im Dezember 1998 wird in einer industrienahen Veröffentlichung [2] festgestellt, daß die Wachstumsrate der Sensorik die höchste innerhalb aller elektrotechnischen Fachbereiche ist. Von einfachen Industrieerzeugnissen bis hin zu komplexen Systemen, von der Waschmaschine bis zum Kernkraftwerk, ist Sensorik und Regelungstechnik entscheidend für sicheren, wirtschaftlichen und umweltverträglichen Betrieb.
Am Eingang des Überwachungs- bzw. Regelungssystems stehen die Sensoren, die als Wandler eine mechanische, thermische, chemische, usw., Meßgröße (engl.: measurand) in einen elektrischen Wert umformen. Dieser wird in der folgenden Signalverarbeitungs-schaltung (meist digital) aufbereitet und zur Steuerung der Maschine bzw. des Prozesses herangezogen.

Die vorliegende Arbeit greift drahtlos auszulesende Funksensoren, die zugehörigen Hochfrequenz Abfragesysteme und Auswerteverfahren heraus. Unterschieden werden dabei lineare und nichtlineare Sensoren sowie Elemente mit und ohne Mechanismus zur Energiespeicherung. Der herausragende Vorteil dieser Sensoren, besonders solcher als Oberflächenwellenbauelement ausgeführter, liegt in ihrer Passivität und Robustheit: Es werden keine temperatur- und alterungsempfindlichen Batterien bzw. ebensolche elektronische Bauelemente sowie fehleranfällige (bewegte) Drahtverbindungen und Schleifringe gebraucht.
Andererseits ist für die verläßliche und genaue Ablesung der Meßgröße vom Sensor ein optimiertes Funkabfrage- und Auswerteverfahren, sowie die Berücksichtigung des bei bewegten Maschinenteilen stark verrauschten und schwundbehafteten Funkkanals notwendig. Da passive Funksensoren und Identifikationsmarken (ID Tags) eingehend erst seit etwa fünf Jahren untersucht werden, war eine zusammenfassende Darstellung dieser Probleme bisher

nicht bekannt.

Insgesamt ist das Ziel der Arbeit, einen Überblick über die bekannten und neuen passiven Funksensorsysteme zu geben, wobei das Hauptgewicht auf die umfassende Quantifizierung der durch den Funkkanal, die Abfragesysteme und die verschiedenen Auswerteverfahren auftretenden Fehler gelegt wird. Einflüsse durch Signalinterferenz und bestimmte Rauschquellen im Radiokanal, die bei der Anwendung auftreten, werden untersucht, notwendige, einzuhaltende Randbedingungen werden angegeben.

Es zeigt sich bei der Auswertung, daß für schnell sich ändernde Meßgrößen breitbandige Abfrageimpulse anzuwenden sind (in der Arbeit mit time domain sampling, TDS, bezeichnet). Eine Genauigkeitssteigerung bzw. Reduktion des Meßfehlers läßt sich hier nur mit integrativen Signalauswertemethoden erzielen. Eine höhere Genauigkeit erreichen von sich aus die Frequenzbereichsverfahren (frequency domain sampling, FDS), bei denen die Sensorantwort mit relativ langen schmalbandigen Signalen der Funkabfrage im Frequenzbereich abgetastet wird.

Im einzelnen wurden Temperaturmessungen an Bremsscheiben von Eisenbahnfahrzeugen, an Stahlkonvertern und an Maschinenteilen im Bereich der industriellen Fertigung, Messung des Luftdruckes in KFZ Reifen, Messungen des Kraftschlusses zwischen Reifen und Fahrbahn, verschiedene Messungen von Schwingungen und Beschleunigungen (z.B. Verzögerung eines Dartpfeiles), Messung des Kolbenringverschleißes, Drehmomentmessungen an Antriebswellen, u.v.a.m. durchgeführt. Einige Anwendungen und Auswerteverfahren sind Gegenstand von in Patenten festgehaltenen eigenen Erfindungen. Für alle diese Anwendungen lassen sich ein auf das Sensorsystem abgestimmtes Pegeldiagramm und die daraus mit den Methoden der Nachrichtentechnik ermittelbaren Meßfehler angeben.

Schwerpunkte der Arbeit werden bei der Systemtechnik, der Schaltungstechnik zur Signalverarbeitung und der Analyse von Fehlerquellen und ihres Einflusses gesetzt. Neben einer überblicksmäßigen Einteilung der Systeme und Verfahren wird versucht, an Hand der Ergebnisse konkreter Beispiele quantifizierbare Aussagen zu machen. Einige experimentell demonstrierte Anwendungen sind in beigeschlossenen Publikationen dargestellt.

Als "sonstige Arbeiten" sind die Arbeiten an einem low-cost Chirp- Bandspreiz-Übertragungsverfahren angeführt. Es wurden Untersuchungen zum Systemdesign wie auch zum Funkkanal durchgeführt. Die Übertragungseigenschaften wurden mit Hilfe von

Simulationen wie auch experimentell überprüft. Um einen sicheren Betrieb im 2.45 GHz ISM Band gewährleisten zu können, wurde vom Autor ein Verfahren zur schnellen adaptiven Störunterdrückung erfunden und theoretisch wie auch im Experiment verifiziert [3], [4]. Entsprechende internationale Patente wurden von unserem Forschungspartner Siemens Schweiz angemeldet [5], [6].

Weitere "sonstige Arbeiten" betreffen Untersuchungen und experimentelle Verifikation von schnellen adaptiven Chirp Transformations- Spektralanalysatoren mit extrem breitbandigen Signalkompressoren [7], [8].

The "Habilitationsschrift" consists of an unpublished introduction to radio sensors and of the review paper, *A. Pohl, "A Review of Wireless SAW Sensors"*, [1], published in *IEEE Transactions on Ultrasonics Ferroelectrics and Frequency Control, in March 2000*. Further parts of this thesis are six selected publications dealing with this topic. The discussion (chapter 7) and the conclusion (chapter 8) of [1] are applicable for this thesis too.

Preface

Due to its high availability, sensor technology is of rapidly growing importance. In December 1998, an industry related publication mentions its growing rates to be the highest in electrical engineering market [2]. More and more processes and procedures in everyday life as well as in industries, a washer in the household as well as a nuclear power plant, are controlled electronically, enabled by and depending on the sensor technology. Control circuits provide a secure, economical and ecological operation. The sensors are the front end components of all control systems. They operate as an interface, converting the mechanical, thermal, chemical, etc. parameters to observe (i.e. the measurands), into electrically readable quantities. The sensors are read out by sensor systems, delivering the information about the measurand for process control to computers, displays and actuators. These readout systems can span from Wheatstone resistor bridges to highly sophisticated data transmission and signal processing circuits.

The current work gives an overview of known and new passive radio sensor principles. It concerns the passive radio transponder sensors, the principles of readout and the circuits employed. For the radio sensors is distinguished between linear and non linear devices and between units with and without energy storage capability. The outstanding advantage of these sensor devices, especially of the surface acoustic wave (SAW) type is their passive operation. Since no active components, no capacitors and no batteries are employed, the effect of aging almost vanishes and they are capable of operation in hazardous environmental conditions.
Then, it is focused to the system engineering, to the signal processing employed and to the sources of errors. The main emphasis is focused to the comprehensive quantification of the occurring errors due to the radio transmission and the sensor signal processing methods.

Effects of noise and interference are investigated, boundary conditions for operation are given. It is shown, that for the evaluation of rapidly changing measurands, wideband interrogation (a time domain sampling, TDS) utilizing wideband signals is applicable only. The energy contents of the signals is rather small and therefore the accuracy of measurement via larger distances only can be ensured utilizing integrative signal processing. For quasistationary measurands, also a narrow band frequency domain sampling (FDS) is applicable, inherently including more signal energy to achieve a better performance without further measures.

To provide a reliable and accurate readout, an optimized radio interrogation and signal processing technique is required. Therefore, the properties of the radio transmission channel, disturbed by noise and interference have to be considered.

Since the passive radio sensors and ID tags are under research and development for a few years only, a comprehensive description was not available up to now.

During our research concerning passive SAW radio sensors, many applications have been verified experimentally. Temperature measurements at brake discs, at machine parts, at steel converters, etc., have been performed as well as the measurement of car tire pressure and of the friction between the tire and the road surface. Further investigations have been done experimentally proving the wireless measurement of mechanical vibration and acceleration and the wear of the wear rings in industrial compressors. These applications and methods partly are the contents of Austrian, German and international patents.

As "other work", publications dealing with low cost chirp spread spectrum systems are attached to the Habilitationsschrift. The work is based on channel measurements and system engineering, e.g. for wireless local area network (WLAN) terminals. To reduce the effect of co-channel interference, a fast adaptive interference cancellation method was invented by the author and has been investigated theoretically and experimentally [3], [4]. Corresponding international patents have been applied by our industrial partner Siemens Switzerland [5], [6].

Additional "other work" concerns Chirp-Transform real-time spectrum analyzers. Here, adaptive systems, employing wideband compressors have been investigated [7],[8].

Acknowledgment

I thank the head of our laboratory and my fatherly friend, Prof. Franz Seifert for an almost infinite number of discussions and scientific advice. I also gratefully acknowledge the support by stimulating discussions with Dr. L Reindl, Dr. C.C.W. Ruppel and W.E. Bulst, from Siemens ZT KM 1, Munich, Germany. Further, I thank all colleagues, especially Dr. G. Ostermayer, R. Steindl, Ch. Hausleitner and M. Brandl, and all diploma students, accompanying the activities for several years.

Last but not least, I want to thank my family, my wife Veronika, my sons Alfred and Thomas and my daughter Veronika, for bearing a lot of absence of husband and father.

1. Introduction - Fundamentals of Radio Sensors

A sensor delivers information about its physical, electrical, chemical, etc., state or its environmental conditions. This also can be the one bit information about the presence of a device or an identification number. In our terminology, we do not distinguish between identification purposes and measurement of a certain measurand, initially. Identification is treated as a measurement with a data decision instead of a readout of measurement result. In other words, the readout information is classified in intervals of discrete valid data. For simple identification (ID) systems this decision is deduced from the signal amplitude with a threshold detector.

For a wide variety of sensor applications, a wired connection between the sensor and the evaluation unit is impractical or cannot be established at all. Collector rings with brushes, e.g. cause additional mechanical and electrical problems (i.e. signal-noise etc.) and make these methods viable for test system use only. Therefore, wireless methods to gain the information have to be employed.

Apart from optical systems, e.g. bar code labels for product ID in every department store, smart radio sensors came into use. In a few years, they supplanted the bar code tags in industrial environments and opened a lot of consumer applications. Today, entrance control and billing systems (e.g. the Austrian Ski Data System) are established employing smart electronic ID labels and a radio frequency (RF) radio link for communication between sensor and tag.

Only for the zero-price application of the article numbering, bar code labels printed e.g. onto the label of the milk bottle and read out optically at the cash desk are still unrivaled. (These well known systems are not discussed here.)

Another well known low cost application is the theft alarm in department stores. Here, passive one-bit wireless radio ID systems have been implemented successfully.

1.1 Radio sensors

A radio sensor system generally employs a radio interrogation unit and one or more distant sensors. Figure 1 shows a block diagram of such systems.

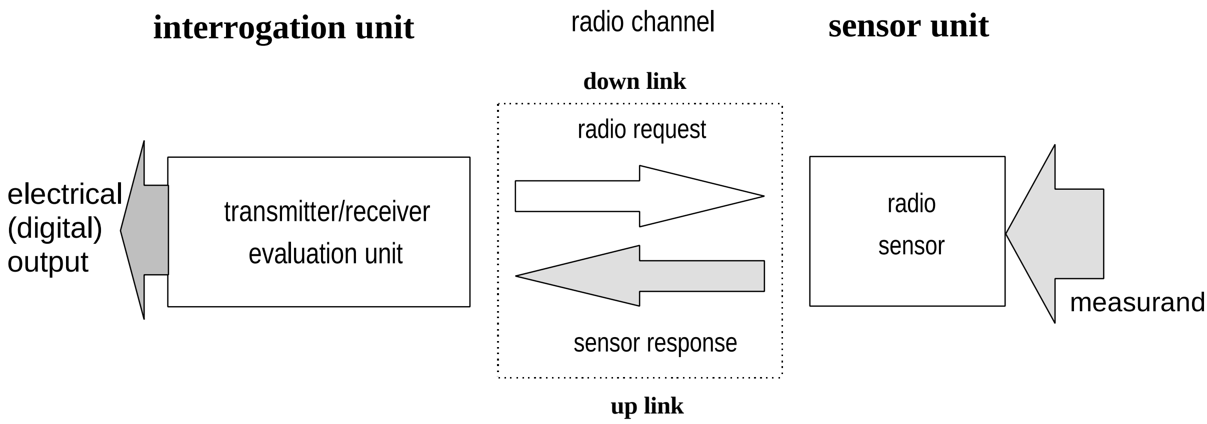

Figure 1: Radio sensor system performing down/up link interrogation of a radio sensor

Since radio sensors have to transmit electromagnetic signals or to retransmit a measurand or ID modulated radio request signal, the sensor units need a more or less extensive signal processing capability to modulate the information on an RF carrier. An important issue is the power supply of the circuits, therefrom, a classification of the radio sensors can be given:

1.1.1 Active radio sensor circuits

For active radio sensor systems, active circuits are employed in the remote unit. This sensor type became very mature up to now. Within a space implantable even into a tiny mouse, the sensor itself, a sensor circuit for identification and for measurements, an RF transmitter integrated on a silicon chip and an on-board power supply are included. Only a small antenna is added. Nowadays, these transmitters are sold cheaply. Their applications cover a wide range from animal tagging on the meadow, burglary alert systems combined with infrared detectors and vibration sensors, to identification and chronometric applications for Marathon runners and to skier identification in the Alps. These sensors are capable to perform read and write cycles, data can be changed or added. The attached battery has the advantage of a fixed, stable power supply; however, its disadvantages are its limited total energy available, its temperature dependency and its relatively short life span. A maintenance interval time of a few years is predicted (e.g. for the tire pressure measurement system [9] available since autumn 1998 for German upper class cars). Due to the on-board supply, the distance range of operation can be large (with the effective isotropically radiated power - EIRP - allowed for these applications, e.g. up to a few hundreds of meters).

The block diagram of an active radio sensor is drawn in Figure 2. The sensor transmits its information via an RF link to the base station. The sleeping sensor is requested by the base station with an RF interrogation signal or it awakes periodically and transmits its data telegram.

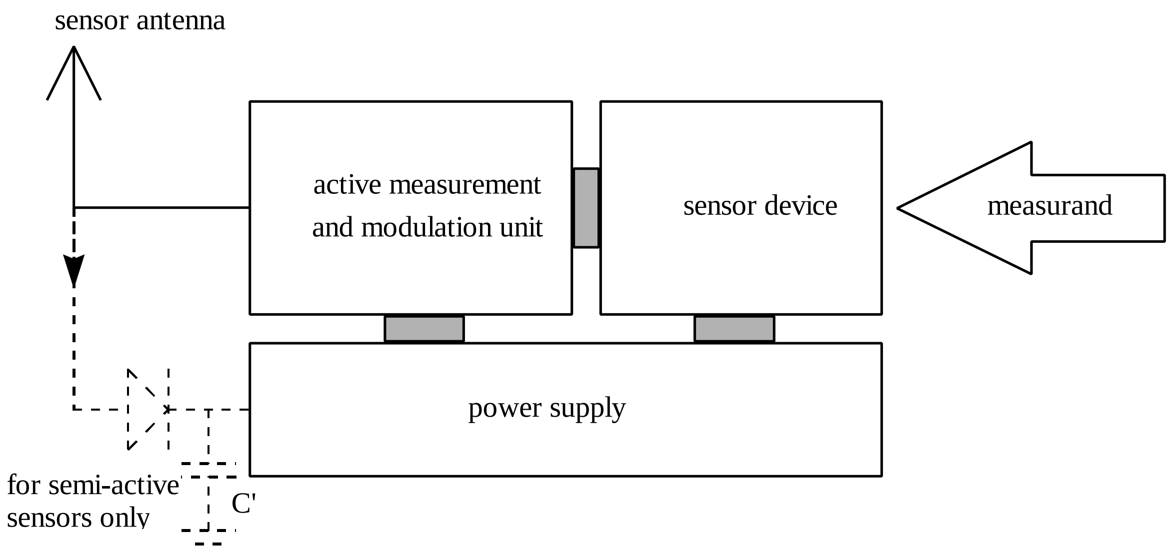

Figure 2: Active (and semi-active) radio sensor unit

The receiver for active sensors usually is a very simple circuit. It only has to detect an RF carrier with the digital data telegram. For low cost response evaluation, super-regenerative receivers are sold for less than 10 $. The data rate is low (some kBit/s), the signal processing in the measurement system is reduced to readout and storage of data. Sensitivity, resolution and accuracy are parameters of the sensor unit and are strictly separated from the radio link. Transmission errors can be coped with error correction codes employed for data modulation.

1.1.2 Semi-active radio sensors

Semi-active sensors are very similar to the active devices, they contain silicon circuits, too. The power supply energy is gathered by inductively near field coupling or by far field coupling from a strong RF radio signal transmitted by the radio request antenna. The RF signal is rectified, stored in C' and used for DC supply of the semiconductor circuits (shown in Figure 2). Both types, active and semi-active, contain signal processing capability in the remote frontend. For digital as well as for analog measurands, preprocessed digital data are transmitted together with additional information (sensor status, etc.). The sensors usually can be programmed to stay in a stand-by mode and respond in case of alert or request only. For data modulation in the near field coupled remote sensor unit, a digital impedance modulation of the sensor antenna is used widely, exciting sidebands of the RF carrier. As for active devices the signal processing effort in the receiver is rather simple. Additional measures are required for remote powering.

1.1.3 Passive radio sensors

To cope with the problem of the required power supply as well as with the limited life time due to batteries and possible damages due to hazardous environmental conditions, e.g. temperatures above 150 °C, hard radiation, strong EMI, etc., and for very low cost one-bit ID applications, passive radio sensors have been introduced. The passive devices employ a linear or non linear distortion of a radio request signal (received by the sensor antenna), transmitted as response signal (usually via the same antenna). The distortion is fix and contains the ID information or it is caused by the measurand. Passive radio sensors not necessarily include semiconductor components or capacitors. As shown in the next chapters, a cavity resonator can be used as linear passive radio sensor too. Since linear or non linear effects of the sensor device to the RF radio request signal have to be evaluated, the signal processing effort in the radio request system is much higher than for the active sensors mentioned above. The request signal is reflected, modulated by the measurand and afflicted with noise and interference. In contrast to active and semi-active circuits, all errors occurring during radio request and response transmission not only cause a (with coding) detectable data error, but yield additional measurement errors inseparable from the uncertainty of the sensor.

1.2 Separation of radio request and sensor response

For radio sensors, the information is transmitted wirelessly in the physical layer of the radio channel. Applying active sensors, the downlink path is occupied by the wake-up signals in a reduced manner only. For semi-active or passive sensor units the uplink RF response, modulated with the sensor information, has to be retransmitted and received by the interrogation system, separated from the (usually much stronger) downlink radio request signal. This task is very similar to the task of a bi-directional (duplex) communication system, where a division between transmit and receive mode, down- and uplink, has to be established. Same principles can be employed to separate subscribers of a radio communication network (multiple access). To separate the signals in the physical layer, the signals have to be orthogonal in space, time, frequency or code. In communication engineering, four basic principles and further some hybrid methods for separation are applied:

- **in space:**
  Space domain division (SDD) and space division multiple access (SDMA), applied to radio links to different satellites, etc.; the different links are operated in different directions via different antennas or beams, respectively.
- **in time:**
  time domain division (TDD) in former radio communication (one user talks, the other listen) and time domain multiple access (TDMA), applied in GSM (Global System for Mobile radio) for user separation in time slots
- **in frequency:**
  frequency domain division (FDD) usually applied to broadcasting, etc. , frequency division multiple access (FDMA) to up- / downlink separation in GSM, UMTS (Universal [future] Mobile Telecommunication System), etc.
- **in spreading code:**
  code domain division (CDD) and code division multiple access (CDMA), for user separation in UMTS (jointly with FDMA and TDMA), IS95 (US spread spectrum standard), etc.
- **hybrid schemes:**
  (TCDMA, TFDMA, FCDMA, ...)

Since for operation of radio sensors, as for all other radio communication systems, only one physical radio channel is available, similar principles of access to the medium are employed:
Space domain division (SDD), sketched in Figure 3, employs the separation of down- and uplink in space, i.e. the linear or non linear sensor unit receives within one antenna beam and transmits over another. Since large antennas with narrow beam width would be required and since the radio sensor is moving in most applications, this method is impracticable for usual radio sensors.

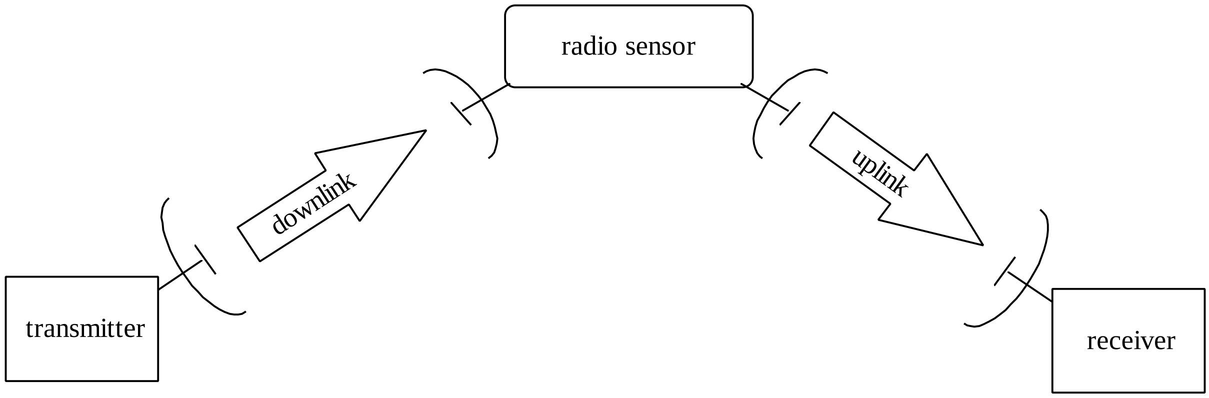

Figure 3: Space domain division

For time domain division (TDD), the sensor responds delayed to the downlink signal via the same physical channel segment in frequency and space. In the sensor a delay mechanism with energy storage is required suitable for (semi-)active sensors as well as for totally passive (usually linear) devices. This principle is widely used for resonant sensors, if the energy of radio request is stored in a high Q resonator. It also is applied in the passive surface acoustic wave (SAW) sensors, utilizing the relatively slow sound propagation of a SAW on a piezoelectric substrate for delay lines. The (acoustic) storage time has to be longer than the duration of the decay of the environmental electromagnetic request echoes of the radio channel. In Figure 4, the radio signals for interrogation of a passive delay line sensor are shown.

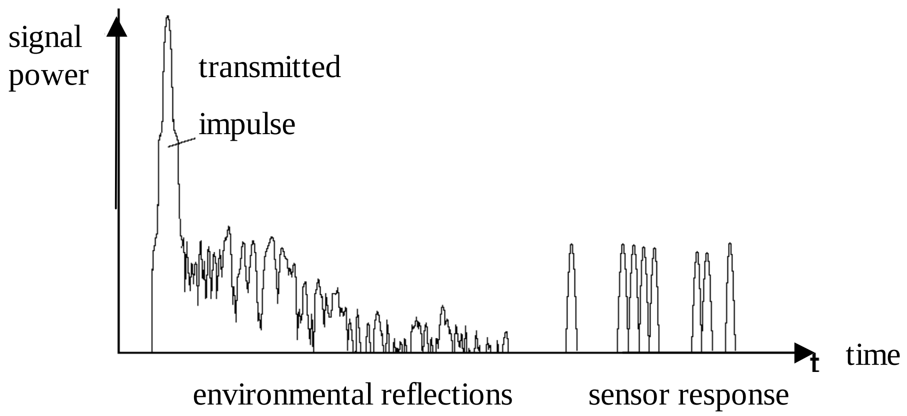

Figure 4: Radio request of passive delay line sensors with time domain division (TDD) between request and response signal.

Frequency domain division (FDD) usually requires additional response frequencies, i.e. a non-linear signal processing within the sensor unit. This is done by modulation of the RF carrier or by switching the reflectivity of an antenna by a diode, e.g. in (semi-) active sensors.
The non linearity causes sidebands and harmonics, detected in the receiver. For FDD no transmit / receive switch but a sufficient separation of the spectra is necessary.

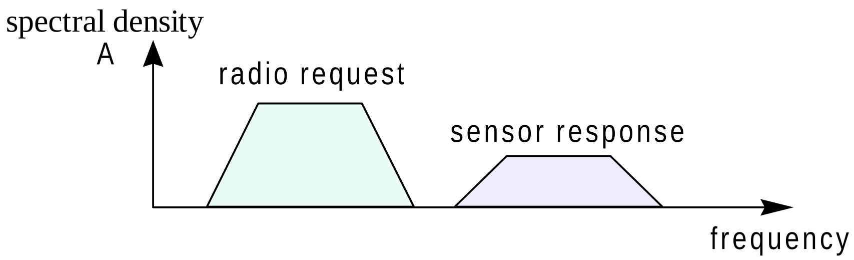

Figure 5: FDD scheme

A passive implementation of the principle employs a non linear element. The non linear element can be a fixed device, e.g. a diode, it also can be affected by external circuits or its non linearity can depend on a magnetic bias field. So, passive sensors with FDD, discussed in chapter 2.2 become feasible.
As an exception, in chapter 4.1.2 a FDD system employing the FM-CW RADAR principle is shown for radio interrogation of passive linear delay lines.
and Hybrid schemes like time/frequency domain division (FTDD) and, due to the near far effect, code domain division (CDD) are not applied for today's radio sensor systems.

1.3 Radio transmission regulations

Radio sensors and the according radio request systems are radio transmission systems and ruled by international and European standards and by the national governmental regulations.

frequency	radio sensors	other restrictions
0-135 kHz	inductively coupled	strong long wave radio stations
6.765-6.795 MHz	ISM band (ITU)	narrow bandwidth, strong short wave radio stations
13.553-13.567 MHz		
26.957-27.283 MHz		license free communication e.g. "baby phone", RF heating systems citizen band (CB) communication: 26.565-27.405 MHz remote control systems
40.660-40.700 MHz	low range inductive coupling	remote control systems
433.050-434.790 MHz	European ISM band, B=1.74 MHz low cost RF systems	amateur radio band 430.000-440.000 MHz wireless communication products e.g. LPD radio sets, keyless entry systems, alarm systems, ...
868.000-870.000 MHz	SRD band in Europe, B=2MHz	former special channel for TV
888.000-889.000 MHz 902.000-928.000 MHz	in USA and Australia only	in Europe GSM mobile communication, CT1+ and CT2 cordless telephones
2.400-2.4835 GHz	ISM band, B=83.5 MHz	Wireless local area network (WLAN, 802.11, Bluetooth, ...) and remote control systems, microwave ovens (P < 1 kW), amateur radio band
5.725-5.875 GHz	ISM band, B=150 MHz	WLAN and remote control systems, amateur radio band, Radar motion detectors
24.000-24.250 GHz	ISM band, B=250 MHz	amateur radio band

Table 1: Frequency bands for radio sensor operation

For telemetry, frequency bands are allocated. Keeping standardized limits concerning the effective isotropically radiated power (EIRP), the bandwidth and the spurious emissions, rules for short range devices (SRD) and low power devices (LPD) with reduced licensing requirements can be applied. In Europe, in the ETSI CEPT/ERC 70-03 regulations, EN300330 (9 kHz - 25 MHz), EN300220 (25 MHz - 1 GHz) and EN300440 (1 GHz - 25 GHz), the limits of operation of radio sensors can be found.

The frequency bands, radio sensors can be operated within, are listed in Table 1 (from [10]).

International definitions of band coverage are defined by the International Telecommunication Union (ITU). Operation in industrial scientific and medical (ISM) bands is allowed, if the bandwidth and the power limits are kept.

The choice of the frequency band for radio sensor operation depends on the sensor type, the RF technology, the admissible antenna size, the distance range, etc. The low frequency bands are characterized by a relatively low bandwidth and therefore by low data rates.

For a more detailed investigation, further, we will distinguish between ID and sensor applications: The frequency allocations listed in Table 1 are allowed for both, identification and sensor purposes. Identification means that in the uplink the sensor responds with its ID code. For measurements, the sensor response contains information about the measurand instead of, or additionally to ID.

1.4 Applications of radio sensors

While identification is a well proven technique employing active, semi-active and passive devices, only measurement systems utilizing active transponders are implemented in high quantities in today's systems. In recent years, semi-active short range telemetry systems came into use. Passive measurement systems nowadays are in the stage of initial development of industrial applications, essentially supported by the research activities in our lab.
In Table 2 an overview of radio sensors and their applications is given.

	identification *)	measurements
active	door openers entry control person and animal tracking	telemetry systems weather balloons tire pressure monitoring
semi-active	car immobilizer fare payment entry control ski ticketing airport check in beacons	short range telemetry systems tire pressure monitoring
passive	anti theft systems (low-Q resonators) automation ID traffic applications (road pricing,...) RF beacons	SAW radio sensors **) high-Q resonators *experimental* non linear sensors *experimental*

Table 2: Examples for RF radio sensors and applications

*) in [10] more than 60 products for RF ID applications are described

**) scientific investigations currently (March 2000) are done:
in the USA, University of Central Florida, Prof. Malocha, jointly with SAW Tek Inc.,
in Germany, University of Illmenau, Prof. Buff,
in Austria, TU Vienna, Applied Electronics Institute, together with Siemens ZT KM1, Munich, Germany.

The current work focuses on the last row in Table 2. It concerns the sensors and the readout

circuits, an overview of the signal processing, employed for passive radio sensors, is given.
A more detailed classification of the passive sensors is made in Table 3. The groups of linear and non linear devices are divided into circuits employing energy storage and circuits without that:

	linear	non linear
employing energy storage (delayed response)	SAW radio sensors High-Q resonators	Modulated resonators
without energy storage (synchronous, not delayed response)	Low-Q resonators	Harmonic sensors Intermodulation sensors

Table 3: Passive radio sensors

Most of the scientific work of our group in the last years was focused on SAW sensors. Therefore, the enumeration of the passive sensors is divided into the groups of the non-SAW passive sensors, dealt with in chapter 2 and the surface acoustic wave (SAW) sensors discussed in chapter 3. Then, in chapter 4 the radio interrogation of passive sensors and the systems employed are discussed.
An essential part of this thesis is the review paper [1], A. Pohl, "A Review of Wireless SAW Sensors", published in IEEE Transactions on Ultrasonics Ferroelectrics and Frequency Control, dealing with SAW radio sensors, the systems and the measurement uncertainty. There, the relation between the parameters of the radio channel, the properties of the interrogation system and the uncertainty are shown and discussed, the results and the prospects are summarized.
In appendix A1, the radio channel and its deterministic and statistical parameters and their implementation in the design of radio sensor systems are discussed by means of measurement results. In appendix A2, further information for the estimation of measurement uncertainty is provided.

2. Passive radio sensors without SAW technology

Passive sensors from Table 3 investigated in our laboratory but operating without SAW technology, are described in this chapter. First the linear sensors are discussed, then the passive sensors employing non linear devices are described.

2.1 Linear passive radio sensors - resonators

Apart from the SAW devices, discussed in [1] and in chapter 3, resonant sensors belong to this group. Resonant sensors can be classified by the quality factor Q.

The quality factor Q of a resonator is defined by the ratio of energy W_r stored in the resonator and the total loss (dissipation) in a period P_v / ω_0.

$$Q = \omega_0 \cdot W_R / P_v \,. \qquad (1)$$

The energy time constant τ in the resonator we get from the well known equation

$$\tau = \frac{W_R}{P_v} = \frac{Q}{\omega_0} \,. \qquad (2)$$

Utilizing high-Q resonators, the signal of the decaying resonator is detected for up to several tens of microseconds after switching off the exciting RF signal.

The resonator's decaying signal at $f_0 = \omega_0/2\pi$ decreases with an exponential function. The Fourier transform of this signal yields an exponential spectral density almost symmetrical to the center frequency f_0 (see also chapter 3.3.4 / Figure 31 and chapter 4.2.2).

High-Q devices are characterized by a Q factor of several thousand. That means, that the losses per period are small, the device is able to store energy during the ring out time. A low Q factor makes a passive resonant device applicable as a radio sensor with frequency selective signal absorption.

2.1.1 High-Q dielectric resonators

Energy storage in resonators is the oldest principle applied to passive radio sensors. Almost thirty years ago, cavity resonators have been introduced for train identification purposes [11]. Representative for different types of high-Q resonators (without SAW technology), dielectric resonators (DRs) are discussed here.

For passive radio sensor purposes, resonators, e.g. DRs, are coupled to an antenna and are excited by an RF radio signal near f_0.

After excitation of the resonator the RF signal is switched off and the interrogation system receives the decaying response at f_0. Here, we have to distinguish between storage of energy in concentrated reservoirs (electromagnetic: capacitor and inductance in LC resonators, mechanical: in a pendulum in different kinds of static or kinetic energy) and storage in waves (as in acoustic bulk or surface waves). Switching off the excitation, in the devices with concentrated storage the system starts oscillating (exchange of energy between the reservoirs) at the resonance frequency f_0 almost within one period. Applying the storage with waves, the oscillation mode at resonance frequency has the largest time constant due to the lowest attenuation (best reflectivity of reflectors, etc.). All other modes decay with a shorter time constant. After a transition time, both passive resonator sensor types transmit a decaying signal centered at the resonance frequency f_0 of the device.

This frequency is a measure of a physical quantity (temperature, stress, etc.) affecting the resonator. The system and the signal processing effort is the same as employed for the SAW resonators (chapter 3.3.3).

Investigations for sensors, e.g. for high temperature measurements on the rotating anode of a x-ray tube, have been performed applying DRs [12]. The DR was fixed to a printed circuit board on a ceramic (Aluminum oxide) substrate with platinum strip lines and ground plane. A strip line for resonator coupling and a patch antenna were arranged on this board.

In Figure 6 the resonance frequency of this passive sensor unit is drawn versus the temperature. Our measurements have been performed in a high temperature oven capable to operate up to 1300 degree centigrade.

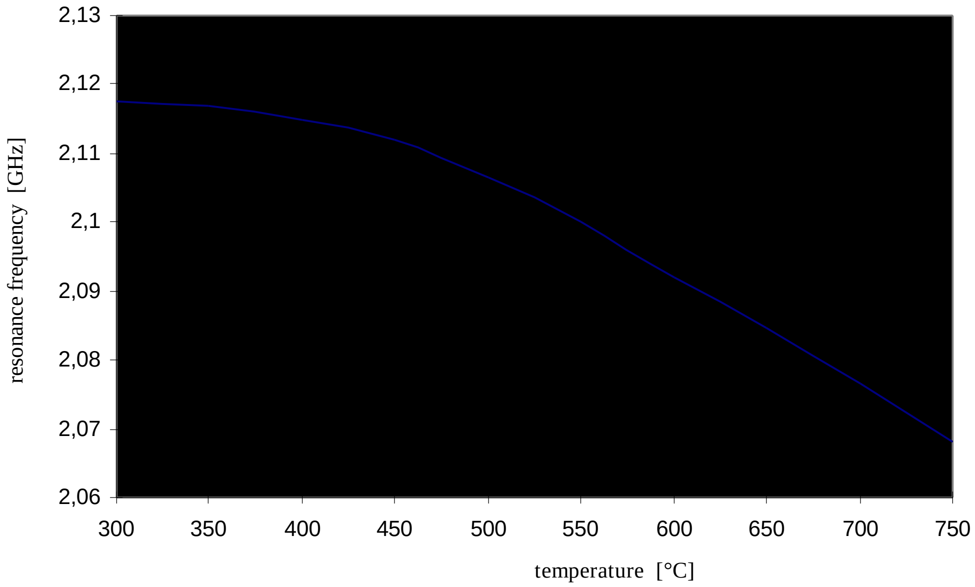

Figure 6: Wirelessly interrogated resonance frequency of DR versus temperature

2.1.2 Low-Q resonant devices

Another type of resonant passive sensors are LC circuits, line resonators, etc. with a low Q factor. This devices are characterized by time constants of some tens of nanoseconds. A time division between exciting signal and retransmitted signal is feasible with extremely high speed signal processing only. Radio interrogation usually is done by near field coupling of the resonators to the readout unit. Due to the low Q factor, the resonance has a wide maximum in frequency domain, a precise detection is difficulty and not applied. The radio interrogation units (one port network analyzer and "grid dip meter" principle) are described in chapter 4.1.3. The sensors are applied as one bit ID systems, e.g. for anti theft systems in department stores. The presence of the sensor is detected by the absorption of energy within a certain bandwidth.
Low-Q resonators are built very cheaply punching an inductance and two capacitor electrodes out of a thin aluminum film and insulating the electrodes by a plastic film. This sensor easily can be included into paper labels, glued onto consumer goods. In Figure 7, a photograph of a low Q resonator sensor for very-low-cost one-bit ID applications is shown. The sensor is canceled after paying the good by a breakthrough of the capacitor in a high magnetic field at resonance.

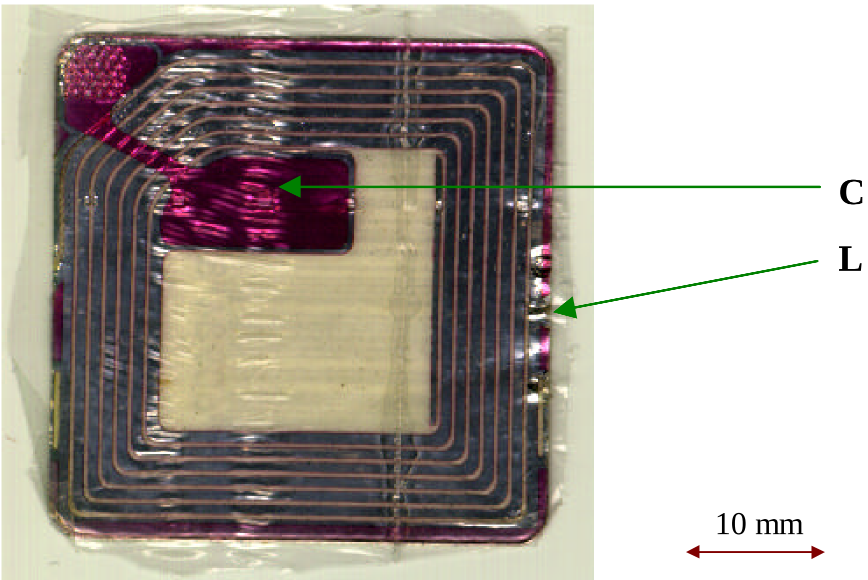

Figure 7: Low Q passive LC resonator sensor label for one bit ID purposes used in theft alarm systems

Further perspectives are offered by materials with a magnetically adjustable mechanical resonance frequency [13]. Therefore, a (long) ductile strip of magnetostrictive ferromagnetic material (= mechanical resonator) is arranged adjacent to ferromagnetic elements, being magnetized (bias elements). The resonance frequency of the (mechanical) resonator depends on the magnetization of the bias elements, it can be read out wirelessly by interrogation coils and detecting a frequency selective lack of energy in a frequency domain scan. If the sensor is carried through the coils at the output of the department store, the alarm bell starts ringing, etc. At the cashier desk, the magnetization and therefore the bias and the mechanical resonance is changed or "deactivated" e.g. by demagnetization. The interrogation system won't detect a resonance at the frequency of active sensors.

2.2 Nonlinear passive sensor devices without energy storage

To achieve a FDD capability to separate the radio request and the sensor response in frequency domain, a nonlinear sensor has to be applied. The nonlinear relation between voltage and current can be provided by a semiconductor diode.

Two types of frequency conversion are discussed here:

2.2.1 Harmonic sensors

One type of nonlinear frequency conversion (e.g. in a rectifier diode) is the generation of harmonics, spectral components at multiples of the radio request signal frequency.

A signal

$s_1(t)=a_1\cdot\cos(\omega t)$ (3)

passing a nonlinear device with a signal transition function

$g(t)=g_0+g_1\cdot s(t)+ g_2\cdot s(t)^2+ ...$, (4)

causes an output signal $s_2(t)$ containing a DC part and harmonics of the original signal.

For a nonlinear one port device, the signal reflection function is its impedance, converting the request voltage nonlinearly to the current through the device. The device can be an active circuit, it also can be a diode as shown in Figure 8, etc.

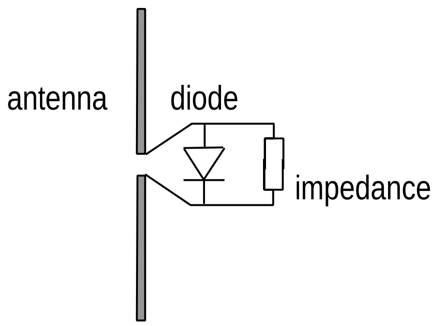

Figure 8: Passive nonlinear radio sensor circuit

If this circuit is requested by an RF radio signal, it excites and retransmits harmonics of the request signal. Detecting these response harmonics yields a simple theft alarm system for department stores etc. Of course, this arrangement is a wideband circuit, a nearby radio station will cause its harmonics too: for implementation a narrowband filtering is necessary. Sensors only can be distinguished by space division. In department stores, as for the low-Q sensors, antennas are attached near the doors, interrogating the theft alarm sensors and trigger the alarm if a sensor is detected.

The sensors discussed above are not suited to be fixed to metallic surfaces, otherwise the resonance, etc., would be shifted and the reliability of detection would be impaired.

Therefore, in today's theft prevention systems, more and more new nonlinear elements are used, operating at very low frequencies of some tens of Hz. In Figure 9, a photograph of such a sensor is shown. It only consists of a strip made of Permalloy and of magnetizable bias elements, and therefore it provides a very-low-cost one-bit ID sensor.

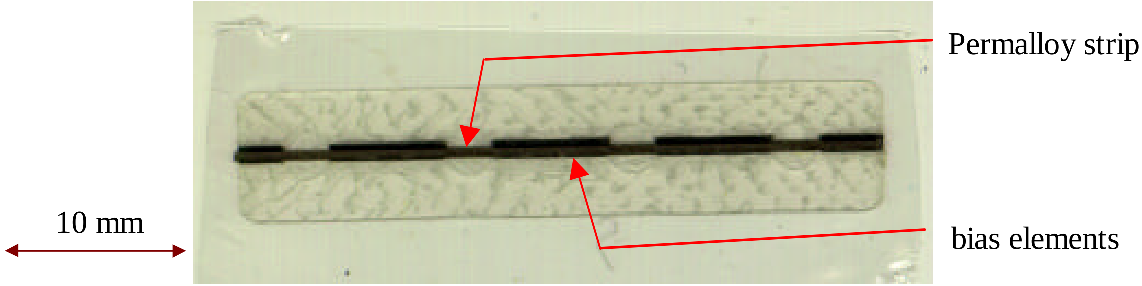

Figure 9: Magnetically biased nonlinear one-bit ID sensor for theft alarm systems

Due to its steep hysteresis flanks, the Permalloy strip provides a nonlinearity if it is magnetized by a low frequency alternating magnetic field. Without a magnetic bias (the bias elements are demagnetized), due to the hysteresis, the Permalloy strip generates nonlinear products at harmonic frequencies of the exciting signal, or intermodulation products of a sum of radio request signals. These spectral components easily can be detected if the sensor is coupled closely to the interrogation coils.

At the cash desk, the bias elements are magnetized, the relatively weak alternating magnetic field of the readout system won't be able to overcome this bias and to change the direction of magnetization, no harmonics occur and no alarm is triggered, if the sensor is carried through the readout coils at the exit of the department store.

The sensor is reprogrammable by demagnetization of the bias elements.

In usual systems, the readout is performed at 20 .. 50 Hz with an overlay AF signal at 3 .. 20 kHz. Due to the low operation frequency, metallic surfaces in parallel to the strip do not disturb the operation.

2.2.2 Mixer sensors

Another nonlinear radio interrogation method employs mixing effects. In RF engineering, the nonlinearity of a two port device causes intermodulation. At the output, due to the nonlinearity, spectral components occur at frequencies $f_e = k \cdot f_1 \pm l \cdot f_2 \pm m \cdot \Delta f$, for $|k|, |l|, |m| = 0, 1, 2...$, depending on the nonlinearity.

Applying a quadratic characteristic (IM2), signals in baseband and at the sum or difference and doubled frequencies occur. A third order nonlinearity causes intermodulation (IM3). Cross modulation is a special case of the IM3: $(f_2 \pm \Delta f) - f_2 + f_1 = f_1 \pm \Delta f$. The modulation with the frequency Δf is partly transferred from the carrier signal at f_2 to the previously not modulated RF carrier at f_1, causing signal components at $f_1 \pm \Delta f$.

Some tens of years ago, the powerful RF signal of Radio Luxembourg modulated other stations by the nonlinearity of the ionosphere. Radio signals being reflected at this layer were modulated by the information of this station. The effect was named "Luxembourg effect".

In Figure 10, the principle of cross modulation is sketched in frequency domain.

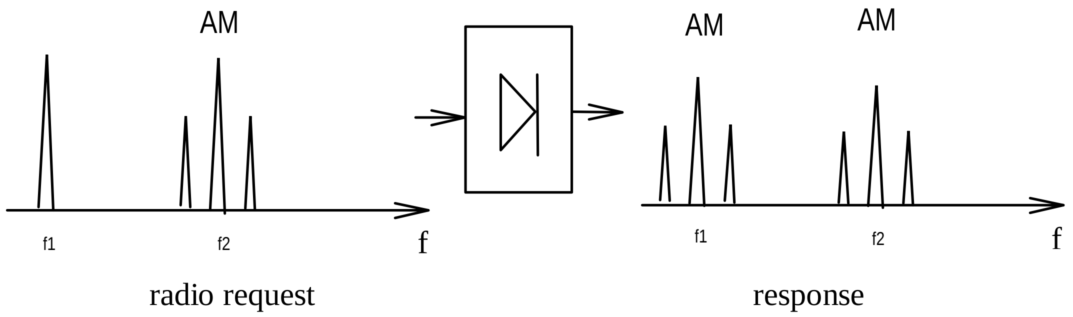

Figure 10: Cross modulation

Now, the idea is to apply these principle to the non linear radio sensors to achieve sensor capability. A radio request signal as drawn in Figure 10 is transmitted. Instantaneously the passive sensor retransmits the cross modulation products, received by the interrogation system. The frequencies for operation much more flexible than for the simple harmonic sensors. To avoid overdrive, f_1 and f_2 can be separated as wide as necessary, they also could be allocated in different ISM bands.

The sensor unit sketched operates in a wide bandwidth. The bandwidth of the f_1 modulating signals to detect in the response is very narrow, the effect of noise is small. To reduce errors due to cross modulation because of powerful broadcast or nearby mobile communication transmitters, appropriate bandpass filters would have to be implemented for actual application. The interrogation unit has to transmit and receive simultaneously. The demodulation can be done by a simple envelope detector. The according radio request system is described in chapter 4.1.4. Demodulation of the response signal around f_1 yields an audio frequency (AF) component at Δf, if the sensor is present. This AF signal can be detected easily, multiple operation of more than one radio request system may be achieved by different AF frequencies Δf.

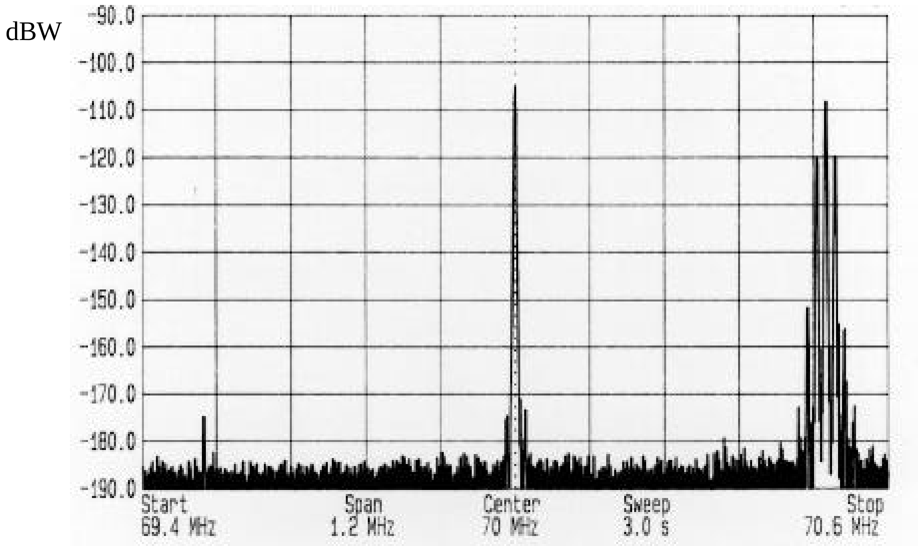

a) **f_1** **f_2**

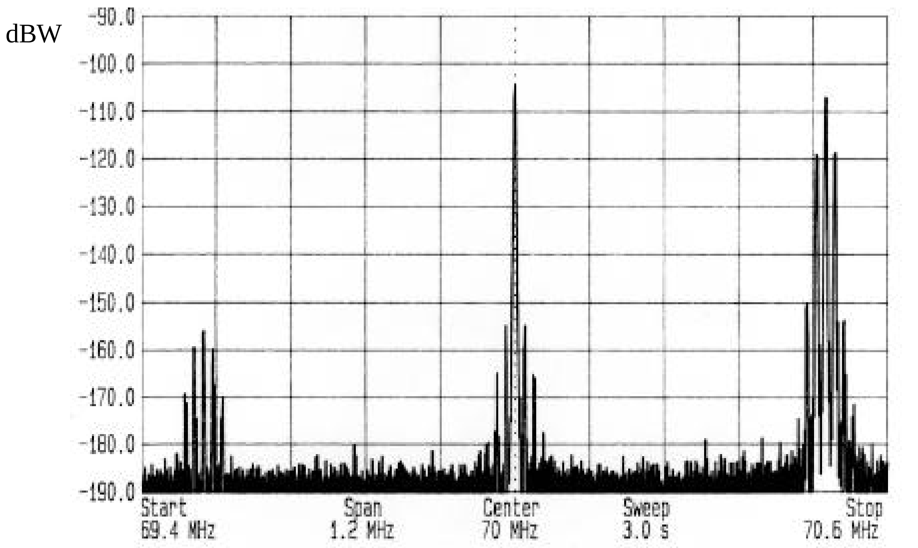

b) **$2f_1$-f_2**

Figure 11: Spectrum at receiver a) without, b) with passive nonlinear sensor present

The advantage of the method is, that no transmit / receive switches and no fast signal processing are required. Disadvantageous is the required signal power for biasing the diodes. In our experiments we used Schottky diodes: For a sufficient nonlinearity, the RF power received at the remote unit had to be higher than -20 dBm, limiting the distance range for application to approx. 1 meter. In Figure 11 the spectrum at the receiver input is shown for a) no sensor present and b) a passive non linear sensor in the operation range of the radio request system. It shows the result of our simple laboratory experiment.

The cross modulation effect can be observed clearly. At $2f_1 - f_2$ the AM signal but no RF carrier from the radio request signal is present. Sideband detection at this frequency avoids interference from the phase noise of the strong, continuously transmitted radio request signal at f_1 and lowers the phase noise requirements to the local oscillator.

The sensor unit drawn in Figure 8 is useful for one-bit identification only. To perform sensor tasks, the nonlinear behavior of the diode can be adjusted by an (active) biasing circuit, controlled by the measurand (Figure 12) or modulated by a code for digital data transmission as actually performed in the semi-active radio sensors (e.g. car immobilizers). Since the principle avoids extensive RF circuits (the RF part of this sensor unit only consist of the nonlinear device and the antenna) it is well suited for low cost applications.

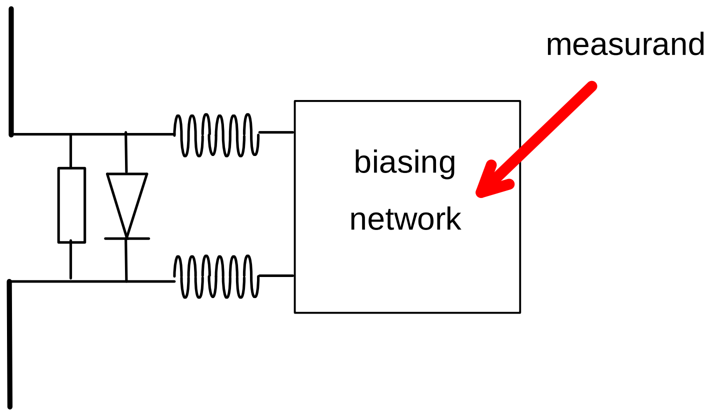

Figure 12: Radio sensor with biasing network for identification and sensor purposes ("backscatter modulation")

For measurements, to avoid an influence of the radio propagation distance, a differential measurement has to be performed. This requires at least two parameters to discriminate in the receiver. The idea now is to employ more than one, at least two AF signals at f_a and f_b, amplitude modulated to f_2 for radio request (Figure 13). Then, the RF voltage at the diode generates a current, containing the two sideband AF components, too. The carrier signal at f_1 and the spectrum at $k \cdot f_1 \pm l \cdot f_2$ is modulated by both, f_a and f_b.

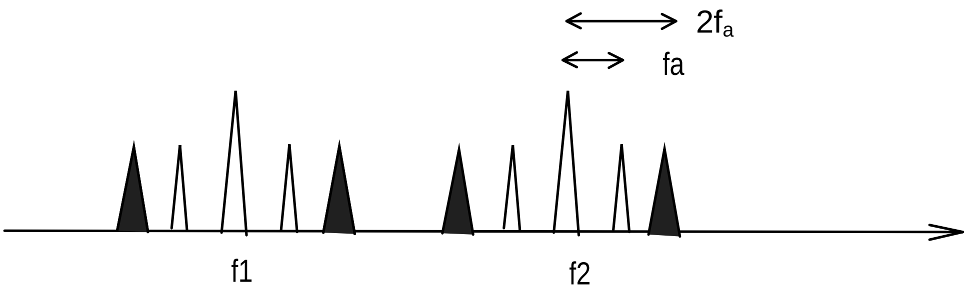

Figure 13: Two tone cross modulation

For sensor capability, the AF signals at f_1 and f_2 have to be differently affected by the measurand in the sensor unit. Then, a discrimination of amplitude or phase difference provides the information in the receiver. To evaluate the phase relation, the AF frequencies f_a and f_b have to be in a discrete ratio and mutually phase locked (Figure 14).

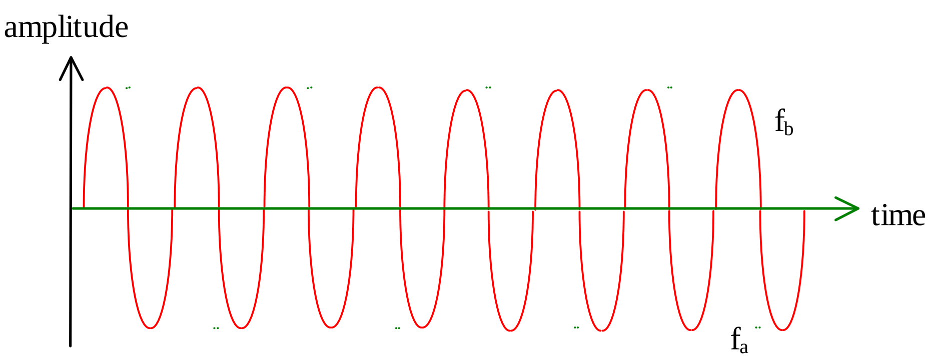

Figure 14: Phase locked AF signals for AM in a discrete frequency ratio of 2 (f_b=2f_a) with equal amplitude.

A simple composite signal with phase locked spectral components is a nonlinearly distorted periodic (e.g. rectangular shaped) signal.

Phase and amplitude distortions caused by the sensor can be evaluated in the receiver. By narrowband filters, the harmonics can be separated. In the sensor circuit, the task of conversion of the measurand into a phase shift $\Delta\varphi(f_a) \neq \Delta\varphi(f_b)$ easily is done by a frequency dependent impedance, e.g. a L-C resonance circuit (Figure 15).

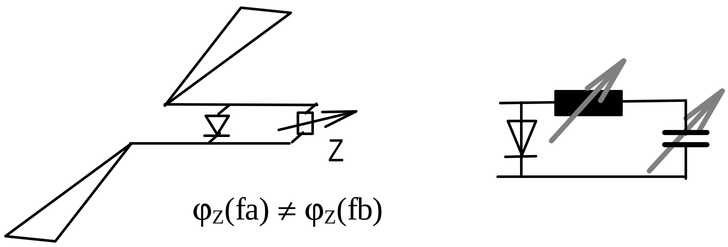

Figure 15: Sensor unit with tunable phase shifts for f_a, f_b

The measurand e.g. affects the capacitance or the inductance of the circuit and therefore the phase shift between the signals f_a and f_b (Figure 16).

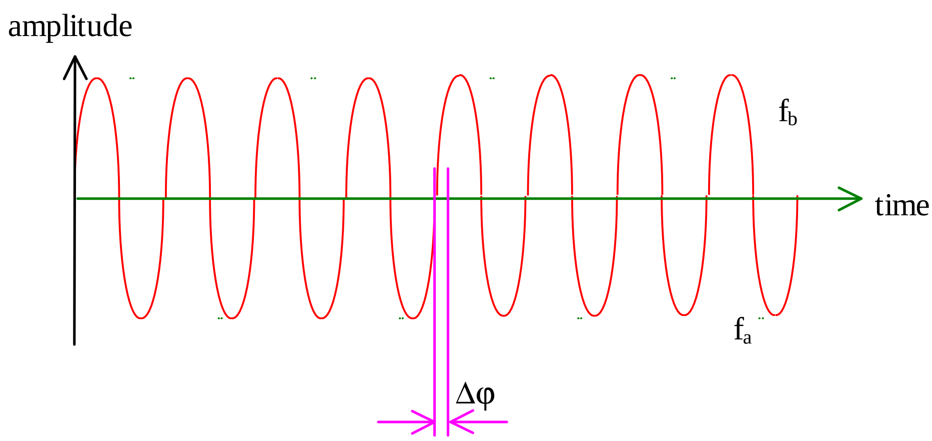

Figure 16: Phase locked but phase shifted ($\Delta\varphi$) AF signal in the receiver (amplitudes not affected here)

The method of passive sensing utilizing cross modulation has shown its feasibility in our experiments. For actual industrial implementation, further work is in progress.

2.3 Non linear sensors with energy storage

Here, the semi-active sensor devices employing semiconductor circuits and a microcontroller would be also included, utilizing remote powering by an RF signal instead of a battery and DC energy storage in an capacitor. On the other hand, we focus to passive devices without a DC supply, therefore these sensors are not discussed.

A noteworthy combination of RF energy storage and non linear signal processing was introduced for a passive radio sensor for the second generation tire pressure control in German upper class cars [14]:

Here, for request an RF carrier frequency (2.45 GHz) is amplitude modulated with two baseband (AF) signals. The passive sensor unit contains a non linear element and two bulk wave resonators (at two different resonance frequencies of approx. 10 MHz), one affected by the measurand, the other for temperature compensation. The radio request signal is demodulated by the nonlinear element, the AF signals excite the resonators. Then, the AM is switched off, the RF carrier signal is still transmitted by the interrogator. By the nonlinearity in the sensor unit, the signals from the (now decaying) resonators modulate the RF carrier. This response signal is retransmitted to the interrogator and coherently demodulated there, the measurand is evaluated. The simplified circuit diagram of the sensor unit is sketched in Figure 17.

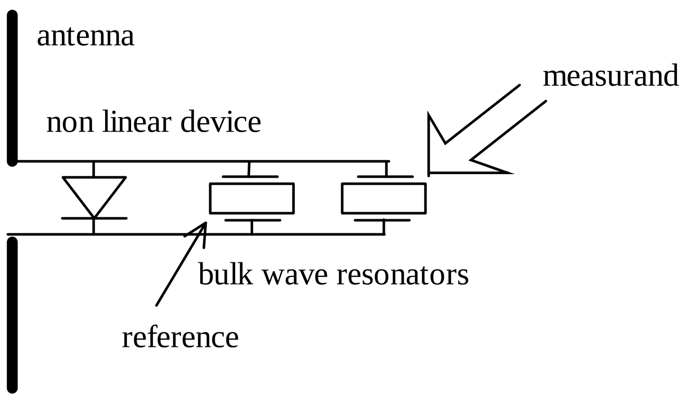

Figure 17: Simplified circuit diagram of a passive non linear radio sensor with RF energy storage

3. Passive SAW sensors

Since in our laboratory a lot of work has been done concerning SAW sensor devices, these will be discussed in this third chapter focusing on the currently applied passive types for radio request. From a lot of applications implemented experimentally, only a few are discussed here. Many of them have been published [1], [15], [16], [17], [18], [19], [20], [21], [22], [23], [24], [25].

3.1 SAW devices and materials

Surface acoustic wave devices have been invented more than 30 years ago [26]. On the surface of a plain polished piezoelectric substrate, metallic structures, interdigital transducers, (IDTs), are arranged [27], [28]. Due to the piezoelectric effect, an electric signal (AC voltage) at the IDT excites an acoustic wave, propagating on the surface (SAW). Vice versa, a SAW generates electric charge in an IDT driving an electric current into an external load.

By weighting of the finger overlap, a spatial weighting of the SAW intensity and therefore an amplitude weighting of the output signal versus time can be achieved, transversal filter structures are assembled: The gain factor of the taps is fixed by the IDT's finger pair overlap, the tap delay by the finger pair position. The summation is done in the bus bars interconnecting the electrodes. For first order filter design, the impulse response is depicted directly into the geometry of the IDT.

In frequency domain an IDT is a bandpass element, the center frequency of acoustoelectric interaction occurs for the acoustic wavelength equal to the geometric period of the electrodes. The Q factor of an IDT (length of impulse response) and of a reflector (number of wavelengths within the reflector) is proportional to the number of electrode pairs.

In Figure 18 a two port SAW device is sketched.

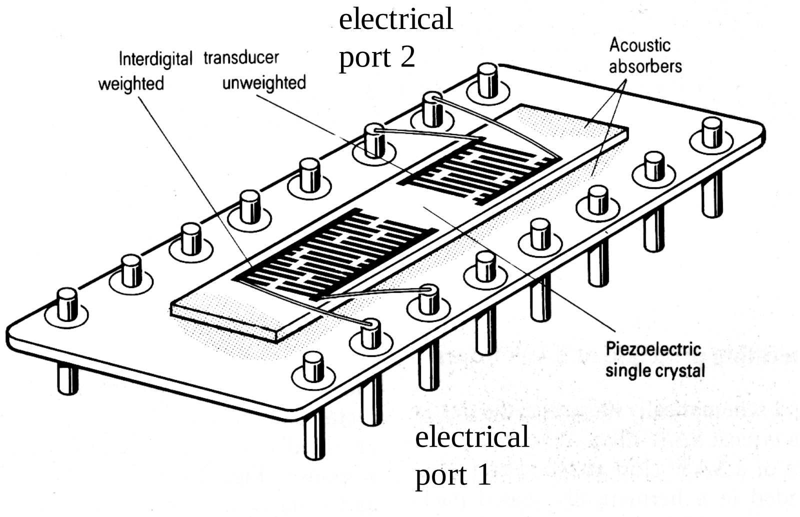

Figure 18: SAW device

While in the first decade, SAW devices were used for military and for special commercial applications only, they captured key positions in most modern communication sets in the last two decades. Today SAW devices are applied to a wide range of filter applications and as resonators for frequency and time reference. SAW devices are free of adjustment, former sensitive (because of the tolerances and aging of the components) filter circuits, sometimes requiring expensive adjustment in manufacturing, have been replaced by simple plug-in SAW components with specified data but without need of any adjustment. Because SAW devices are manufactured using one photolithography process only, the components remain low cost for high quantities. Today, SAW components are implemented in almost every color TV set, in personal mobile communication systems, in RF remote control systems, etc.

The market for SAW devices is still growing, manufacturers (e.g. Siemens Matsushita Components) produce more than 300 million of SAW filters for mobile phones and color TV sets per year. Mobile communication yields growing sales of SAW components. Upcoming low power radio systems, e.g. for remote control, wireless data transmission, radio sensor systems, etc., operating in the 433.92 MHz and the 2.45 GHz "industrial scientific and medical" (ISM) band yield a further need for SAW devices. Finally, since the sensor market grows with high rates today, the SAW sensors described in this work have a high potential for a wide spread application in industries, traffic and automotive systems, etc.

Our investigations in this topic have been accompanied by an increasing interest of the Austrian and the European industry, expressed by permanent inquiries and the start of industrial projects in cooperation with our permanent scientific partner Siemens Corporate Technology in

Munich, Germany.

With a SAW propagation velocity of 3400 m/s, the acoustic wavelength for an acoustic 1 GHz wave is 3.4 µm. Due to the optical resolution of the photolithographic manufacturing process of approx. 50 - 100 nm, the upper frequency limit for industrial sold SAW devices is approx. 3 GHz today. In scientific laboratories, SAW components up to 16 GHz have been built [29]. The lower frequency limit is given by the geometrical size of the substrate. Commercial SAW devices are deliverable from 30 MHz up.

At the beginning of SAW technology, Quartz (SiO_2) or Lithiumniobate ($LiNbO_3$) monocrystals have been used as substrate material, usually.

Since Quartz has a very low acoustoelectric coupling K, the insertion loss of such SAW devices is high. If the number of finger pairs is increased to reduce the insertion loss, the bandwidth is decreased. The temperature coefficient of ST cut quartz substrates has a wide minimum for room temperature and is neglected in many applications ("quartz stable operation").

A very high coupling coefficient K is found for $LiNbO_3$, its temperature coefficient TK (for velocity) is approx. -72 ppm/K using a 128° rotated Y/X cut. For the Y/Z standard cut it is approx. -92 ppm/K. Therefore, although the insertion loss is low, filter devices on $LiNbO_3$ have poor specifications because of their thermal drift. For intermediate frequency (IF) applications operated within the temperature range of a television set, a thermal frequency deviation of approx. -50 kHz will occur [30].

Up to now, a lot of alternative materials have been found. A substrate, widely used for RF filters and resonators, is Lithiumtantalate, $LiTaO_3$. It yields low insertion loss due to a high acoustoelectric coupling and a medium temperature coefficient (TK) of approx. -18 ppm/K for the 112° X/Y cut, up to -30 ppm/K for the 36° rotated Y/X cut. The SAW propagation loss is rather high.

In Table 4, the properties of the usually used SAW substrate materials are listed:

Material	Crystal orientation		v	K^2	S_T^v (TK)	Attenuation (dB/μs)	
	cut	propagation	(m/s)	(%)	(ppm/^{0}C)	433MHz	2.45GHz
Quarz	ST	X	3158	0.1	0	0.75	18.6
	37°rotY	90°rotX	5092	≈ 0.1	0	-	-
$LiNbO_3$	Y	Z	3488	4.1	-92	0.25	5.8
	128°rotY	X	3980	5.5	-72	0.27	5.2
$LiTaO_3$	36°rotY	X	4112	≈ 6.6	-30	1.35	20.9
	X	112°rotY	3301	0.88	-18	-	-

Table 4: Properties of usually used SAW substrate materials

For filter applications, new investigations to combine Galliumarsenide (GaAs) amplifiers and SAW filters in one chip are known. For sensors, high temperature SAW substrate materials have been found.

As one of the most important advantages of SAW radio sensors, their wide temperature range of operation is considered. In general, the lower limit of the temperature range of SAW devices is the vaporization temperature of the gas (e.g. Nitrogen) inside the package.

For a temperature increase of 100 K, an additional SAW propagation loss of approx. 2 dB / 100 K / µs delay can be observed.

The upper temperature limit is given by the lowest of various upper limitations:

(a) Exceeding the melting temperature of the IDT's metallization causes a total defect of the device. Usual SAW devices are metallized by aluminum with an approx. 400 °C melting point. For high temperature applications, a platinum / tungsten metallization was investigated successfully.

(b) If the piezoelectric Curie temperature is exceeded, the piezo-effect vanishes and therefore the device cannot be operated any more. New high temperature materials [31] are Berlinite ($AlPO_4$), Lithium tetraborate ($Li_2B_4O_7$), Langasit ($La_3Ga_5SiO_{14}$) and Galliumorthophosphate ($GaPO_4$), with Curie temperatures of more than 1000 °C.

(c) Lithiumniobate is used in a mixture with unbalanced energy conditions (it is not stoechiometric). Therefore, a process of de-mixing takes place continuously. This effect is very slow for low temperatures, a lifetime of many hundred years is predicted [32]. Investigations [33] show, that this de-mixing is uncritical below 300 degree centigrade in general and for industrial polished surfaces up to 600 °C.

(d) An upper temperature limit is given by packaging, contacting and by the antenna design (for SAW radio sensors). For commercial SAW components, the substrate is glued into the package by an adhesive. To avoid mechanical stress to the substrate, the thermal extension of package and adhesive has to be considered.

Especially at enhanced temperatures, usual adhesives tend to vaporize some parts of their contents. This yields a layer deposited to the substrate's surface, causing a mass loading. Thus, the SAW velocity is affected, changing the acoustical delay and the frequency of acoustoelectric interaction of an IDT. Further the layer yields an increased insertion loss of the device and it may become useless for the particular application.

SAW resonators are subject to aging due to the oxidation of the aluminum metallisation, causing stress loading, raising the SAW velocity. This is not affecting SAW delay lines, since the delay mainly depends on the propagation length across the free surface.

The most important parameters for RF front end applications are the insertion loss and the compatibility of the filter to an RF transfer power of several Watts. Applying coupled resonant structures, the insertion loss of a narrow band SAW device was reduced from more than 30 dB ten years ago to less than 2 dB for modern RF and IF filters in mobile phones [34]. The power capability is limited by the electrical field strength between the IDT electrodes and the mechanical stress occurring due to the piezoelectricity. For SAW devices below 1 GHz, a maximal power capability up to 30 dBm is attained today [35].

3.2 SAW sensors

With SAW devices, an electrical delay is achieved by an acoustic propagation length, frequency selectivity by the geometry and period of the IDT electrodes. Since the SAW propagates with a factor 10^5 slower than an electromagnetic wave (EMW), electric delays up to several tens of µs, corresponding to a few km EMW propagation, can be implemented in a small analog passive device.

In Figure 19, a two port SAW delay line, an input burst signal and the corresponding output signal are sketched versus time. Actually occurring unwanted effects (triple transit signal, etc.) are neglected here as well as the impulse widening due to the convolution of the burst with the burst response of the IDTs.

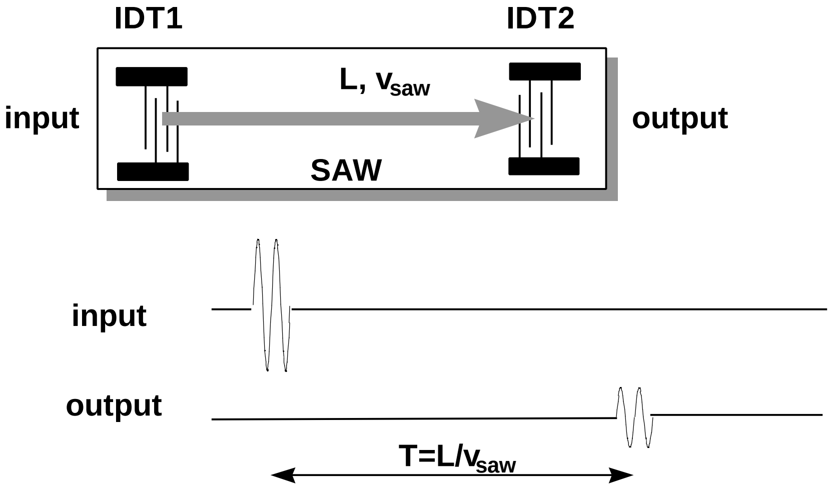

Figure 19: SAW delay line

The propagation of the SAW depends on the geometry of the substrate and the material parameters. These material constants are subject to environmental conditions.

The electrical behavior of the devices can be designed to be insensitive against physical effects of the environment. A lot of work has been done to make SAW devices to operate well in the desert as well as flying in an airplane with high g-load in a height of 20000 meters at -60 °C. Due to the low temperature coefficient of special crystal cuts, SAW devices are used as "quartz stable" filters and resonators for frequency reference. A special packaging prevents the SAW devices from mechanical and chemical stress.

Vice versa the components without compensating arrangements can be used for measurement, evaluating the electric response of the SAW device, affected by temperature, mechanical stress, strain, mass loading, etc.

The measurand usually affects both, the elastic constants of the crystal and its mechanical dimensions. For an ST-Quartz substrate the thermal extension is compensated by the change of velocity. This yields the almost vanishing temperature coefficient. For $LiNbO_3$ the change in velocity predominates the thermal extension. If more than one parameter is affected by the measurand, cross sensitivities occur.

Since many years, SAW resonators or two port delay line sensors are implemented into the feedback loop of oscillator circuits (Figure 20) and the change of output frequency is discriminated for measurement.

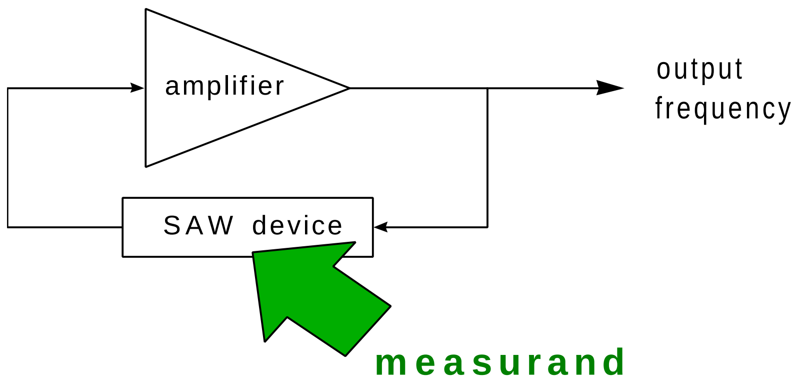

Figure 20: Oscillator circuit utilizing a two port SAW sensor device in the feedback loop

For a classification of the SAW sensors, we will divide into two categories of SAW devices, delay lines and resonators:

SAW delay lines utilize the propagation delay T= L/v_{saw} between IDTs, the ratio of length and velocity (Figure 19).

In Figure 21 a SAW resonator is sketched. The resonance frequency is determined by the geometric reflector period $d=\lambda_{saw}/2$. For sensor purposes, the reflectivity (in frequency domain) of the acoustic reflectors with fixed geometric period d and therefore the resonance frequency is shifted due to the change of velocity and wavelength λ_{saw}.

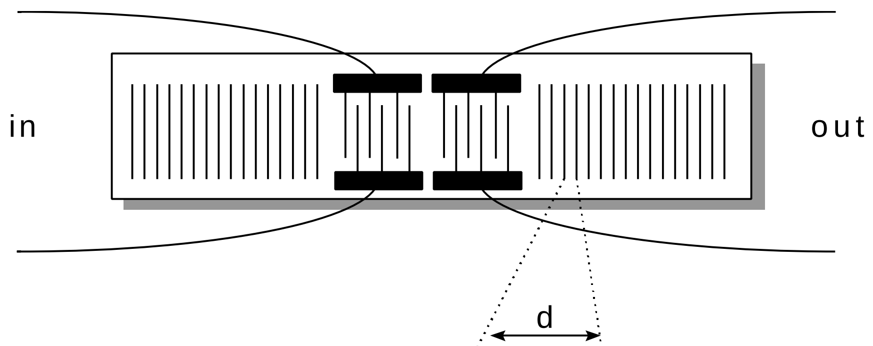

Figure 21: SAW resonator

Usually, to avoid errors due to cross sensitivities for temperature, etc., a differential measurement is performed. As shown in Figure 22 two oscillator circuits controlled by SAW devices are employed. One of the, e.g. SAW resonators is affected by the measurand, the other is insulated from this. Both are exposed to the same temperature, acceleration, etc. The output signals are multiplied. Only the difference frequency, carrying the information of the measurand but compensated for temperature, passes the low pass filter (LPF).

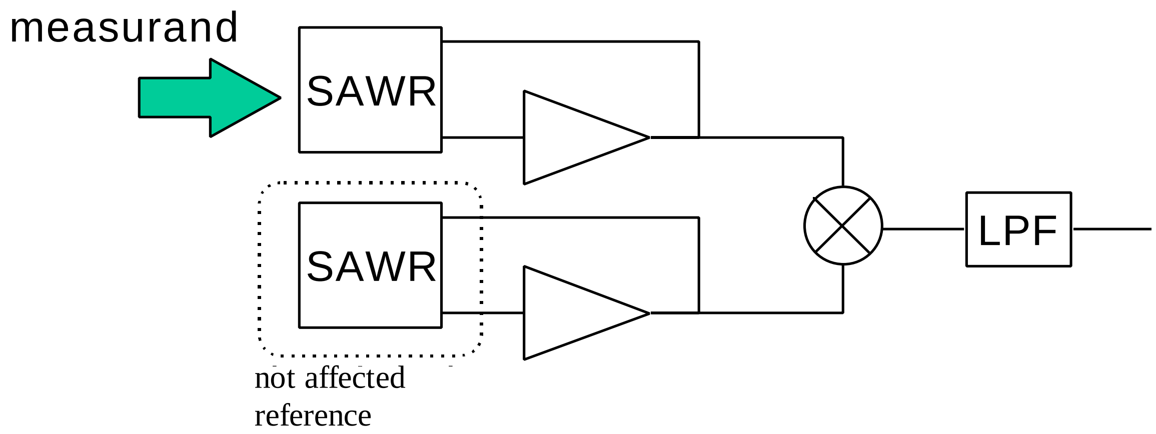

Figure 22: Compensated measurement circuit

With "wired" SAW sensors implemented into active circuits, a lot of sensor tasks have been solved satisfactorily. Sensors for many mechanical, chemical and even biological measurands have been published [36], [37], [38], [39], [40], [41].
The effect of the measurand to delay and resonance frequency is the same as for the passive SAW radio sensors, discussed in [1].

3.3 Radio requestable SAW sensors

For radio sensor applications, one port surface acoustic wave devices electrically connected to an antenna, came into use. Initially, these passive circuits have been invented for the identification of animals [42]. The first industrial application was a road pricing system for the Norwegian highways around Oslo [41]. SAW devices are linear, time invariant and passive. The division between radio request and the sensor response is performed in time domain (TDD). As defined above, radio interrogation (or sensor readout) summarizes RF request, RF response, its reception and evaluation of measurand (Figure 23).

Though in SAW interrogation systems in some implementations the sensor is in the near field (see appendix 1) of the interrogation antenna, for the interrogation process it is considered in the far field always, i.e. no direct interaction (without time delay, or equal time request and response) is employed.

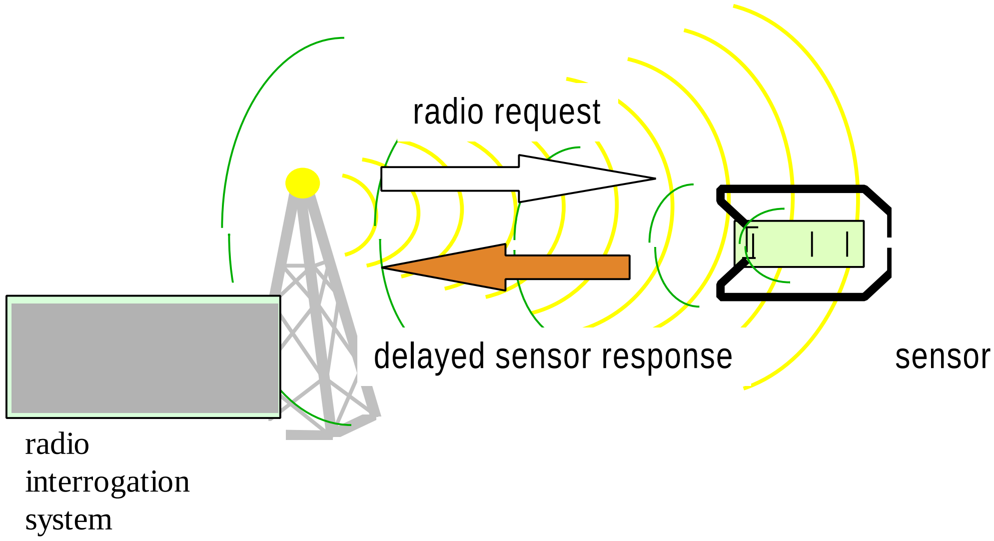

Figure 23: Radio interrogation (= request + response + evaluation) of passive SAW sensors

Employing TDD, the radio request system transmits an RF signal and switches to receive mode then. After a delay time, the convolution of the radio request signal and the reflective SAW device's RF response (burst response, if a burst was transmitted), carrying the information about the measurand, is transmitted back to the receiver and the evaluation unit.

In Table 5, the SAW devices, today employed for sensor applications, are marked by an "x". The others ("-") are currently subject of research activities.

	delay lines		**resonators**
	wideband	dispersive	
one port	x	x	x
two port	x	-	-

Table 5: SAW devices actually used for radio sensors (marked by "x")

3.3.1 Wideband SAW delay line sensors

A comprehensive survey of SAW delay line (DL) radio sensors is given in [1]. There, it is distinguished between directly affected (one port) and indirectly affected (two port) devices. Employing directly affected devices, the measurand changes the SAW velocity or the substrate dimensions, determining the delay, by a direct affect to the substrate.

In Figure 24, a reflective SAW DL with the IDT and the reflectors R_1 and R_2 is sketched.

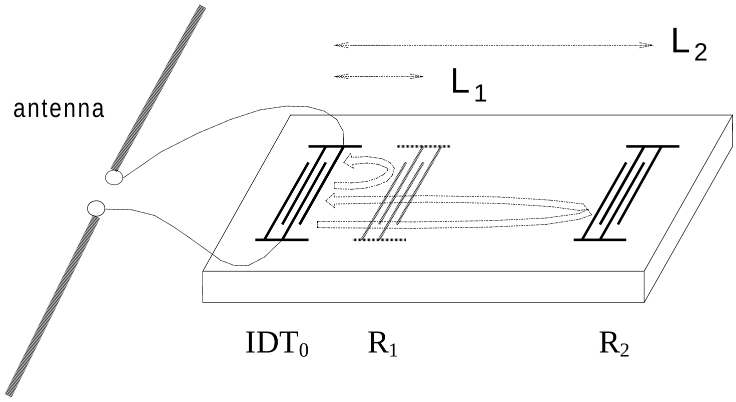

Figure 24: One port (reflective) SAW DL

Indirectly affected SAW sensors utilize a reflective IDT R_2 (a second electrical port), loaded by an external load impedance, changing its reflectivity [43]:

The SAW arriving at the reflector R_2 generates electric charge on the electrodes, i.e. an electric voltage between. An external electrical load connected to R_2 discharges this voltage and affects or avoids a re-generation of a SAW and therefore it affects the reflected radio response after a delay 2. L_2 / v_{saw}. If the voltage is short circuited, almost no reflection of the SAW will occur.

From [27] the reflection and transmission coefficients for IDTs are calculated utilizing the P matrix:

$$b_1 = P_{11} \cdot a_1 + P_{12} \cdot a_2 + P_{13} \cdot u_3$$

$$b_2 = P_{21} \cdot a_1 + P_{22} \cdot a_2 + P_{23} \cdot u_3 \qquad (5)$$

$$i_3 = P_{31} \cdot a_1 + P_{32} \cdot a_2 + P_{33} \cdot u_3$$

The terms a_i are the incoming, b_i the reflected acoustic waves. The electric current into and the voltage at the IDT (e.g. R_2) are given by i and u.

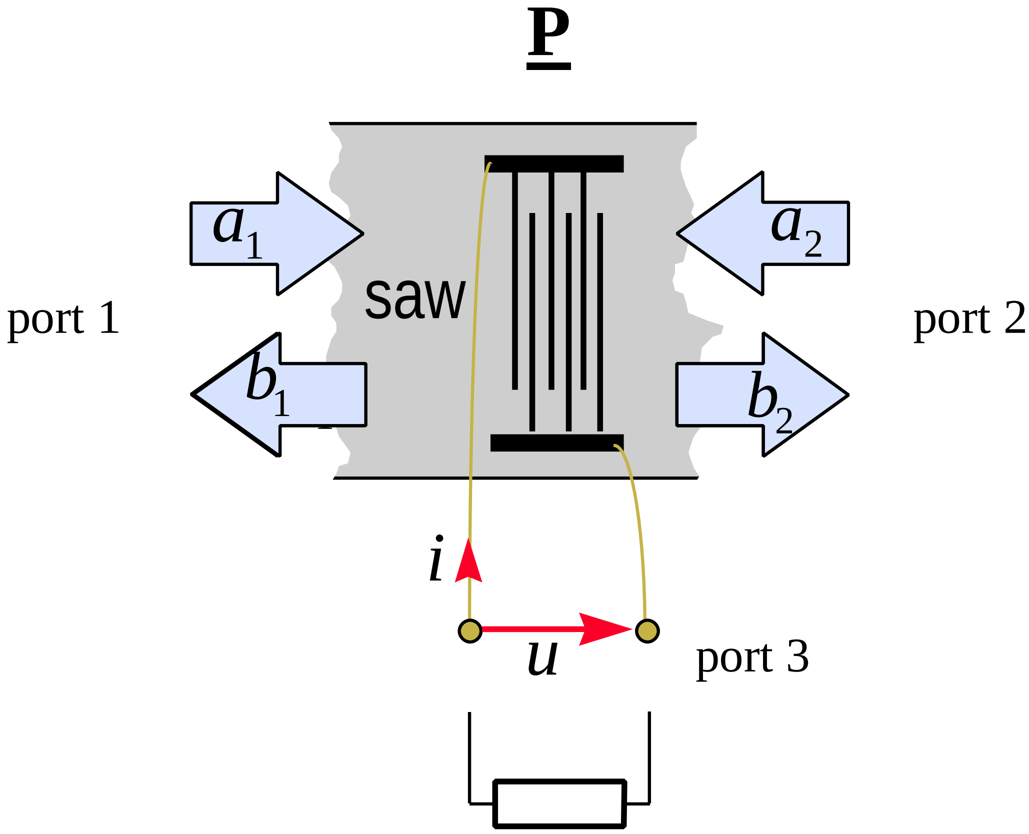

Figure 25: Three port IDT for P-matrix description, acoustical ports 1 and 2, electrical port 3

As also discussed in [1], the reflectivity of an IDT as a function of a complex impedance Z_{load} at its electrical ports is calculated with the P-Matrix formalism from P_{11}:

$$P_{11}(Z_{load}) = P_{11}^{sc} + \frac{2P_{13}^2}{P_{33} + \frac{1}{Z_{load}}} \qquad (6)$$

Here, P_{11}^{sc} is the acoustical reflection coefficient of port 1 with the electrical port 3 shorted (u_3=0). Since the reflection coefficient is a complex parameter, the according signal of the sensor response is affected in magnitude and phase. In Figure 26, the acoustic reflection coefficient is plotted in a polar diagram, a comparison of theory and our measurement is shown.

Actually, the passive electrical load impedance Z_{load} consists of a serial-circuit of a sensor impedance (resistive, capacitive or inductive) with the inductance of the bonding and connecting wires. The smaller this (unavoidable) inductance is, the further the short-circuit point moves towards zero reflection (center of the polar plot). Vice versa, for increased inductance (between the SAW device and the external sensor contacts) the shortcut-point moves outwards. The open point is determined by the IDT capacitance of the SAW device and by P_{13} and P_{33}, respectively.

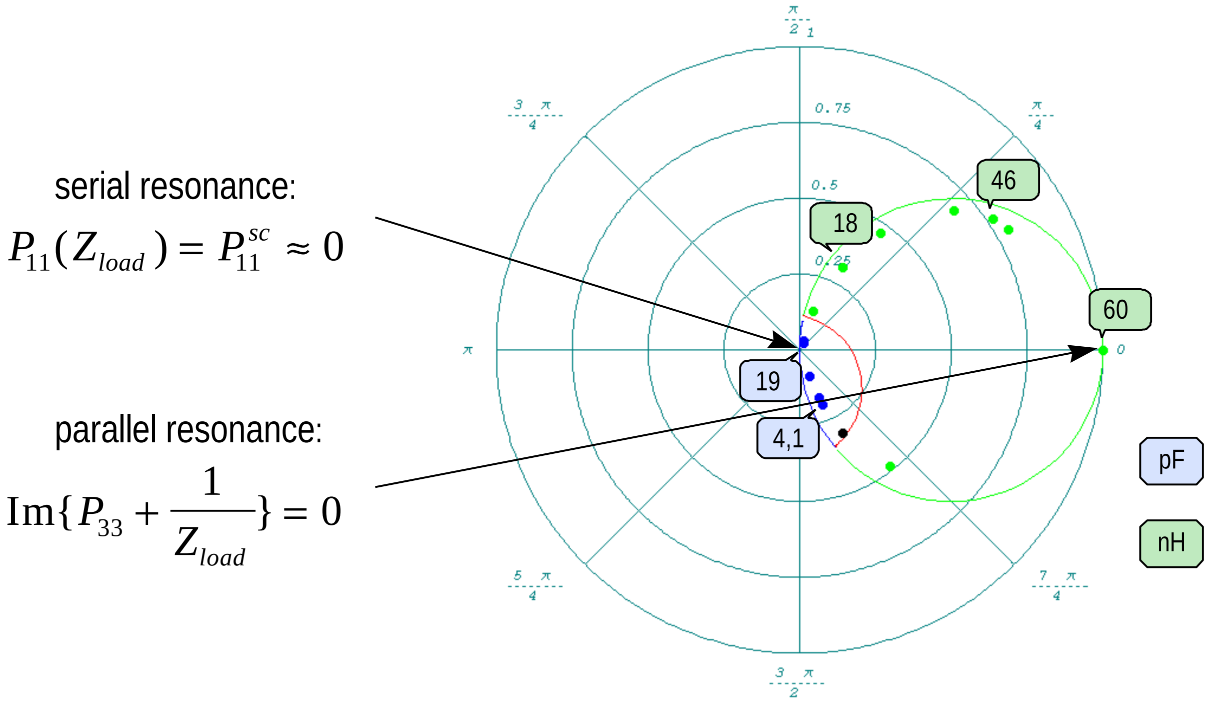

Figure 26: Polar diagram of the acoustic reflectivity $P_{11}[Z_{load}]$ of a split finger IDT as a function of its electrical load, comparison of theory and experimental results

Employing this principle for passive radio sensor circuits, the SAW device operates as a delaying RF transponder only, the sensor element is a conventional from stock sensor device where Z_{load} depends on the measurand. It is not necessary to construct the SAW device especially for the specific application, a standard type can be used. The SAW can be encapsulated and protected from mechanical stress, etc., cross sensitivities are reduced drastically due to the separation of sensor and delaying transponder task.

The resolution is determined by the external sensor device as well as by the nonlinear relation between the load Z_L and reflectivity $P_{11}[Z_{load}]$ of the reflector R_L. In actual use, the resolution is better than 1 % in worst case.

Sensors for a lot of measurands have been experimentally investigated. With capacitive sensors, pressure, distance, temperature, etc. have been measured wirelessly [17]. Applying Giant Magneto Impedance (GMI) wires as external load, we built sensors for magnetic field [18].

The external sensor device is electrically operated (excited) at high radio frequency. Many (semiconductor) sensors cannot handle this. A new idea from the author [16] is to separate the RF transponder and the sensor path utilizing a varactor diode loading the IDT as a capacitance, controlled by a DC or AF voltage (Figure 27).

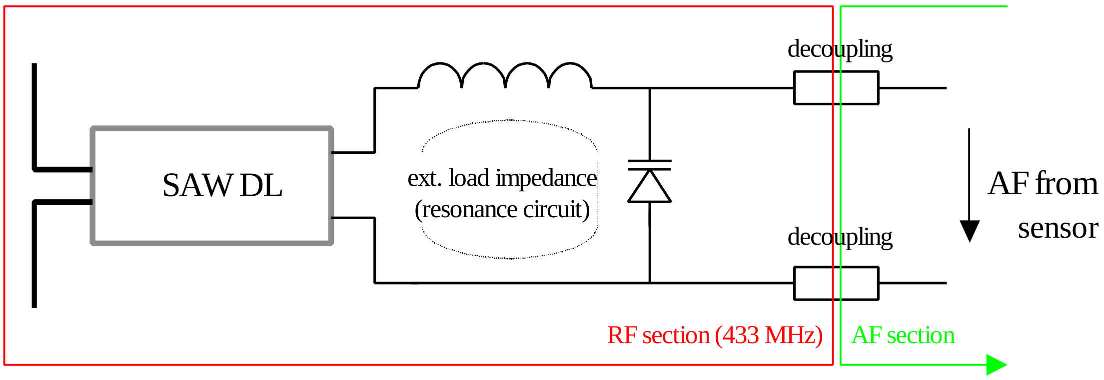

Figure 27: Indirectly affected SAW radio sensor for AF voltage measurements

So, measurands exciting an AF (from DC to more than 100 kHz) voltage can be measured. The principle successfully has been utilized for the measurement of dynamic mechanical parameters. There, the sensor, converting the mechanical strain into a voltage was a from stock piezo element. Due to the high input impedance (loss resistance) of the varactor for its bias signal, a time constant of a few seconds, and therefore a lower frequency limit of approx. 1 Hz has been achieved even for piezo elements with very small internal capacitance (a few pF only, which are discharged slowly over the loss resistance).

3.3.2 Dispersive SAW delay line sensors

SAW devices are well known for matched filter applications e.g. for chirp impulse compression. The linear chirp signal is characterized by its bandwidth B, its duration T and the sign of the dispersion coefficient μ (up or down). A mismatch of the chirp signal and the compressor yields a time shift of the compressed impulse, i.e. an error if Doppler shift occurs, but is essentially in compressive receivers [7], [8].

As sketched in Figure 28, an on-chip chirp impulse compression is applied by dispersive delay line sensors (DDL) [40].

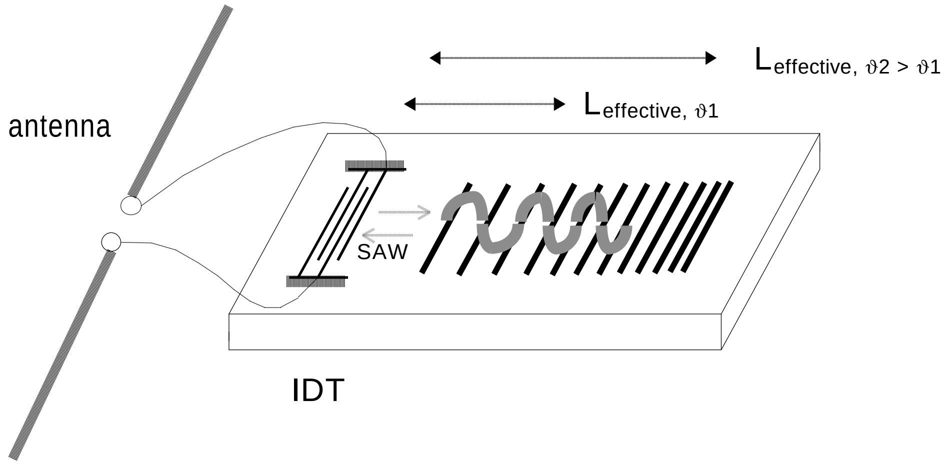

Figure 28: One port SAW DDL with impulse compression on the sensor chip

The radio request signal is a chirp matched (i.e. it is time inverse) to the sensor dispersion. The sensor responds with a bandpass impulse compressed in time to a 3 dB width of 1/B.

On the other hand, the sensor can be utilized as a chirp expander, excited by the radio request signal. Then, the compressor is implemented in the receiver.

Affecting the dispersive reflector in the sensor (e.g. thermally or mechanically) yields a change of the total delay due to a shift of the effective reflection location for each frequency within B. The shift of geometry causes a shift in frequency of acoustoelectric interaction, the chirped SAW (propagating on the sensor in Figure 28) delivers a compressed output signal, e.g. earlier for a temperature $\vartheta_1 < \vartheta_2$.

In Figure 29 the principle is shown in a time / frequency diagram for a "cold" and a "hot" temperature sensor with a positive change of delay versus temperature.

It is important to consider the principle of stationary phase. Then, the frequency used in Figure 29 is the differential $d\varphi/dt$ of signal phase φ and time t.

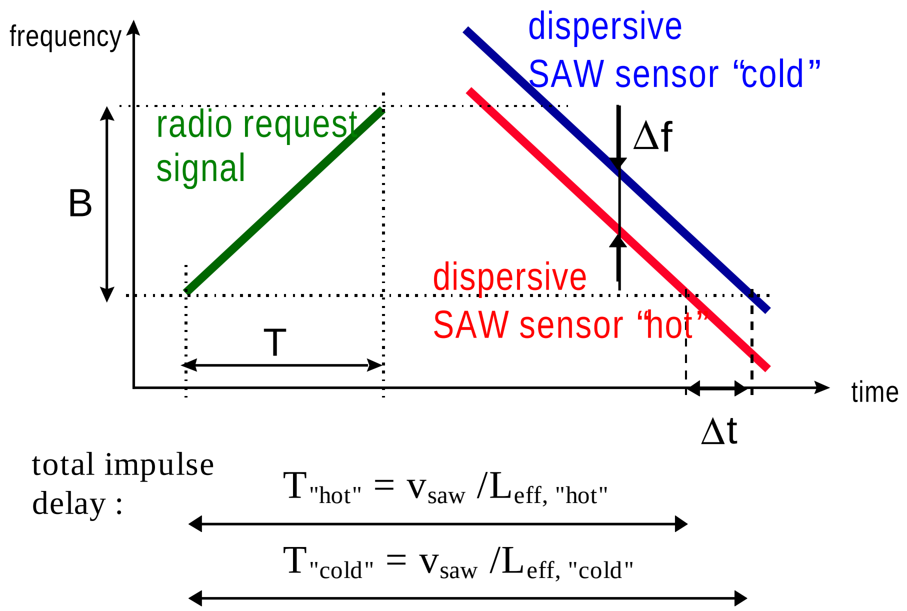

Figure 29: Principle of a one port SAW DDL

The shift in delay of the compressed impulse's envelope is amplified compared to a wideband delay line

$$\Delta t = \Delta f \cdot \frac{T}{B}. \tag{7}$$

The amplification of sensitivity compared with a wideband delay line is

$$\eta = \frac{\Delta t_{ddl}}{\Delta t_{dl}} = \frac{\Delta f \cdot \frac{T}{B}}{\varepsilon \cdot T} = \frac{\varepsilon \cdot f_{center} \cdot \frac{T}{B}}{\varepsilon \cdot T} = \frac{f_{center}}{B} \tag{8}$$

with ε, the scaling of the sensor's response in time due to the measurand [40], [44].

3.3.3 SAW resonator sensors

SAW resonators (SAWR) are applied as passive sensors with RF energy storage in the SAW. After excitation by an RF signal, the resonator transmits a decaying signal at its resonance frequency [45]. In Figure 30 a SAWR radio sensor is sketched, in Figure 31 the resonator response signal in time and its FFT spectrum is shown.

The scaling factor for delay is calculated from $1+\varepsilon = 1 + S_T^y \cdot y$ with the relative sensitivity

$$S_T^y = \frac{1}{T} \cdot \frac{dT}{dy} \qquad (9)$$

of the parameter T to the effect y, e.g. in ppm/K.

The effect of a measurand y to the frequency of a resonator is

$$\Delta f = \frac{S_T^y \cdot y}{d/v_{saw} \cdot \left(1 + S_T^y \cdot y\right)} . \qquad (10)$$

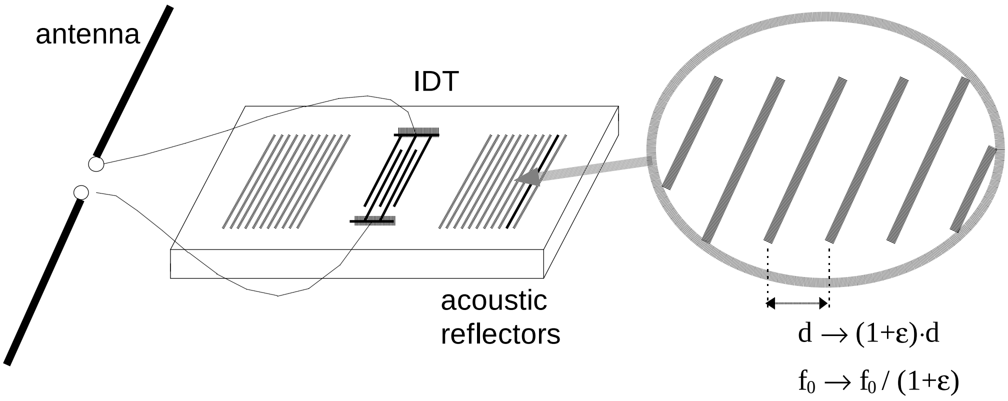

Figure 30: One port SAWR

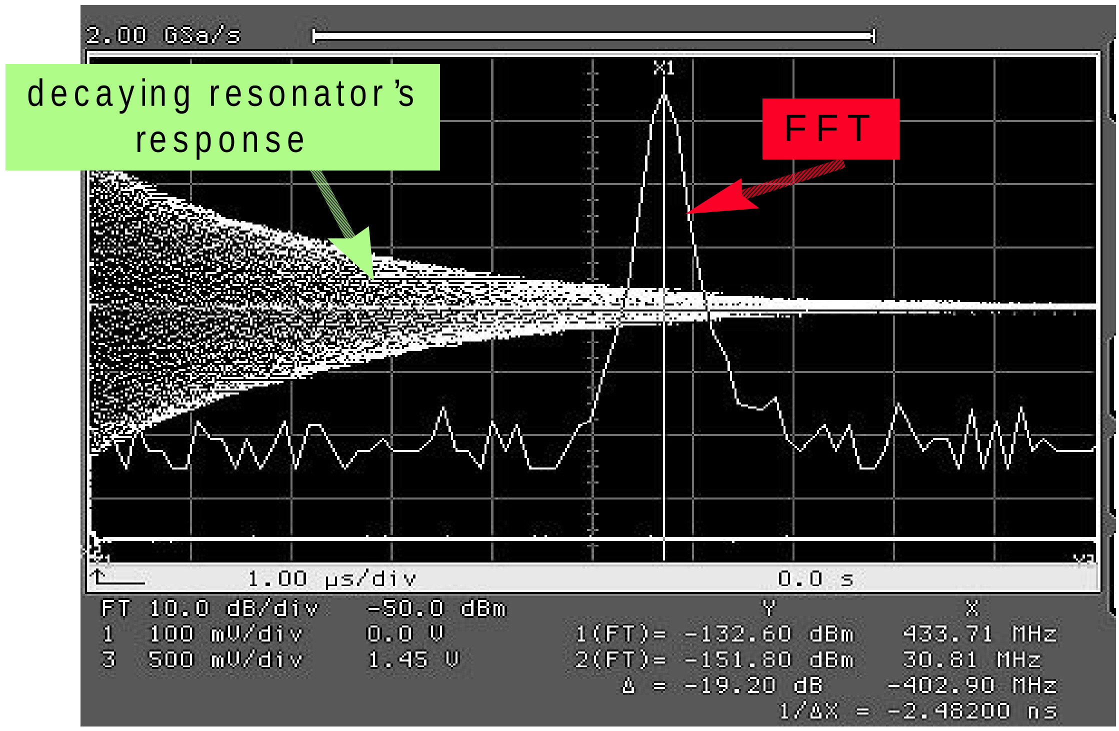

Figure 31: Screen shot of the response signal of a one port SAWR at 433.71 MHz on a digital storage oscilloscope with decaying RF signal (1 µs/Div.) and FFT (1 MHz/Div., center 433

MHz)

To achieve identification capability or to design a multi-channel sensor, resonators at different resonance frequencies are switched in parallel.

The operation temperature range of the SAW radio sensors is the same as for the other SAW devices described above. SAW radio sensors are totally passive, contain neither active elements nor batteries or capacitors. Since no semiconductors are applied, the sensors withstand a high rate of hard radiation and a powerful electromagnetic interference (EMI). With suitable packaging, the sensors are applicable in dusty environments with high load and withstand severe environmental conditions.

SAW radio sensors can be requested by radio signals in a frequency range between approx. 30 and 3000 MHz. The operation in the ISM bands is recommended or necessary, respectively.

Utilizing SAW radio sensors, a wide range of sensor applications, including automotive, have been investigated.

4. Interrogation systems for passive radio sensors

As mentioned above, we disregard the interrogation systems for active and semi-active radio sensors here. These units usually respond with a digital data telegram. The interrogation system contains a rather simple AM or FM receiver, the data are processed in a microcontroller.

But, whatever kind of wireless passive radio sensor is employed, the sensor responds with an RF signal derived from the radio request signal by a linear or a non linear effect due to the measurand. As for RADAR systems, the oscillators in the receiver usually are phase-coupled to the transmitter, coherent detection is easier than for interrogation of active sensors.

4.1 Radio request methods

As discussed in [1], a classification of the radio request methods can be established by the domain of initial signal detection. Further, a distinction between TDD sampling methods and FDD continuous measurement is applicable.

We investigate the actually employed methods and classify:

- Time domain sampling (TDS), wideband or full band sampling with TDD and
- Frequency domain sampling (FDS), narrowband or partial band sampling with TDD
- Continuous frequency domain sampling (CFDS) with FDD

The measurement system can be separated into an RF part (RFU) and an evaluation unit (EU). In the RFU, the response signal is demodulated, sampled and usually digitized. For the wireless readout of moving passive sensors a very special RFU circuit design has to allow for the d^p (see appendix 1, e.g. d=4) dependence of the response signal strength on the length d of the radio channel. So, automatic control circuits (gain, frequency, etc.) operate in the RFU exclusively but the parameter settings can also be controlled by the EU.

The interface between RFU and EU is a matrix of data, representing the sensor response amplitude and/or phase versus time or frequency, or the frequency versus time. The interfaced data is complex valued, a real and an imaginary part is handed over. The EU processes this data and calculates the estimated measurand for display, control, etc. Data reduction processing, as discussed below, require an enhanced interaction between RFU and EU.

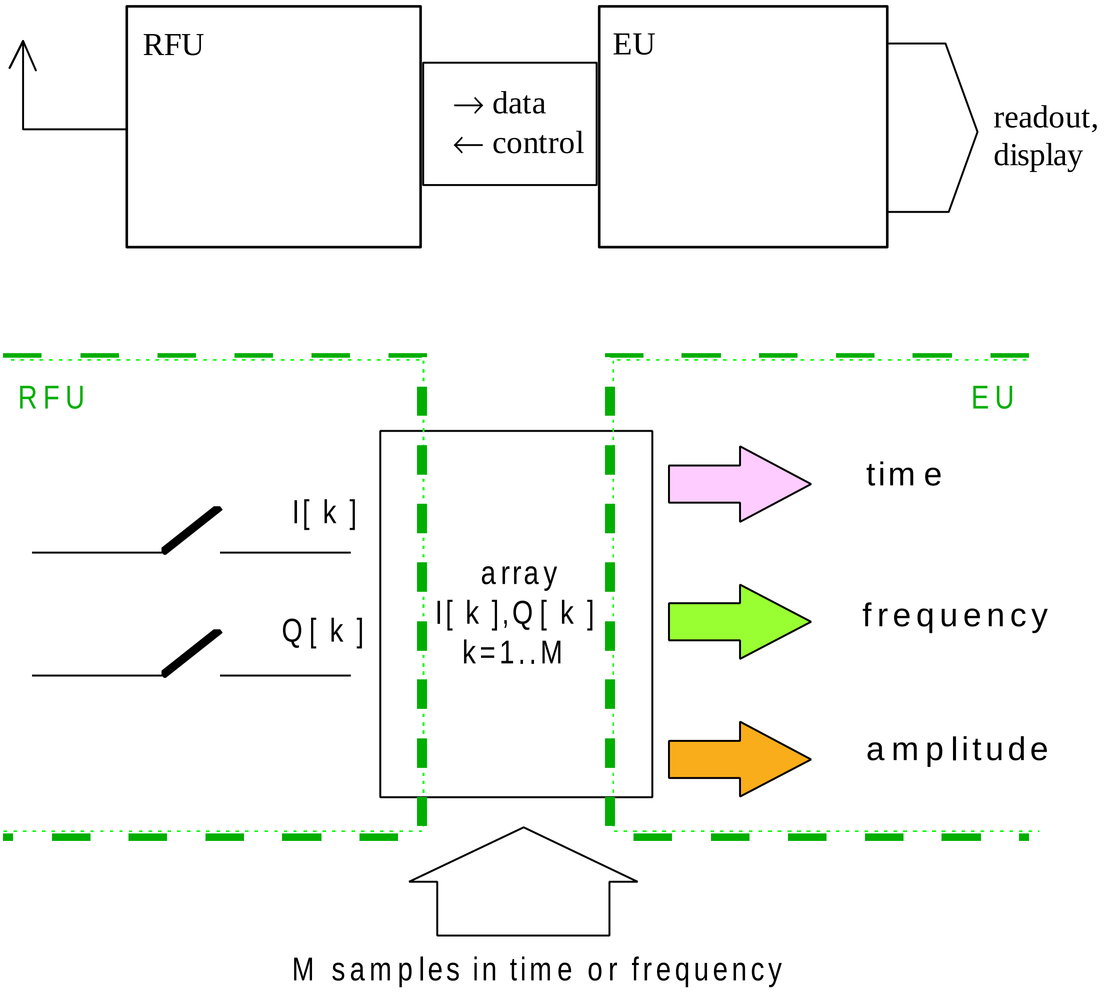

Figure 32: Interface between RFU and EU

The RFU yields the detected response in time or frequency domain.

The principle of the EU hardware (Figure 33) is almost identical for all methods of radio request. It consists of the memory buffer to convert the serial input data into the array of data. The calculation of the measurand is performed in a microcontroller, also capable for system control and interfacing the results to a display unit or to a data bus, e.g. via RS232, GPIB (IEEE 488), CAN bus for car applications, etc.

The effort, and the price of the EU mainly depends on the speed of signal processing. Applying data reduction processing, a very low cost solution based on a 2..5 $ Risc processor (e.g. PIC 16C...) was built in our laboratory.

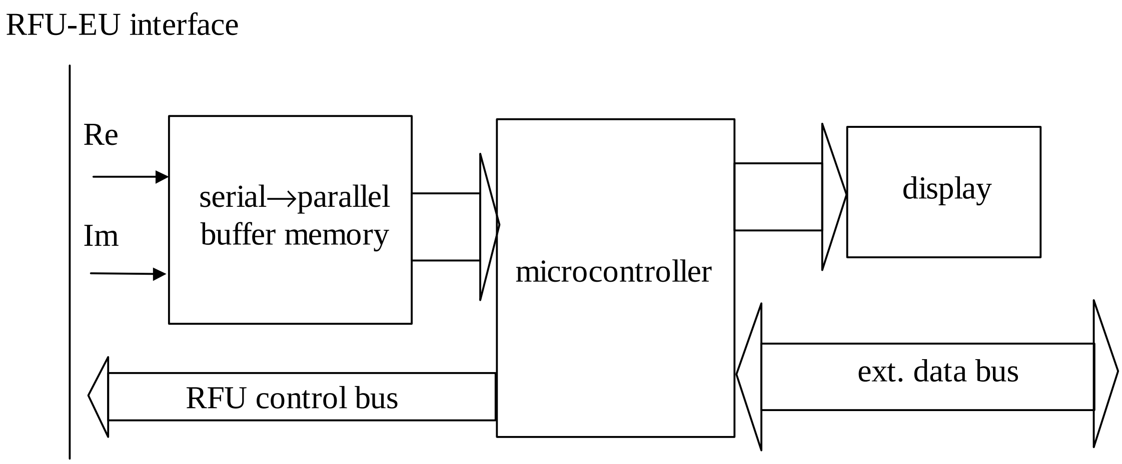

Figure 33: Block diagram of the EU: instead of real (Re) and imaginary part (Im) of the analog baseband signal, magnitude (Mag) and phase (Ph) can be delivered digitally from the RFU

Now, the RFU principles are discussed, providing the different methods of radio interrogation:

4.1.1 Time domain, full band sampling

For time domain sampling (TDS), (with TDD), resolution in time is achieved by a transmitted radio request signal, covering the total system bandwidth at once (full band). This signal could be a simple burst or an amplitude weighted burst to shape the signal in frequency domain and to keep the allowed bandwidth. Preferably the signal can be a spread spectrum signal, a chirp or e.g. a Barker code sequence. The spreading gain exploitable is limited by the maximum length of the radio request signal (to provide TDD between request and response) and the bandwidth of the sensor. For SAW DL sensors, to achieve low insertion loss, the bandwidth is approx. 10 MHz (for a 433 MHz device). Assuming a basic delay (until the first response signal occurs after request) of 1 to 4 µs for usual ID and sensor devices, a spreading gain of only approx. 6 dB is feasible (10 to 20 dB with special sensors).

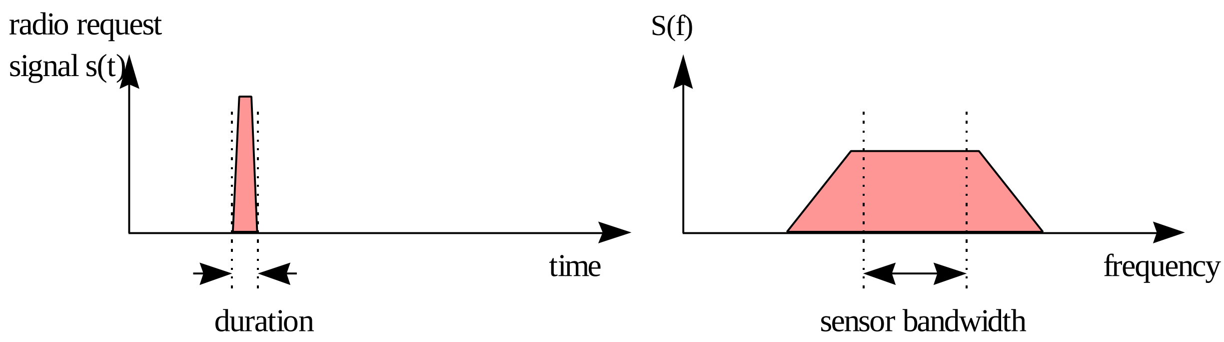

Figure 34: Full band sampling, TDS with burst signals

To gain full information from the sensor, the request signal's bandwidth (with "flat top" = constant power density) has to be wider (if allowed) than the sensor bandwidth. Then, the sensor impulse response is measured or, at least it can be calculated, if the condition "flat top" is not fulfilled.

It has to be noted, that if the RF bandwidth of the sensor limits the total RF bandwidth asymmetrically (e.g. due to the measurand), during coherent demodulation a residual frequency occurs due to the different center frequency of the received response signal and the frequency of the local reference oscillator. This yields distortion of the detected signals and complicates the data evaluation.

The radio sensor responds to each radio request signal with one (e.g. single resonator) or a number of (e.g. DL) response signals. A wideband detection and sampling of the response signal is performed in the receiver (Figure 35).

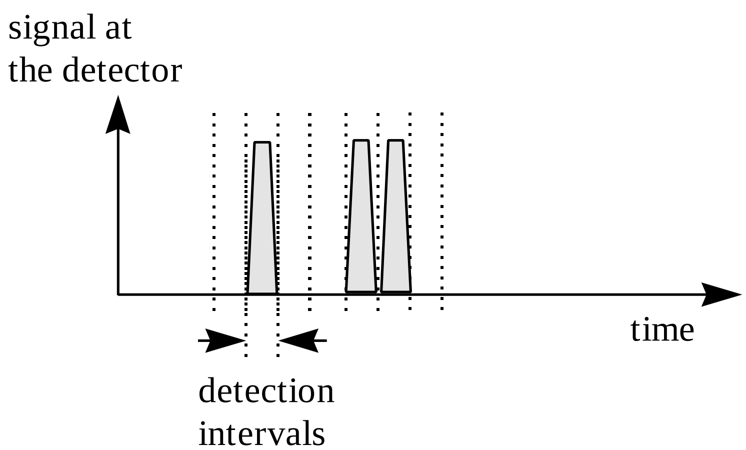

Figure 35: Signals in the receiver

For the interrogation of a SAW DL, the bandwidth has to be high enough to distinguish the response signals from different reflector signals, i.e. to make these orthogonal in time (or orthogonal in frequency, if chirps have been transmitted).

Employing an ID tag, i.e. a delay line with a characteristic code, the response signal is the convolution of the request signal and the impulse response. Requested with a single burst, the tag responds with the code. On the other hand, a code matched radio request signal (i.e. the time inverse of the sensor impulse response) yields a compressed impulse as sensor response and, interrogating with another code yields the crosscorrelation of the request code and the time inverse response code. A lot of system solutions for a multiple access scenario are feasible as shown below and in [46].

Requesting resonators, the signal bandwidth has to be capable to excite the oscillation of all resonators to be interrogated.

TDS is a single scan measurement method, the whole sensor response can be recorded in one radio interrogation cycle. Wideband RF signal generation and high speed signal processing are necessary. Due to the wide bandwidth and the small spreading gain (due to the maximal request signal length) available, the energy contents of one scan is small [1]. The SNR at the detector, applied to estimation of the measurand, is enhanced by coherent integration (see chapter 4.4) at the expense of measurement speed. Smart data collection (selective non periodic sampling) yields a reduced effort in signal processing (chapter 4.3).

Usually, coherent demodulation of the received signal r(t) is performed for a number M of sample points t_m in time (Figure 36), i.e. the time discrete response (e.g. burst response) of the sensor to the request signal s(t) is evaluated.

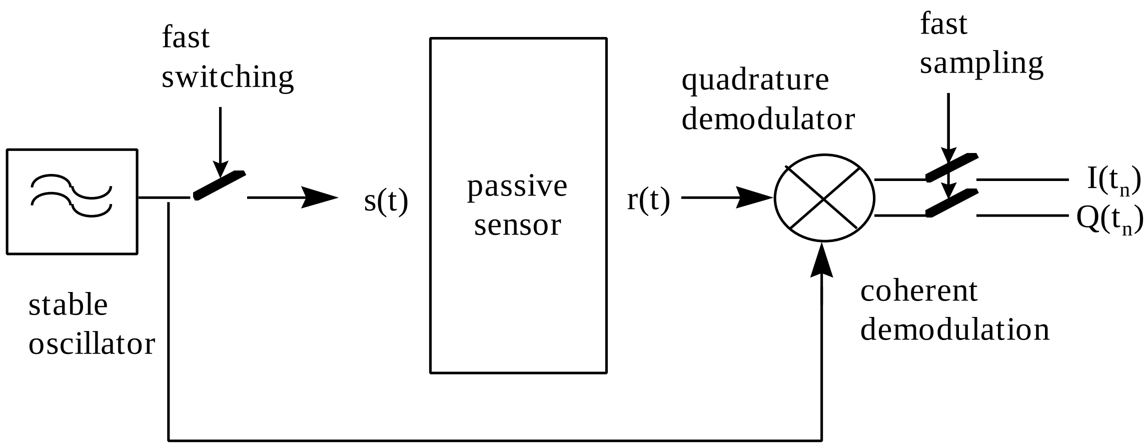

Figure 36: TDS / TDD RFU with quadrature demodulator

In Figure 37 the block diagram of an actual TDS system, built in our laboratory and applied to readout of passive sensors is drawn.

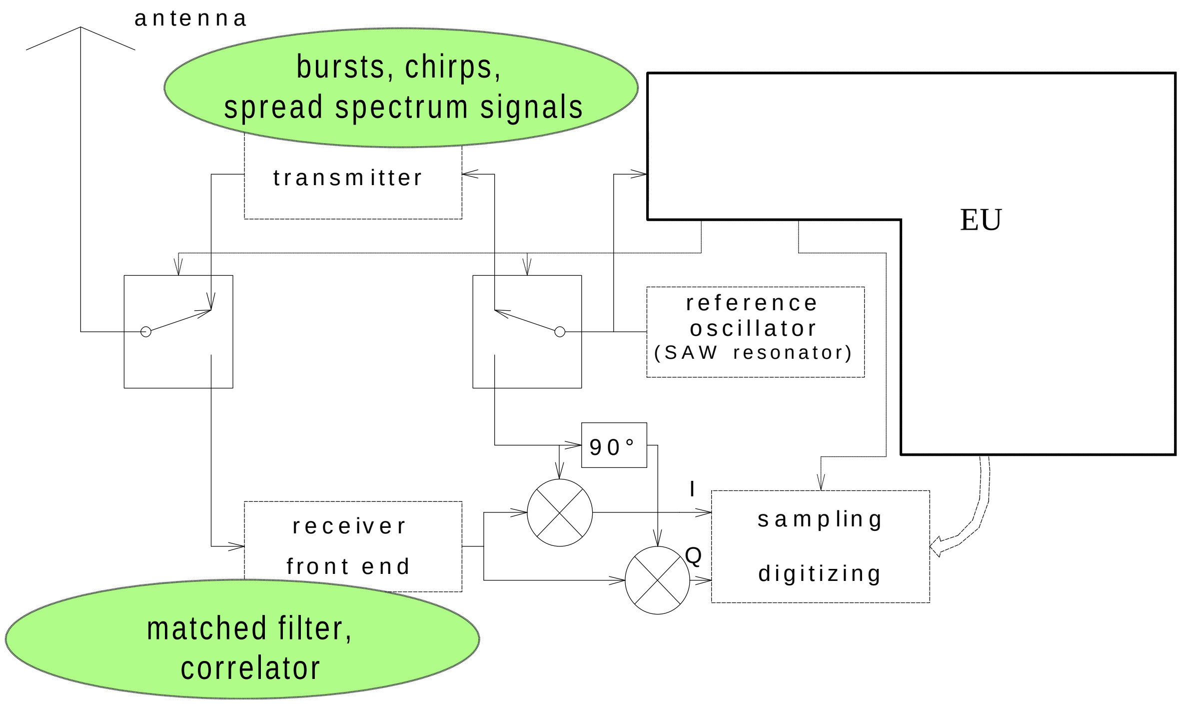

Figure 37: Block diagram of an actual TDS interrogation system

In another proven concept, the quadrature demodulator is replaced by a logarithmic amplifier with one output logarithmically proportional to the radio signal strength (RSSI) and a limiter output with true phase transfer from the input signal. Then, the magnitude (Mag) is measured (sampled) directly, the phase (Ph) is evaluated by a digital phase discriminator.

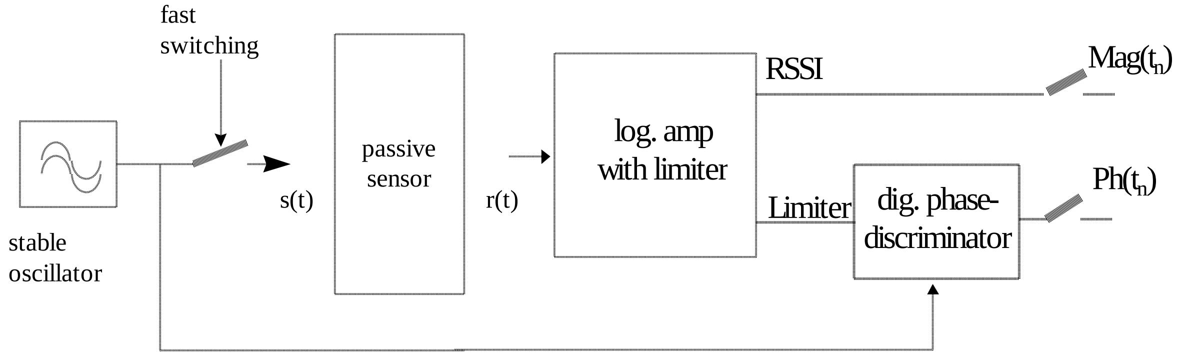

Figure 38: TDS / TDD RFU with logarithmic amplifier receiver concept

Due to the fast response of the logarithmic receiver for RSSI, the system is capable to operate without additional gain control with a typical input signal's dynamic range of up to 100 dB.

At sampling, attention has to be paid to the effect of the convolution of the sampling window with the signal. Of course, the sampling theorem applies, the sampling has to be performed with at least twice the bandwidth of the baseband signals.

4.1.2 Frequency domain sampling

Time and frequency domain can be transformed into each other by (discrete or fast) Fourier transform (FFT) and the inverse (IFFT).

Frequency domain sampling (FDS) or partial band sampling means successive scanning of the total bandwidth step by step in the frequency domain. As performed in a vector network analyzer, the sensor response is measured for a number M of request center frequencies f_m.

To achieve high resolution, M has to be high and the bandwidth of each step at f_i must be low. Therefore a relative long duration of the request signal and a long total measurement time are required, on the other hand, the total energy for detection is enhanced. The principle of FDS is discussed in [1] and sketched in Figure 39.

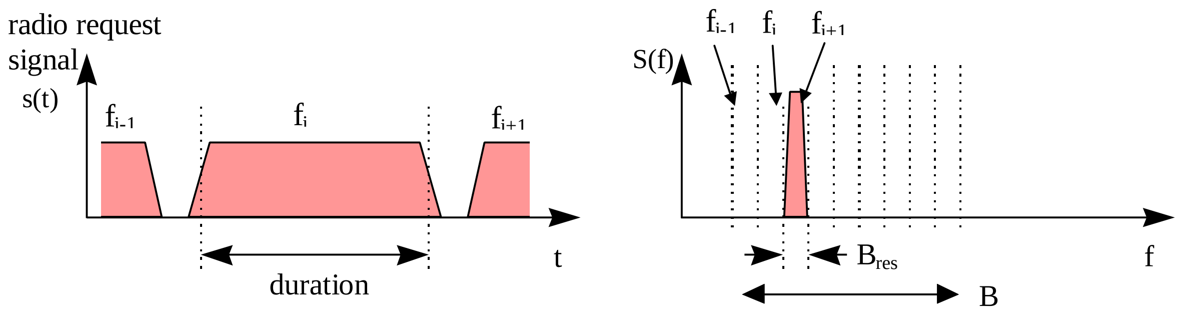

Figure 39: FDS / TDD, partial band sampling

In Figure 40, the RFU of a FDS / TDD system is sketched. As for the TDS system (Figure 36), the RF signals preferably are derived from one oscillator to allow coherent demodulation.

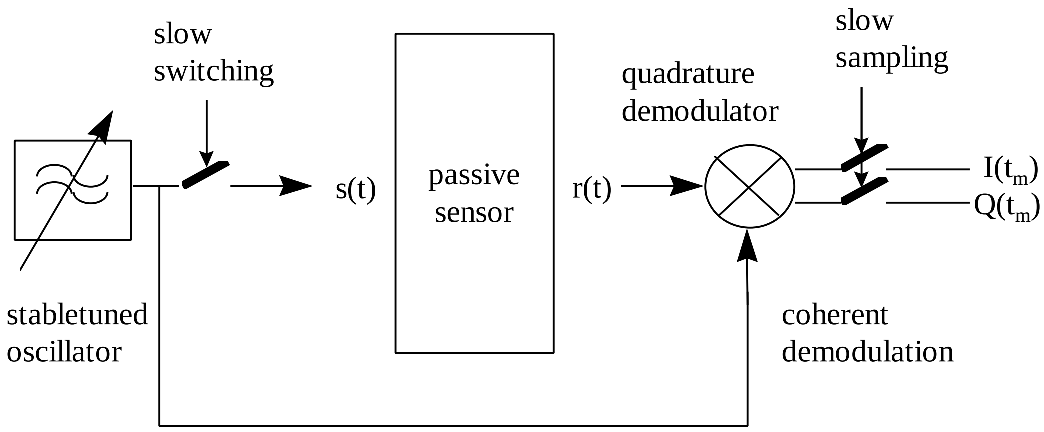

Figure 40: FDS / TDD transmitter and receiver principle

As for the TDS system a logarithmic amplifier with limiter output can be employed here.

In

Figure 41 a block diagram of a FDS system is sketched. As discussed above, the operation is very similar to that of a vector network analyzer (VNWA) for S11 measurements with time gating. Controlled by the EU the oscillator is tuned to the frequency f_i. In time domain division (TDD) between request and response detection, the frequency selective response is measured. The time gating can be done by a transmit /receive (T/R) switch or by software. Then, the T/R switched is replaced by a coupler, as applied in a VNWA. The output of the receiver delivers real and imaginary part, or magnitude and phase, of the reflected response signal. To gain the information for the present frequency f_i, sampling and digitizing is performed.

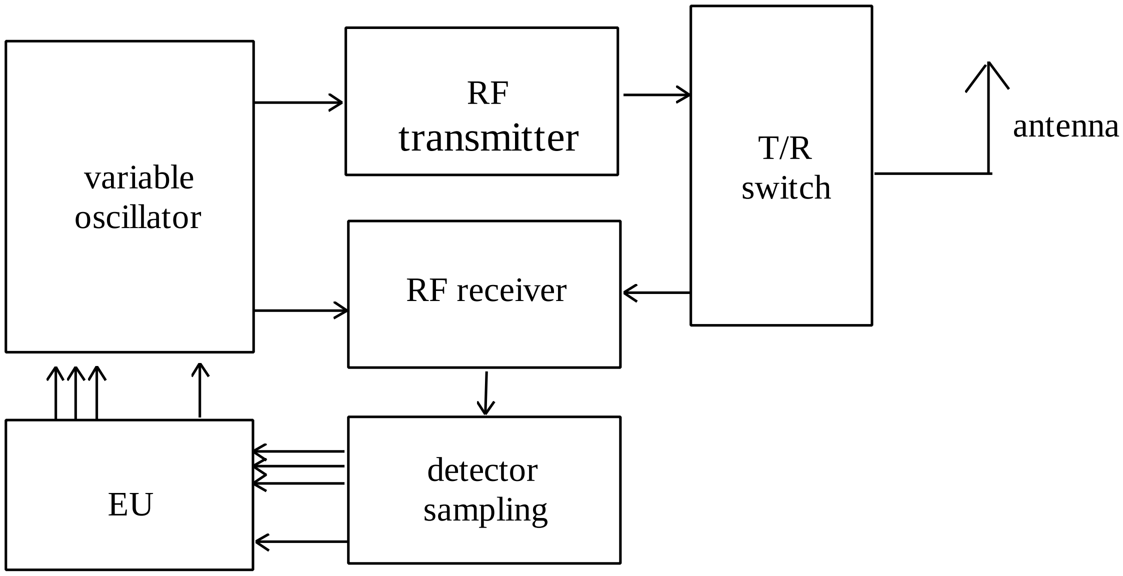

Figure 41: Block diagram of a FDS / TDD interrogation system

The output array of inphase I(1...M) and quadrature Q(1...M) signals contains the real and imaginary part of the time gated reflection coefficient versus frequency f_i, with i=1 to M. If the logarithmic receiver is employed, the data array contains magnitude and phase versus frequency. The time response can be calculated by IFFT.

FDS is a multi-scan measurement. To gain the information of a number of M points in time, M frequencies have to be scanned. The total measurement lasts in minimum M times one measurement cycle of TDS. Simultaneously, the RF energy for one interrogation and therefore the distance range or the reliability of the measurement (due to the enhanced total SNR) are high. Employing the method for an N-bit ID application requires at least M=N sampled frequencies, enlarging the required interrogation time by a factor N compared to a TDS set.

A special derivative of a FDS / TDD system has been invented by the author:

In order to find a principle for a radio interrogation system for high-Q resonators without high signal processing effort, the principle of the phase synchronization in PAL color TV has been employed. Figure 42 gives the block diagram of this system. A wirelessly closed, gated phase locked loop (GPLL) locks the local oscillator to the radio response signal of a decaying resonator sensor. Thus, after acquisition, the local oscillator of the system tracks the frequency of the resonator. A simple frequency counter is employed as display unit for the frequency and the measurand.

Since the loop is not continuously closed but operated in TDD, different distances between the interrogator and the sensor yield errors only when the distance is varied, i.e. the sensor is moved in radial direction with velocity v_r. Since a movement for one wavelength corresponds to a phase shift of 2π, a radial movement correspondents to an error frequency f_e in the PLL of $f_e = v_r / \lambda$, or analog to a Doppler shift $f_e = f_0 \cdot (v_r/c)$, with f_0 the PLL center frequency, and c the velocity of light.

Without movement, only the absolute phase of the received signal is shifted, not affecting the loop after acquisition.

The principle has been evaluated by an experimental setup, the results have been published in [45].

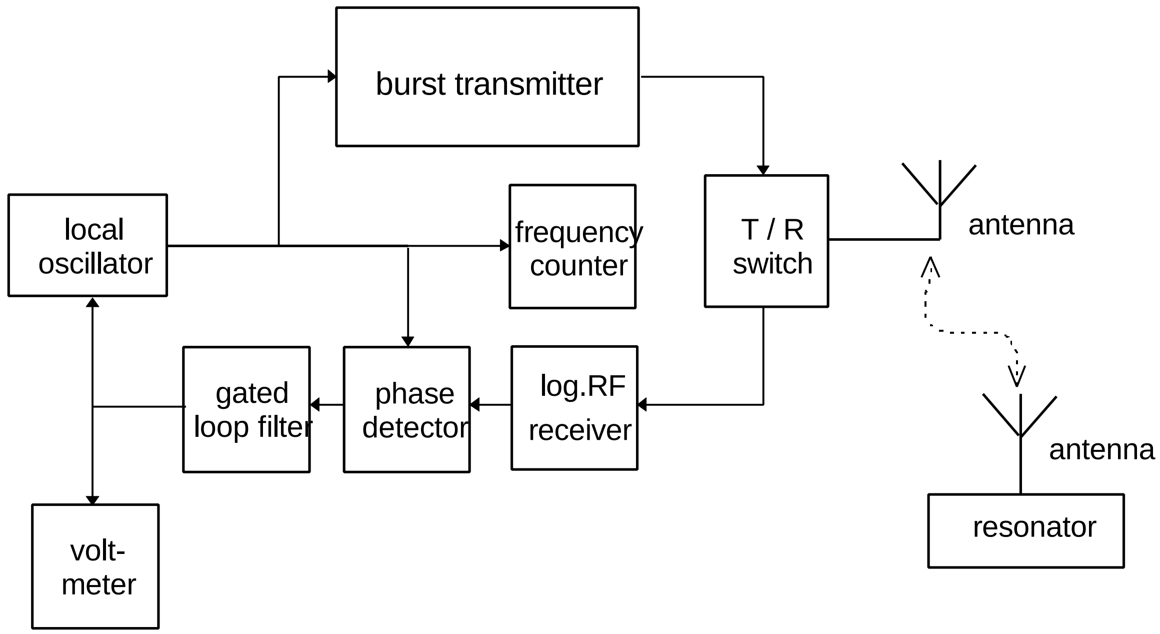

Figure 42: Block diagram of a GPLL self locking FDS system for wireless radio interrogation of resonant devices [45]

Apart from the GPLL circuit, a logarithmic amplifier is employed to linearize the exponential decay of the resonator signal. As display unit, a frequency counter, measuring the frequency of the local oscillator, and a simple panel voltmeter, measuring the loop control voltage have been used. A gated loop filter, employed to suppress drift effects and to facilitate the periodical phase acquisition is described in [45].

Compared to other methods, the advantage of the system discussed above is, that no EU and no microcontroller are necessary, of course at the expense of additional analog circuits. The most important disadvantage is the SNR (approx. > 10 dB) required for reliable acquisition and tracking.

In the introduction, FDD was mentioned to be applicable almost without exception for non linear sensors. A FDS system with FDD for separation of radio request and sensor response for linear sensor devices is employed in FM-CW Radar. The request signal is a linear or nonlinear frequency modulated (FM) continuous wave (CW). The received time delayed response signals are thus shifted in frequency (Figure 43), depending on the dispersion coefficient of the modulation $\mu = B/T$ and the distance. As applied for Radar distance measurements, the request signal is multiplied with the response received. From the frequency difference Δf between the transmitted signal and one individual response the respective propagation delay ΔT is calculated with $\Delta T = \Delta f / \mu$. In actual systems, the information of propagation delay of reflected signals is gained from an FFT of the low pass filtered demodulation product. The applicability to passive DL sensor systems is limited by the necessary large dynamic range of the receiver and the insertion loss of the, e.g. SAW, delay lines. Since instantaneous transmission and reception is required, the T/R switch is replaced by a T/R coupler or a circulator like in microwave Radar systems.

Figure 43 shows the block diagram of a FM-CW interrogation system.

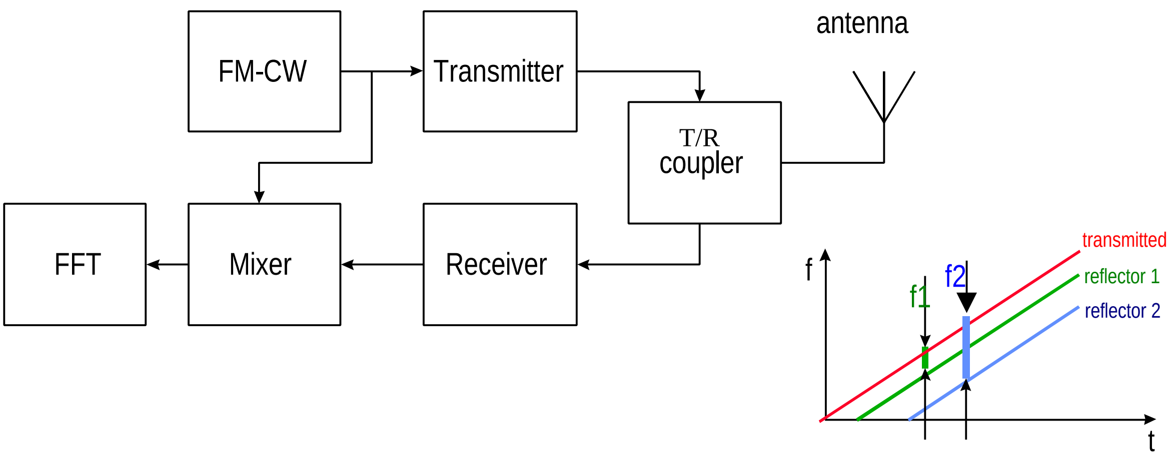

Figure 43: Block diagram of FM-CW Radar system for FDS / FDD

Data reduction is achieved by a model based parameter estimation of the transfer function of known sensors. A new method, utilizing frequency selective mutual cancellation of the response signals originating from two adjacent reflectors of one sensor, was invented by the author, and has been experimentally verified and was published in [47]. The used hardware is similar to that shown in

Figure 41. Principle and performance are discussed in chapter 4.3.2.

If no energy storage is feasible in a sensor, radio request and measurement have to be performed simultaneously as shown in the introduction and the following circuits:

4.1.3 Frequency domain sampling with frequency domain division for non linear passive sensors

Nonlinear passive radio sensors generate harmonic signals or cross modulation products. They are interrogated with an RF signal within a bandwidth B_t, centered at f_t. At the same time the response signal is detected at f_r with bandwidth B_r. Therefore, the interrogation is performed as a (continuous) FDS of the sensor response with FDD between request and response.

Figure 44 shows a block diagram of such an interrogator. As discussed above, no T/R switch and absolutely no fast signal processing is necessary. Choosing appropriate frequencies, the requirements to the receiver band pass and its dynamic range, etc., are designed.

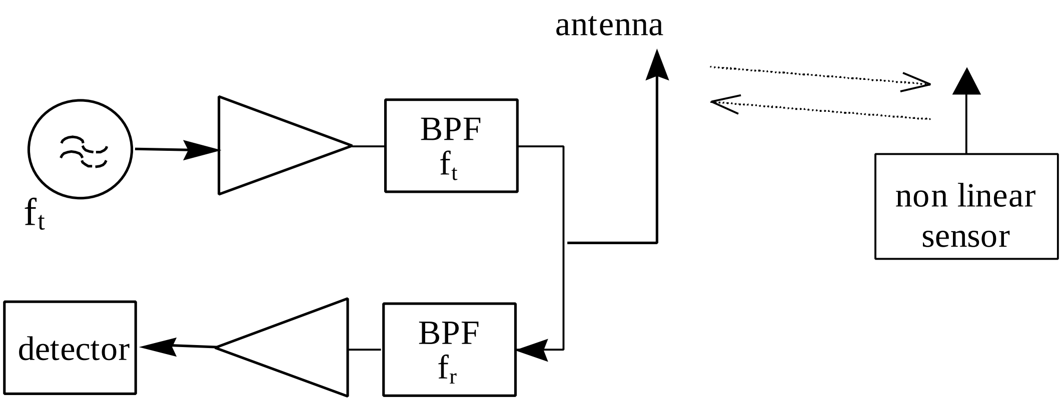

Figure 44: Block diagram of a radio interrogation system with single tone modulation for non linear passive sensors (harmonic sensors $f_r=2f_t$)

Radio request of mixer sensors requires two RF signals in the transmitter (dual tone modulation) and an AM demodulator in the receiver. The according block diagram is sketched in Figure 45. Directional couplers, or frequency duplexers, are used to combine f_1 and f_2 request signals and to separate transmit and receive path.

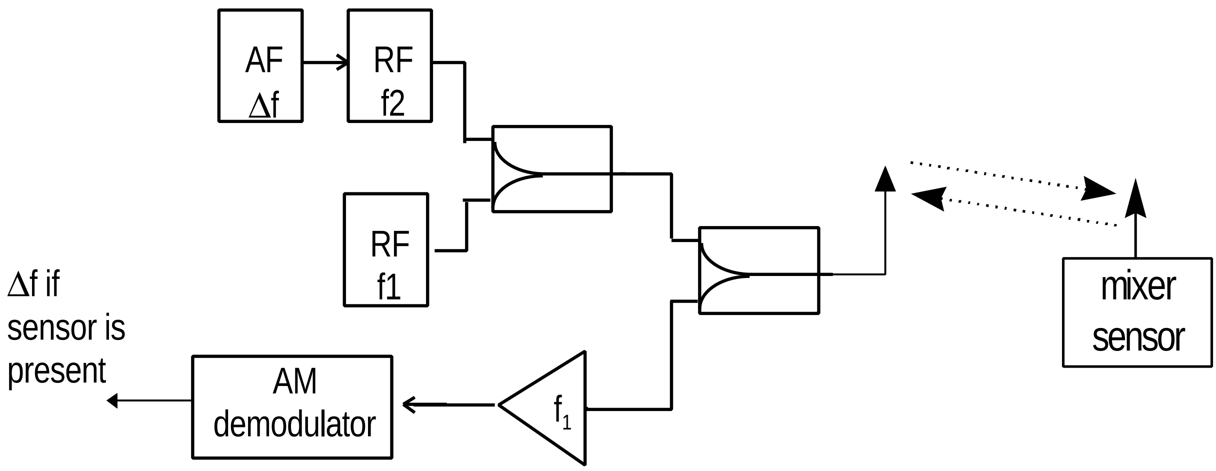

(or e.g. $2f_1$-f_2)

Figure 45: Radio interrogation unit for passive nonlinear sensors utilizing cross modulation

For sensor applications, the system sketched in Figure 45 is extended by a second AF modulation frequency in the transceiver and an FFT processor after the AM demodulator in the receiver. The FFT processor of course can be replaced by a filter bank with detectors.

4.1.4 Continuous Frequency domain sampling (CFDS) for linear devices

Linear, passive low-Q resonant sensors as shown in Figure 7 are interrogated in frequency domain by measuring the "dip" of energy due to a resonance circuit coupled to the sensor. The principle was widely used in the so called "Grid dip Meters" a lot of years ago. The (LC-) resonator of an oscillator circuit was near field coupled to the resonant device under test (DUT), e.g. an antenna. Then, the oscillator was tuned manually and the anode- or collector-current (I_C) was monitored. If the oscillator's frequency was equal to the resonance of the DUT, the resonant energy flow was observed by a current change.
Applying low-Q resonators (afflicted with losses) for one bit ID purposes, the presence of sensors in the near field of "antennas" can be detected monitoring the supply current of the oscillator (Figure 46). The system scans the frequency range (CFDS) and measures instantaneously e.g. the supply current. From the characteristic of the current versus frequency, the approximate resonance frequency of sensors can be found. To find sensors with a well known resonance frequency (as for theft detection), the oscillator can be fix tuned to that

frequency.

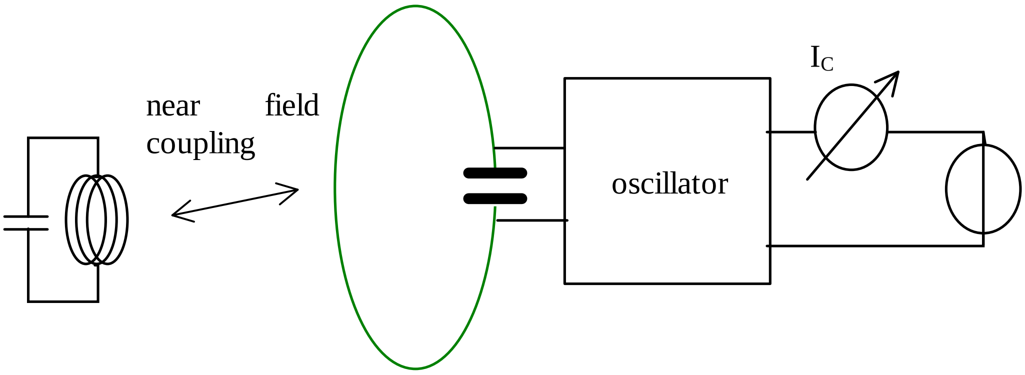

Figure 46: One-bit ID system with low-Q resonators

Measurement of the reflection coefficient S11 utilizing a VNWA can be applied also. Nevertheless, due to the low Q factor (or the wide bandwidth of the resonator), the resolution of a conceivable measurement is rather poor. The sensor principle is applied for one-bit ID detection only. Also it has to be kept in mind, that the principle is usable only with a sensor closely coupled (in the near field) to the interrogation antenna.

4.2 Evaluation of measurand

The measurand is evaluated from parameters of the RF response signals, applying the known sensitivity of e.g. delay for temperature. The parameters are time delay, frequency or phase difference, they have to be measured, or estimated, in the interrogator.

In most systems, the analog response signal r(t) is demodulated, sampled and digitized by an analog to digital converter (ADC). The (digital) data is included in the two column, M row array, mentioned above. The row number indicates the discrete time for TDS methods or the frequency (i.e. the center frequency of the measurement bandwidth) for FDS systems.

In Figure 47, the received response signal r(t) of a 3 bit DL and the time discrete inphase $U_I[n]$ and quadrature $U_Q[n]$ components of the complex valued coherent demodulator output are sketched versus time. A delay line sensor with response signals approx. at the sample positions 4, 8 and 16 has been interrogated with a TDS system. (The data also could originate from a FDS interrogator with frequency responses at 4, 8 and 16.)

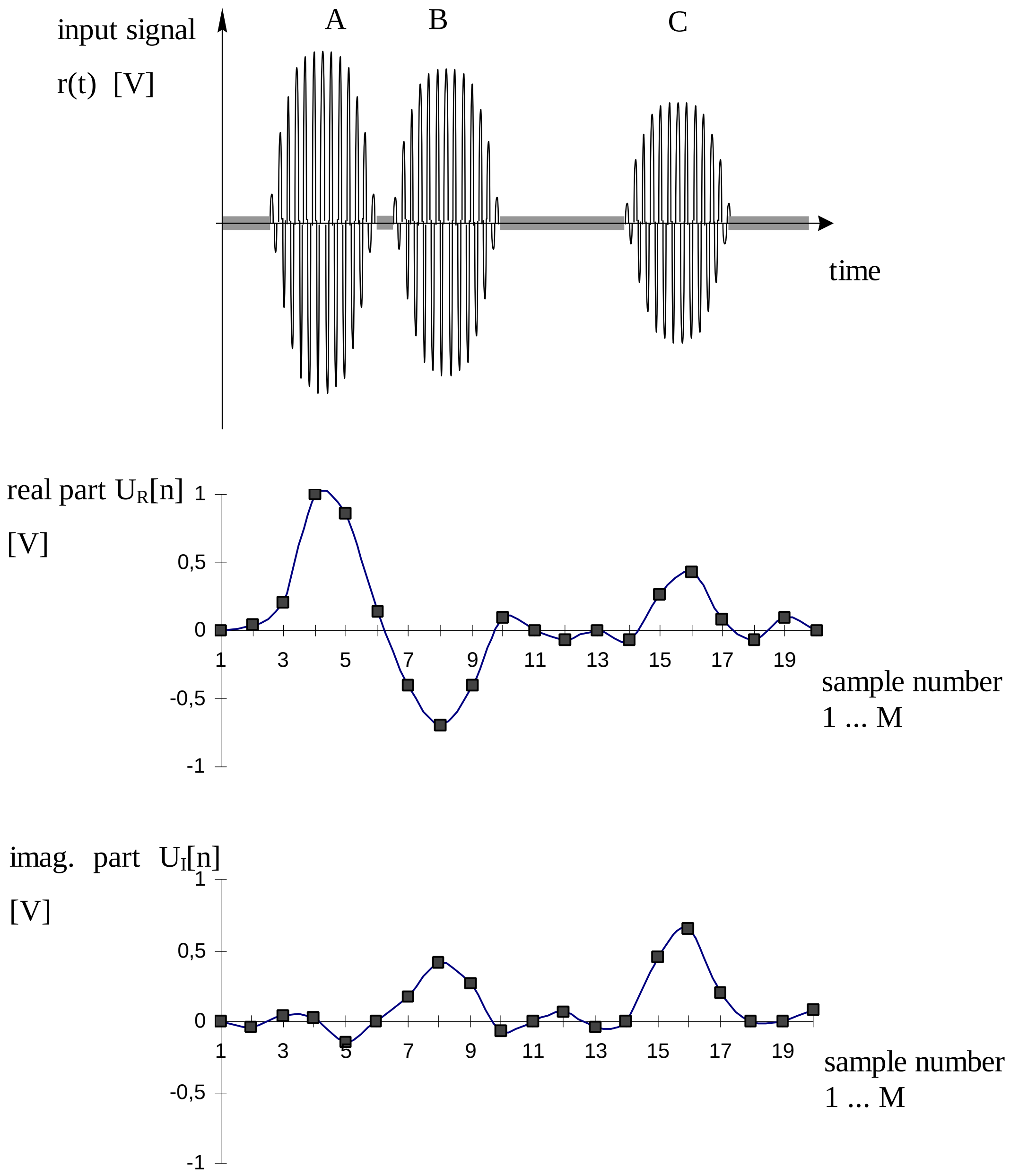

Figure 47: Received signal r(t) and time discrete real (I[n]) and imaginary (Q[n]) part of the demodulator output

4.2.1 Measurement of time

The measurement of time is performed for different purposes in different ways. We assume two impulses in the baseband or bursts in RF bandpass range with a time delay of $\Delta\tau$.

From the TDS data array, the time usually is estimated from a phase measurement.

Phase measurement

The response signal r(t) is coherently demodulated by multiplication with the orthogonal base signals cos(ωt) and sin(ωt) with an integration over a carrier period T:

$$I(t) = \int_0^T r(t) \cdot \cos(\omega t) dt \qquad (11)$$

$$Q(t) = \int_0^T r(t) \cdot \sin(\omega t) dt \qquad (12)$$

For actual implementations, the stable reference oscillator and a 90° shifted version are used as base signals. It is assumed, that the received signal consists of a number of band limited bursts (Figure 47: A, B, C) without dispersion but with linear phase. The phase $\theta_{r(t)}(t)$ of the received signal versus time and so the phase of each burst $\varphi_A(t)$, $\varphi_B(t)$, etc., referenced to the orthogonal base can be calculated from

$$\theta_{r(t)}(t) = \arctan\left(Q(t) \big/ I(t) \right) \qquad (13)$$

Further, it is assumed, that the phase of the response signal within the burst remains approximately constant, i.e. $\varphi_i(t)=\varphi_i$, (i = A, B, C, ...), which actually can be observed.

The orthogonal components of the base band signal are sampled $U(t = t_n) \rightarrow U[n]$ and digitized. The calculations are performed with the digital data, e.g. $\theta_{[n]}=\arctan(Q[n]/I[n])$, afflicted with the additional digitization error (see appendix 2).

To compensate the measurement for the (changing) propagation distance and other electrical delays, usually the phase difference between the response bursts is employed.

In Figure 48, the principle of time measurement by phase detection for DL sensor purposes is drawn:

The bursts A and B are detected with a phase of φ_A and φ_B. The phase interval is assumed to be $\{0 \ldots 2\pi\}$. The phase shift $\Delta\varphi$ corresponds to a time delay Δt

$$\Delta t = \frac{\Delta\varphi}{2\pi \cdot f_c} , \qquad (14)$$

with carrier center frequency f_c. For a 433 MHz RF carrier frequency, a period length is approx. 2.3 ns. A phase resolution of only $\pi/6$ yields a resolution in time of 0.19 ns. This resolution never can be attained by determination of burst maximum with $|r(t)|$, i.e. envelope, alone.

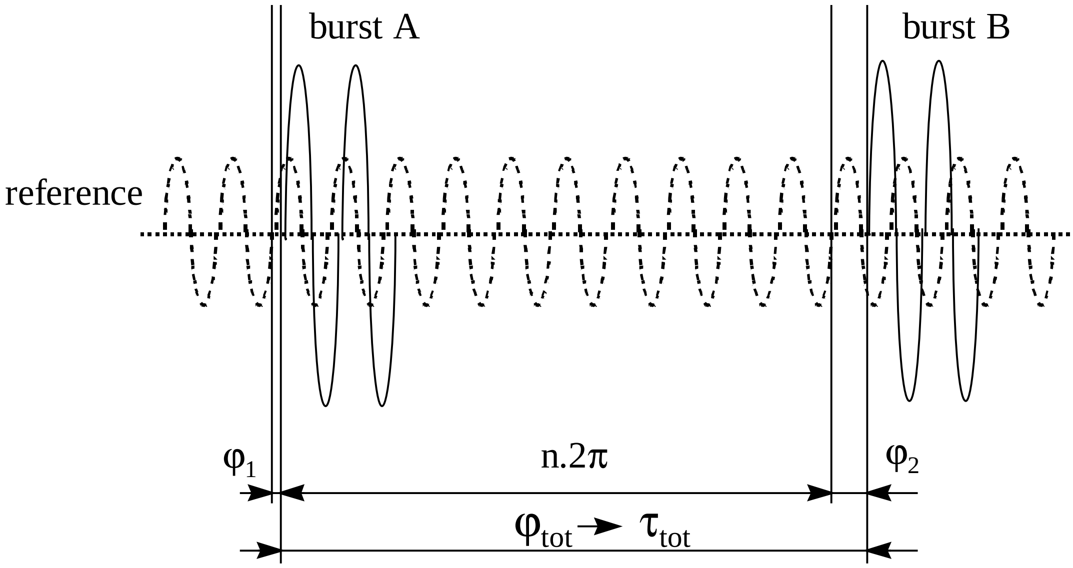

Figure 48: Phase detection for time measurement, stable carrier dashed

In Figure 48, an ambiguity can be observed for a phase shift > 2π. The factor n has to be measured utilizing other methods, it also can be estimated from a third delay position in a geometrically fixed ratio. With n, the total phase φ_{tot} is calculated from

$$\varphi_{tot} = (\varphi_2 - \varphi_1) + 2n\pi. \qquad (15)$$

Then, the total delay τ_{tot} is

$$\tau_{tot} = \frac{\varphi_{tot}}{2\pi \cdot f_c}. \qquad (16)$$

The time measurement for DL sensors by phase detection was developed by our group to technical maturity and is the commonly employed method in today's SAW radio sensor systems. Applying coherent phase detection instead of envelope delay evaluation, the relative resolution for a 3 µs sensor delay interval is enhanced from 10^{-3} to 10^{-6}.

As an example in Figure 49 the measurement readout is shown for a $LiNbO_3$ temperature sensor with a 5 µs delay. In the first part (a) of the graph, keeping temperature constant, envelope detection was executed only, the resolution of temperature was poor, approx. 10 K. Then, the system was switched to coherent mode with phase evaluation (b), yielding a temperature resolution of less than 0.1 K. In this mode a three step heating of the monitored oven was measured. From the enlarged part of the graph around 103 °C the actual resolution can be observed to be approx. 0.01 to 0.02 K. The steps of heating up and cooling down of the thermo-chamber by the control circuit to keep the specified temperature error less than 0.5 K can be seen.

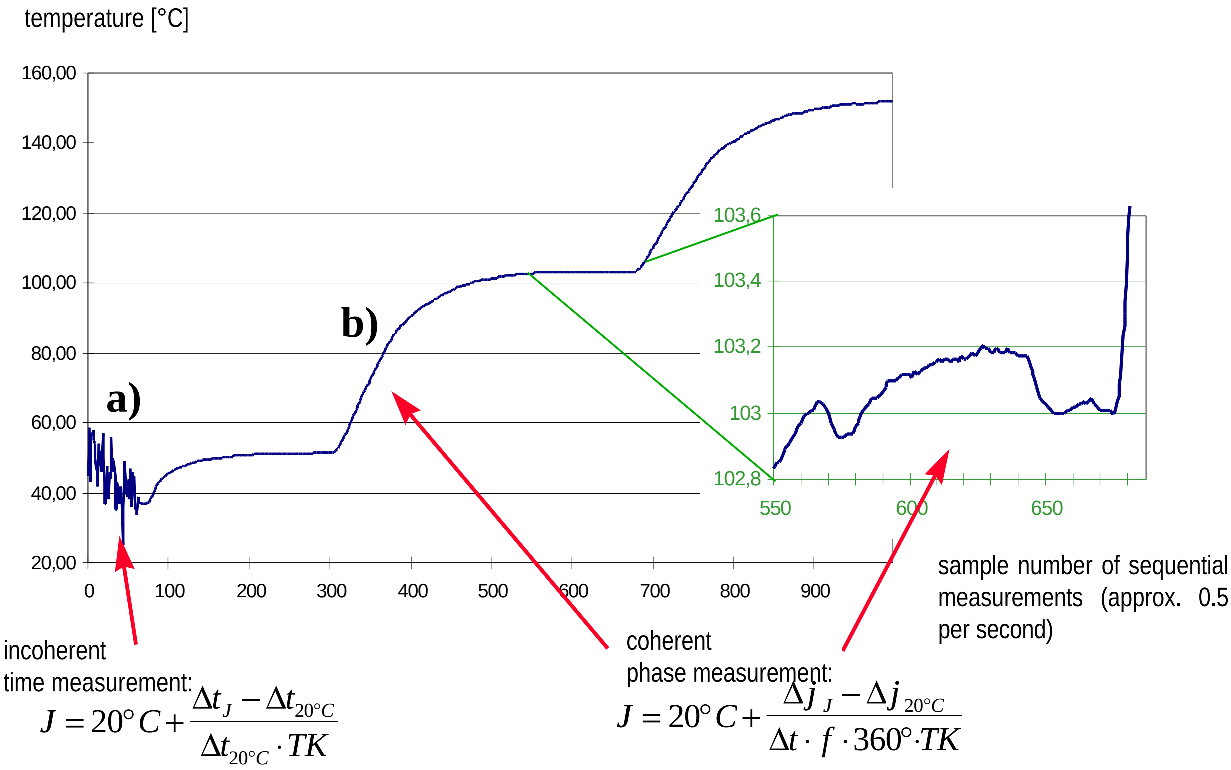

Figure 49: Readout of a temperature measurement system utilizing $LiNbO_3$ SAW delay line sensors ($\Delta\tau$ = 5 µs), with a) envelope delay detection and b) phase evaluation

First moment

From the digital data array, the mean delay, the first moment of the response burst can be calculated easily. This method of course is limited by the sampling rate too. We apply it for coarse measurement of delay and for acquisition of phase. The resolution achieved mainly depends on the SNR of the analog signal, in our applications we attained a resolution of approx. a tenth of the sample period.

IFFT of the frequency discrete frequency response S11(w)

Employing FDS, the time domain response can be calculated employing a discrete Fourier transform algorithm.

The transform is done with equ. (17), the well known discrete Fourier transform and with equ. (18), the inverse discrete Fourier transform [48].

$$S_d[k] = \sum_{n=0}^{M-1} s_d[n] \cdot e^{-j\frac{2\pi nk}{M}}, \qquad \text{for } k = 0 \ldots M-1 \qquad (17)$$

$$s_d[n] = \frac{1}{M} \cdot \sum_{k=0}^{M-1} S_d[k] \cdot e^{j\frac{2\pi nk}{M}}, \qquad \text{for } n = 0 \ldots M-1 \qquad (18)$$

The result of the transform is periodical in time ($s_d[n]$) or frequency ($S_d[k]$) domain, with a period of M points. The period is divided into M divisions, the resolution is 1/M. The resolution in time achieved by an inverse discrete Fourier transform (or an Inverse Fast Fourier Transform IFFT) is 1/B with B the total bandwidth (e.g. sampled by the FDS). An enhancement of the resolution is achieved e.g. with zero stuffing. So, for the band limited signal a higher sample rate is simulated, the additional samples are set to zero, providing no additional errors in the observed interval but less energy per sample in the domain transformed to. DFT and the inverse DFT deliver periodical discrete signal information in time or frequency domain. Information between the samples has to be interpolated if required.

Notch determination

A model based parameter estimation for, e.g., a two bit delay line applied for radio sensor purposes is discussed in [47] and chapter 4.3.2.

Especially if high speed sampling and fast and consequently expensive data processing has to be avoided, methods are employed, to evaluate the demodulated analog base band signal:

Counter

The simplest method for the measurement of time between a start and a stop signal is to count the periods of a high frequency reference in the interval. The actual problems arise, looking for these trigger signals. A noisy signal causes phase jitter when observed for threshold crossing, changing maximum amplitudes of band limited signals yields additional errors. To find the time of the peak voltage (if no ambiguity exists), a peak detector with a differentiation (high pass filter) and a threshold detector is used. To avoid errors from noise during time intervals with low signal strength, the system has to be controlled by an amplitude detector. The upper boundary of resolution in time is given by the inverse RF reference frequency, e.g. it is 1 ns for a 1 GHz clock. It is trivial that the relative error increases for a smaller total delay.

Time to voltage converter

An analog method of time measurement, applied in dual slope ADCs and Austrian police's Laser vehicle speed observation sets, is the analog conversion of time into a voltage: With start and stop impulse, gained with the problems discussed above, an electrical constant current source is switched on and off. An integrator (a capacitor) summarizes the charge and yields an output voltage increasing with time, afterwards sampled and digitized in a low speed signal processing unit. The resolution is limited by the speed of amplitude rise, the hold drift and the resolution of the digitizing unit, etc.

Time to digital converter

Integrated silicon time to digital converters (TDCs) are available from stock [49]. The time between the trigger impulses is compared to a logic gate delay. A high resolution of currently approx. 50 ps is feasible with this devices, the readout is provided by a parallel digital data bus. TDCs also can be applied to a digital phase and frequency measurements. For frequency measurements, the period length is measured. For a digital phase discriminator the reference is fed into the start, the input signal into the stop input. The time between zero crossing and therefore the phase is delivered as digital data word.

Time to frequency conversion - FM CW

See Figure 43.

4.2.2 Measurement of frequency

In general, we deal with short time signals, here. Definition of frequency may not be feasible. Then, the instantaneous frequency, $d\varphi/dt$ can be applied only.

As for the time delay, the measurement of frequency preferably is performed from the digital data array discussed above. For discussion we assume a high-Q resonator as radio sensor. Here, a response signal with an exponential decreasing spectral density centered at the resonance frequency can be observed for e.g. 10 µs, i.e. for at least 5000 periods.

FFT of the time discrete response r[n] = I[n] +jQ[n]

Applying TDS, the response signal is sampled for the time of decay. To enhance the FFT resolution in frequency, zeros are stuffed yielding an enhanced resolution at the expense of signal energy. Then, the discrete spectrum is calculated. As discussed above, the resolution depends on the number of points during the total time interval. FFT usually is applied to test systems, if a digital storage oscilloscope is used as ADC and FFT processor.

Time domain sampling and parameter fitting

The response signal is sampled by a TDS system. Then, by parameter fitting, the signal is matched to an estimated exponential decay of the resonator with a time constant τ and a center frequency f_c. The mean square error is minimized. The principle is successfully employed in actual radio sensor applications [50].

For some applications as well as for the measurement of time and phase, analog frequency measurement methods are employed:

Measurement of time between zero crossings

The duration of one or a few periods is measured, utilizing the methods discussed in 4.2.1.

Measurement of periods within a reference period

Applying a counter, within a gate time the number of zero crossings is detected. Since the gate time is rather short, e.g. 10 µs for a decaying resonator, the resolution achieved is very poor for passive resonators.

Gated phase locked loop (GPLL)

Like discussed as a FDS method in chapter 4.1.2 and shown in Figure 42, the frequency of a sensor response, e.g. shown in Figure 31, advantageously is measured by a gated phase locked loop (GPLL) [45], [51].

4.2.3 Measurement of amplitude

Since amplitude is influenced strongly by the radio transmission, apart from the detection of absorption due to low-Q resonators, in passive radio sensor applications, it is used rarely. Today amplitude only is evaluated for readout of the indirectly affected SAW transponders (see chapter 3.3.1).

In time domain, the signal is sampled with a rate fulfilling the sampling theorem (in minimum twice the signal's bandwidth), or asynchronously in proper time slots (chapter 4.3.1). As shown in the appendix 2, the ratio of signal and self provided ADC noise is enhanced for approx. 6 dB / Bit. As employed for digital storage oscilloscopes, with e.g. oversampling and a sin(x)/x approximation, the envelope can be interpolated with good accuracy.

Employing FDS, the time amplitude in time domain is calculated from the result of an IFFT.

The deterministic error of amplitude measurement's resolution mainly is determined by deviations from linearity of the amplifiers in RF, IF and baseband frequency range, different gain factors in parallel base band channels, hold drift in sample / hold circuits and by errors in the ADC unit.

4.3 Data reduction methods

Opposite to the resonant sensors, where measurement time and collected data directly determine the performance of the measurement, for delay line interrogation the information can be extracted from a reduced quantity. Here both, TDS and FDS, data reduction is feasible, by neglecting time or frequency intervals containing no essential information.

4.3.1 Sampling on demand for TDS

The output of the coherent detector of a TDS system sketched in Figure 37 yields two base band signals I(t) and Q(t) for digitizing and digital signal processing. With a 1 MHz baseband bandwidth for a 433 MHz system (or >20 MHz for a 2.45 GHz set) and a total response interval length of 10 µs, at least 40 (or 800) samples have to be recorded. The analog to digital converters, the digital memory and the microcontroller have to be designed to fit this requirement in signal processing speed. On the other hand, only the phase difference between e.g. two response bursts are important. The required information can be gained from 4 samples only, i.e. 10 % of full sampling (or 0.5 % for the 2.45 GHz system).

Sampling on demand employs asynchronous sampling of the baseband channels for the time slots of interest only. The analog amplitudes of the response are pre-stored in e.g. 4 properly triggered sample/hold circuits, CCD devices, etc. Then, the contents of these circuits is read out and digitized sequentially by slow and therefore low cost devices. The signal processing effort for data collection is reduced by a factor 10. In Figure 50, the principle is sketched and a block diagram of the baseband unit of a TDS sampling on demand system is shown.

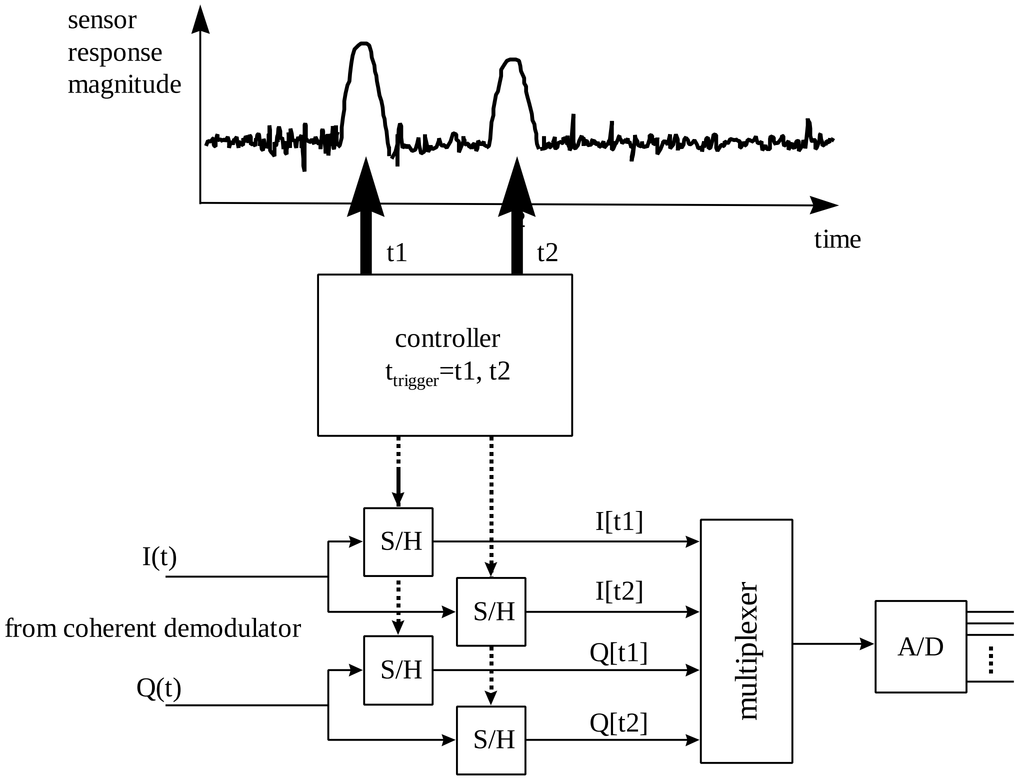

Figure 50: TDS sampling on demand

Employing the principle for low speed identification applications, only one time slot has to be sampled during one radio interrogation cycle, the M time slots are sequentially sampled within M radio interrogation periods, the signal processing effort is further reduced. Employing this methods we built low cost TDS radio request systems for SAW delay line sensors and ID tags.

The state of the art technology of systems utilized for radio interrogation of passive DL sensors is described in [52].

4.3.2 Reduced FDS - "Notch sensor" application

A model based parameter estimation e.g. for a two bit delay line, applied to radio sensor purposes has been invented by the author and was verified in our laboratory. It is discussed in [47]: The theory of a two path radio channel, characterized by frequency selective fading of the transmission function, is applied to radio sensors. A dual reflective wideband SAW delay line has the same impulse response h(t) and therefore the same transmission function H(ω) in frequency domain as the two path radio channel, the insertion loss of each reflector can be interpreted as the loss of the corresponding path. In Figure 51 the magnitude of the measured reflection coefficient $S_{11}(\omega)$ of a dual reflective delay line is sketched.

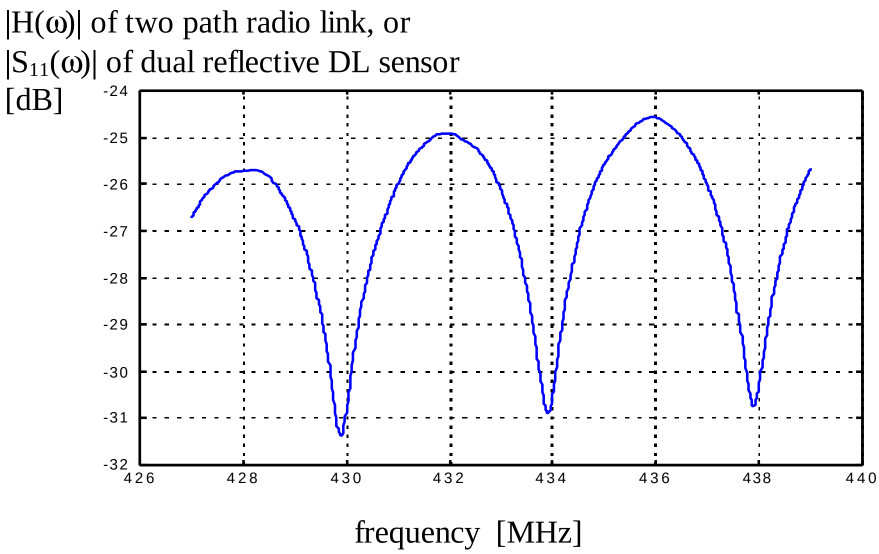

Figure 51: Measured reflection coefficient S11(ω) of a dual reflective delay line with constant insertion loss, (equal to the transmission function H(ω) of a two path radio channel with equal path attenuation)

The deep valleys (notches) occur periodically at frequencies

$$f_{notch} = (2k-1)\cdot 2\ MHz\ \Big|_{J=20°C} \qquad (19)$$

with k = 1, 2, ... (∞).

Employing FDS for delay line sensors with a known structure with U unknown parameters, only U samples are necessary in frequency domain. The parameters of the mentioned dual reflective delay line are:

1.) the amplitude ratio of the two signals arriving at the receiver via the two reflectors,
2.) the delay between the first and the second signal arriving and
3.) the frequency and therefore the phase shift for a delay

With a fixed amplitude ratio of 1, two samples are sufficient. Data reduction by a factor 20 is achieved, of course, at the expense of the robustness of the measurement.

Due to the FDS principle, only a few narrow band radio interrogation cycles are necessary. Enhanced resolution by phase measurement is included inherently in the principle.

As parameter, representative for the measurand, the position or the shift of one notch frequency can be evaluated. Assuming a wide band SAW delay line with two reflectors, a delay difference Δt and a temperature coefficient TK of the substrate, the temperature sensitivity $S^{\vartheta}_{\Delta f}$ and the absolute sensitivity $S_{notch,\vartheta}$ of the shift of the k-th notch at frequency f due to temperature is

$$S_{notch,\vartheta} = f \cdot S^{\vartheta}_{\Delta f} = \frac{-\Delta f}{\Delta\vartheta} = \frac{2k-1}{2 \cdot \Delta t} \cdot TK \cdot \frac{1}{1 + TK \cdot \Delta\vartheta} . \qquad (20)$$

In comparison to the time measurement, operating at the same center frequency f, the sensitivity is enhanced by a factor of

$$G_{S,n} = f \cdot \Delta t . \qquad (21)$$

The principle, the measurement parameters and an experimental verification of the method is given in the included publication [47]. Accuracy and unambiguity are mentioned there. Since the overlap of the two reflected impulses adjacent in time is evaluated here, in [47] the term inter symbol interference (ISI) is used. Of course, ISI originally was coined for digital data communications. In Figure 52 the actually measured position of one notch frequency is drawn versus the temperature affecting the sensor.

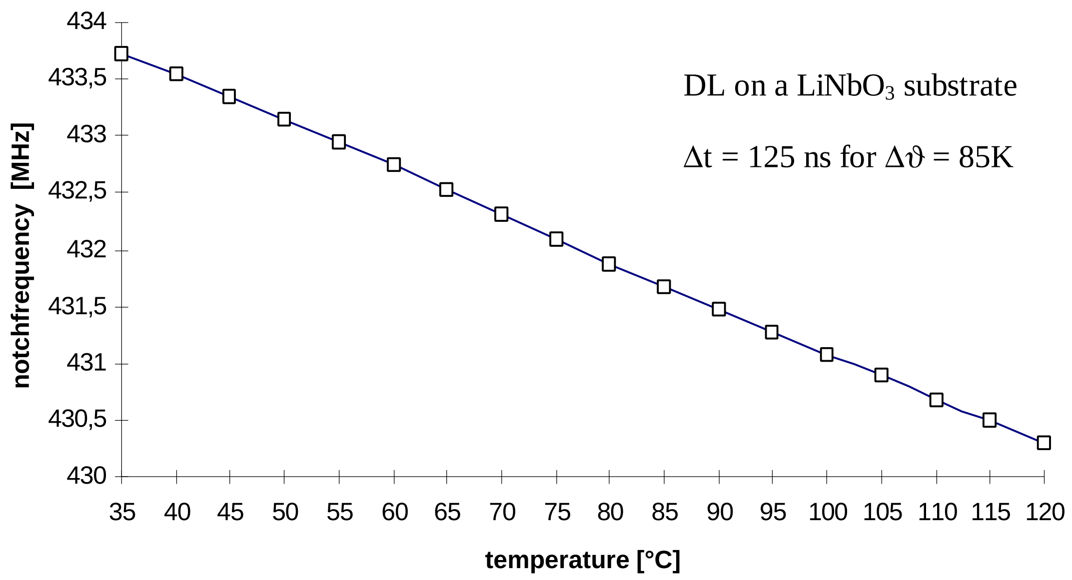

Figure 52: Notch frequency for a wideband delay line with two reflectors spaced by 125 ns versus temperature [47]

4.4 Signal integration methods

An essential advantage of passive wireless sensors is the lack of an on-board power supply. On the other hand, the retransmitted response is generated from the radio request signal. The same radio channel is passed two times, for request and response. Thus, for medium range applications with distances of 5 to 20 meters, the remaining energy of the received response signal decreases in minimum by the fourth power of distance and equally the ratio of signal power to noise added during transmission (SNR) decreases.

A severe problem is the (incoherent) co-channel interference from other radio communication systems, etc. Moreover, to obey national governmental regulations, the transmitted peak power of the sensor system is limited. The signal to interference ratio (SIR) cannot be enhanced arbitraryly. To achieve the required propability of correct signal detection and to keep the error limits, we need a sufficient SNR and SIR for decision.

We implemented integrative processing for radio request of passive SAW sensors. We discriminate between coherent and non-coherent integration:

Coherent integration is a linear operation, samples of signal amplitude $s_k(t)$ of different interrogation cycles are summed up with correct phase. The SNR, the ratio between signal and noise power, is increased by a factor N, the optimum for all integration methods. Coherent

integration is a well known method for signal energy enhancement in Radar and measurement technology.
Coherent integration and the achievable gain are discussed in [1], chapter 3.4.
If no correlation between signal and interference signal exists, coherent integration is also applicable for SIR enhancement. On the other hand, coherent feed through effects of the local oscillator within the radio interogation system cannot be coped with.

After nonlinear signal processing, e.g. incoherent demodulation, other, less effective integration methods can be implemented. Nonlinearity causes an irreversible correlation between signal and noise terms. The gain of nonlinear integration methods is expected to be smaller than that of coherent integration, a threshold effect occurs, similar to the AM threshold for non coherent detection [53]. A type of nonlinear integration is post-detection integration, where an average of a number of results is calculated after a nonlinear data decision. It only is effective above the SNR threshold mentioned above.
The errors due to coherent integration of non stationary measurands are discussed in the appendix A2.

4.5 Multiple access

The problem of multiple access, of the individual access of one interrogation system to a number of different passive radio sensors is discussed in [1], chapter 3.5.

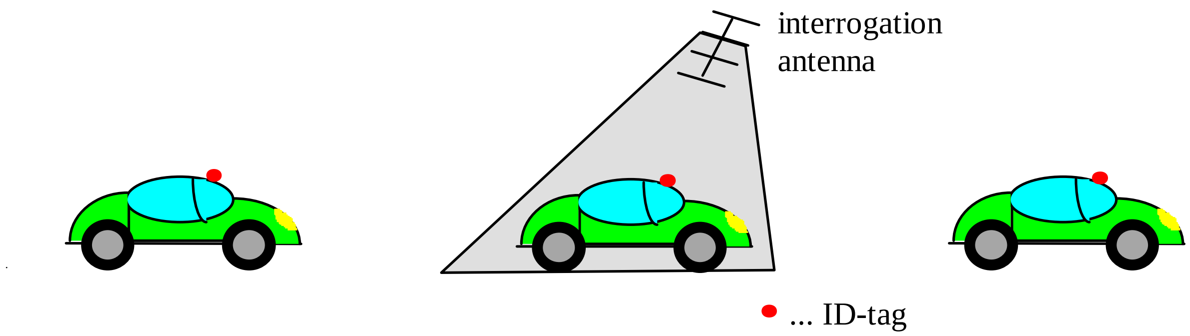

Figure 53: SDMA to passive sensors utilizing the d^4 law for the radio signal attenuation

Division in space (SDMA) is suitable, where the sensors and e.g. the work pieces to monitor, the cars for road pricing, etc., only are allowed to move in certain ways and with sufficient distance from the next one. Then, due to the beam width of the antennas and due to the d^4 propagation attenuation (the sensor to be interrogated is much narrower to the interrogation antenna than the others and is located in the center of the antenna beam), the amplitude of the selected response is large enough to avoid interference from the others. For SDMA, gain controlled and logarithmic amplifiers have to be limited in their dynamic range. An estimation of errors due to other sensors yields the maximum allowed response signal, received from the adjacent sensors. The maximum amplitude error occurs if the interfering signal s_i, e.g. a burst signal from the response of another sensor at the same time with the same (constructive) or inverse (destructive) phase. Then, after normalization to the signal vector s_0, the amplitude error is

$$E_{a,\,max} = \pm\, s_i/s_0. \qquad (22)$$

An amplitude ratio of -20 dB yields a maximum error of 1% in amplitude.

The maximum phase error $\Delta\varphi$ due to a response signal from other sensors is

$$\Delta\varphi_{max} = \arcsin\{s_i/s_0\}. \qquad (23)$$

Therefore, for a phase error limit of 1 degree, the interfering signal s_i originating from the other sensors, must be smaller than $0.0175{\cdot}s_0$, i.e. -35 dB.

Employing SAW sensors, space division mainly is applied for identification purposes, where the amplitude and phase error effects are less significant, e.g. for the Norway road pricing system KOFRI [41]. The advantage of SDMA is, that with exception of a start and a stop bit the whole code family can be exploited. With a 32 bit code and on / off keying, 2^{30} sensors can be distinguished.

For sensor purposes, usually TDMA is applied. The response signals of the sensors to the request are separated interleaving them in time in corresponding time slots. In Figure 54 the TDMA principle is drawn for four time slots, or sensors, respectively. The two-bit sensors 1 and 2 are available here. The measurand is evaluated from the delay of the response signals within the time slots 1-1, 2-2, etc.

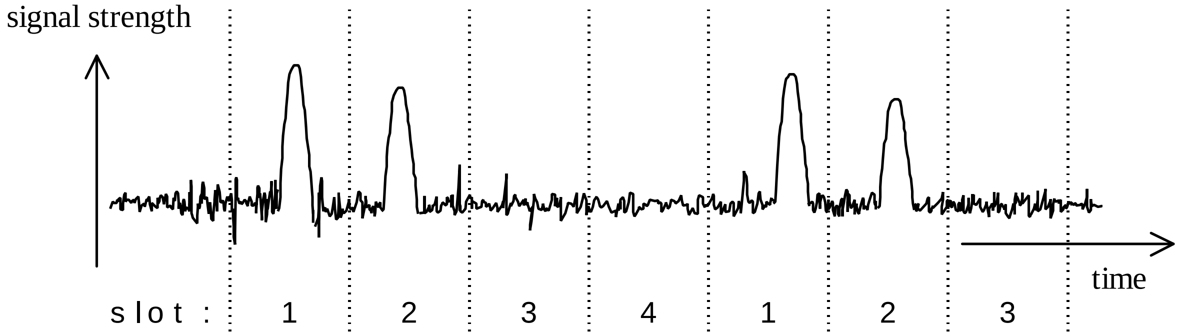

Figure 54: Principle of sensor TDMA, response signal power at the receiver versus time

With TDMA, interference between the sensor response signals is minimized. The system is almost not affected by a near far effect. The time slots have to be wide enough, that the response signals do not leave them due to the measurand's effect. The spacing required is discussed in appendix 1.

Code division (CDMA) is difficult due to a severe near far effect occurring for passive radio sensors. Some work has been done for SAW sensor CDMA in our laboratory, results have been published [54], [55]. Best results have been found by a combination of CDMA with TDMA (TCDMA). Therefore, the code selective addressed sensor responds in a characteristic time slot, where the interference from the other sensors can be minimized by proper choice of codes and timing [46].

4.6 Overview of usually employed methods for radio request of passive sensors

In Table 6, the actually used radio request methods for passive sensors are summarized.

	Request signal	Receiver	Detection	Comments
Wideband DL sensors				
	burst TDS 100 ns up to 2 µs 10 ... 40 dBm E_{tot} = 1 nWs to 20 µWs	AGC or limiting receiver	coherent TDS, I / Q sampling, coherent integration for e.g. 128 radio interrogation cycles	for high speed sensor applications with high resolution, data reduction by non periodic sampling
			incoherent detection envelope sampling	for low range, low cost ID purposes, data reduction by non periodic sampling
	stepped FDS impulses e.g. 32x 10 µs 0 ... 30 dBm E_{tot} = 0.3 ... 300 µWs	linear receiver	coherent FDS	for sensor and ID applications with low speed requirements but high distance range
Dispersive DL sensors				
experimental only	burst τ<< 1/B	matched filter	incoherent detection envelope sampling	
Transponder DL with external sensors				
	burst TDS 100 ns up to 2 µs 10 ... 40 dBm E_{tot} = 1 nWs to 20 µWs	AGC or limiting receiver	coherent TDS, I / Q sampling, coherent integration for e.g. 128 radio request cycles	for high speed sensor applications with high resolution,
			incoherent detection envelope sampling	for low range, high SNR applications, only less signal processing effort
Resonators (high-Q) sensors				
	burst 10 ... 100 µs 0 ... 30 dBm E_{tot}=10 nWs... 100 mWs	linear receiver	TDS, high rate sampling, digital MSE criteria processing	high resolution radio request of high-Q resonators with a relatively long off line processing time
		logarithmic receiver	GPLL	real time signal processing, sufficient SNR required, no multisensor request feasible
Resonators (low-Q) sensors				
	CFDS energy dip in coupled coils at resonance frequency, operating at a few 100 kHz	near field coupled signal reception	detection of energy loss at resonance	for lowest cost ID labels, e.g. for anti theft systems erasable at cash desk

	Request signal	Receiver	Detection	Comments
Non linear sensors				
	CW transmitter, high power (e.g. 30 dBm) to achieve sufficient voltage at the sensor	narrow band receiver at twice the RF frequency	narrow band detection of energy received	for low cost harmonic sensor ID labels, e.g. for anti theft systems, one bit ID tags
experimental only	two band RF CW transmitter modulated by AF signals	narrow band receiver at a known RF frequency	narrow band detection of modulation energy received, detection of amplitude or phase relation of AF signals	mixer sensors for identification and passive sensing

Table 6: Currently employed radio request methods for passive radio sensors

4.7 Radio interrogation systems

Different types of interrogation systems have been developed and investigated in our laboratory. Our related work started in the early 1990's with the first ideas concerning passive radio sensors and the prototype system shown in Figure 55.

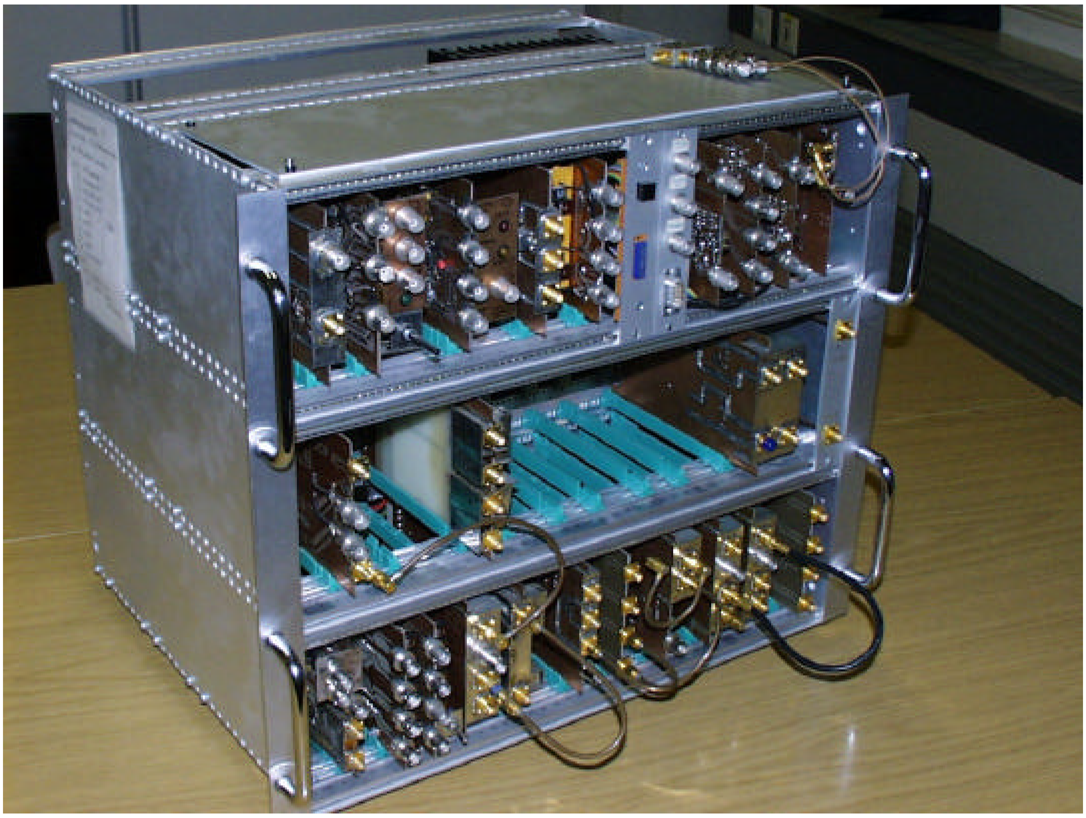

Figure 55: Modular multi-purpose radio interrogation rack

Our response to the demand for all-inclusive low-cost interrogation sets was a small sized ID and sensor system in 1999, shown in Figure 56, suitable for industrial manufacturing.

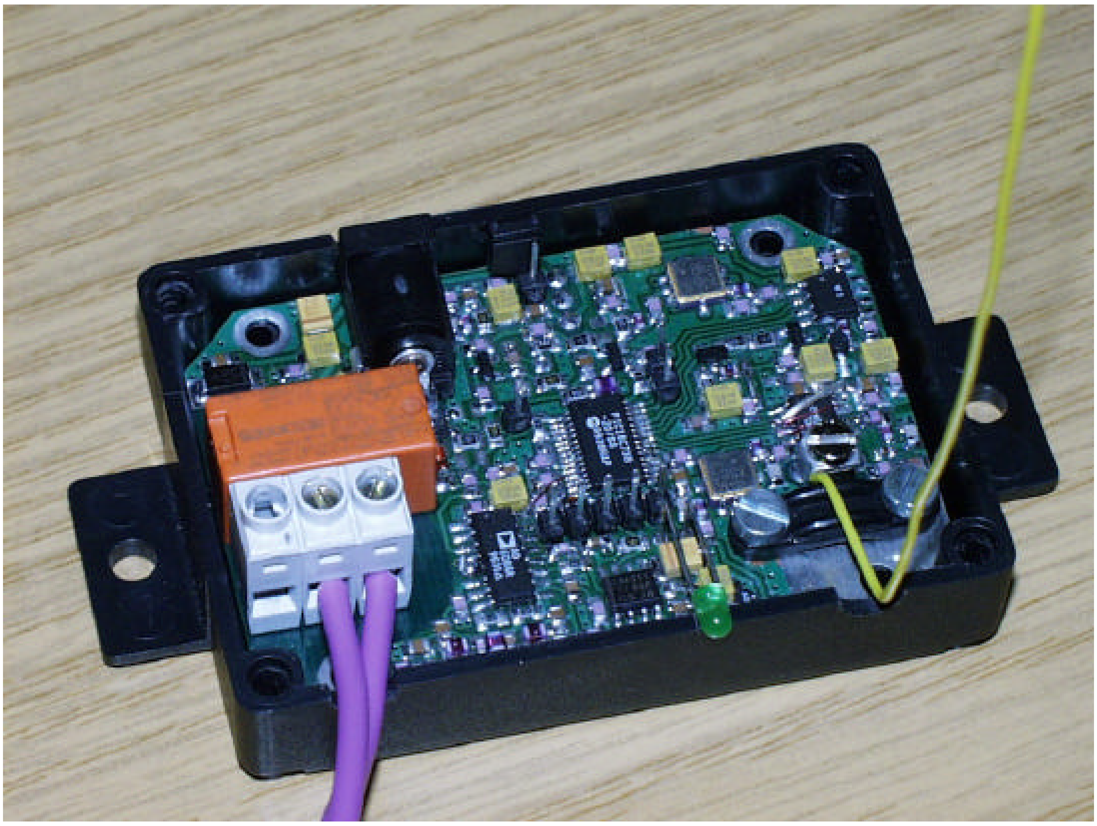

Figure 56: Small-sized (50x70x20 mm^3) low-cost radio interrogation system for SAW DL sensors

Appendix 1 - Radio channel

In this chapter additional information is provided, which is a fundamental of and anticipated in the main part [1] of this thesis.

A1.1 Characterization of the radio channel

A comprehensive introduction into the field of radio transmission is given in [56].
Radio request and response signal retransmission are performed via a radio channel, employing a transmitter, a receiver and at least two antennas. A transmitted RF signal s(t) at a carrier (center) frequency f_c may be modulated in amplitude (AM), frequency (FM), phase (PM), etc.

$$s(t) = A_m \cdot g_T(t) \cdot \cos\{2\pi f_c t + \Phi(t)\} \qquad \text{(A1. 1)}$$

The function $g_T(t)$ is the baseband amplitude modulation, A_m the signal amplitude, $\Phi(t)$ the modulation in frequency and phase, respectively.

An important parameter in radio transmission is the signal attenuation between the transmitter and the receiver. The signal power P_t is assumed to be radiated from an omnidirectional isotropic antenna. The Pointing vector represents the power density $P_t/(4d^2\pi)$ flowing through the sphere's surface in a distance d. For transmission to an omnidirectional isotropic receiver antenna (with the so defined effective area $\lambda^2/(4\pi)$) in a distance d, the signal attenuation for free space propagation is given by

$$a_{free\_space} = \left(\frac{4 \cdot p \cdot d}{l} \right)^2 \qquad \text{(A1. 2)}$$

with light velocity c and wavelength $\lambda = c/f_c$.
This d^p law for signal attenuation with p=2 applies for free space propagation only.
For actual radio channels the exponent p varies from less than 2, e.g. for guiding effects within metallic structures, up to 5 ([56]) for mobile communication radio channels without a direct path (non line of sight, NLOS). Wave radio propagation in tunnels (also line of sight, LOS) may be characterized by an evanescent mode, if the tunnel diameter is in the vicinity of $\lambda/2$ or

less.
The formula given above is valid only in the far field region, where the real component of RF power is dominant. The boundary between the near field region with extensive reactive power flow and the far field region is given by the Rayleigh distance

$r_2=2D_0^2/\lambda$, (A1. 3)

where D_0 is the maximum linear geometrical dimension of the antenna.
For small antennas ($D_0 << \lambda$) the boundary between near and far field is given by the estimation

$r_1 \approx \lambda/2\pi$. (A1. 4)

For the radio sensor applications to machines, within closed process chambers, or under the fender of a car, metallic parts in the near field region of the antenna are electromagnetically coupled and enlarge the effective dimension D_0 of the - usually small - interrogation antennas. For these applications the distance to the sensor antenna usually is smaller than the actual Rayleigh distance r_2. The free space attenuation equ. (A1.2) does not apply, the actual signal attenuation has to be evaluated by a measurement e.g. with a Network analyzer (NWA). For an example in [1], figure 6, the path attenuation is shown for the radio link between the interrogation antenna under the fender of a car and the sensor antenna within the tire. Here, as for similar applications, the path loss mainly depends on the geometry of the system, misadjustment of the antenna polarization becomes an important factor. The two graphs shown in this figure represent two different request antenna positions.
For radio transmission with a distance larger than r_2, obstacles within the Fresnel ellipsoid [56] cause a wideband signal fading.
An important effect in radio transmission is multipath propagation [56], [57], [58], [59]. The radio signal propagates from the transmitter to the receiver via different paths and these are summed up in the receiver antenna. In actual mobile communication radio channels, a time variant and frequency dependent signal fading can be observed caused by changing multipath propagation and shadowing.
As mentioned above, for the short range scenario under the fender of a car, the geometry provides two main propagation paths with different signal losses for the interrogation signals. For the measurement result drawn with the dotted line (in [1], figure 6), the signal is handed over from one to the other path with a maximum in attenuation and a significant phase transition at a wheel rotation angle of approx. 120 degree. Here we cannot use the term

multipath propagation because only two major paths exist and the transmission is mainly due to near field coupling.

A link budget, a sketch of the signal power levels at characteristic points of the transmission channel can be drawn for radio transmission systems. The transmitted signal power, the sensitivity of the receiver, the system's noise figure, the system's dynamic range, the signal detection error, etc. can be put into the evaluation and one of these can be calculated from the others. As a design rule for actual systems, the mathematical relation between these parameters is given in [1] (equ. 32). In [1] (figure 7) the link budget for an outdoor keyless entry system is shown. Here, some estimations and simplifications have to be observed:

Considering the actual implementation without shadowing of the radio transmission and with minor multipath propagation effects, only deterministic parameters are considered. The signal attenuation during transmission is assumed to obey the p=2 law (equ. A1.2). For calculation the gain of the antennas was assumed to be 0 dB to take into account a misadjustment of polarization, e.g. due to non parallel linear antennas, etc.

To other environments, e.g. indoor applications, or for larger distances, the simple deterministic model cannot be applied. For estimations at least a margin for both types of fading (shadowing and multipath propagation) has to be added.

Multipath fading strongly is influenced by moving antennas and moving scatterers and reflectors in the surroundings. A movement of approx. a tenth of the wavelength yields a totally changed scenario. Therefore, multipath propagation is characterized by statistical parameters [57]. In time domain we find:

The **mean delay** is the averaged delay of the signal energy from the transmitter to the receiver. Since the minimum signal delay of the LOS path is not known in all cases, the statistically averaged mean excess delay is used usually.

The **mean excess delay** $\bar{\tau}$ is the first moment of the power delay profile. If k samples a_k of the received signal's amplitude a(t) versus the discrete samples τ_k of time are recorded, $\bar{\tau}$ can be written as

$$\bar{\tau} = \frac{\sum_k a_k^2 \cdot \tau_k}{\sum_k a_k^2} = \frac{\sum_k P(\tau_k) \cdot \tau_k}{\sum_k P(\tau_k)} \qquad \text{(A1. 5)}$$

with the signal power $P(\tau_k)$ at time τ_k.

A further important parameter of a multipath radio channel is the **rms delay spread** σ_τ. It is the square root of the second moment of the power delay profile

$$\sigma_\tau = \sqrt{\overline{\tau^2} - (\bar{\tau})^2}\ , \tag{A1. 6}$$

with

$$\overline{\tau^2} = \frac{\sum_k a_k^2 \cdot \tau_k^2}{\sum_k a_k^2} = \frac{\sum_k P(\tau_k) \cdot \tau_k^2}{\sum_k P(\tau_k)}\ . \tag{A1. 7}$$

Usually zero delay is attributed to the first detectable signal arriving at the receiver. The relations rely on the relative amplitudes of the multipath components within $P(\tau)$. Typical delay spreads are some µs for outdoor and a few tens of ns for indoor channels.
Mean delay and delay spread are deduced from each individual measurement of the specific power profile. For characterization of a radio channel in an environment, many measurements have to be made and an average of the results has to be calculated or a probability distribution function for a statistical description has to be found.

The **maximum excess delay {-x dB}** (eds -x dB) is the delay of the received power profile during which the multipath energy falls to x dB below the maximum. For GSM, x is set to 9 dB, since this is the upper limit the system can accept as (self-) interference. For the radio interrogation of passive sensors with time domain division of request and sensor response signals (e.g. a SAW delay line), echoes interfering with the subsequently reflected waves yield errors depending on the ratio of signal to the interfering echo (i.e. for x dB margin, the amplitude error due to signals outside this amplitude window is smaller than $100/\left(10^{x/20}\right)$ %).,
As shown in [1] and in appendix A2, the resulting error or, for system design, the required timing limits of the delay line sensors and consequently the number of SAW reflectors per substrate length are calculated from this parameter.

Less important for relatively wideband passive radio sensor systems but essential for mobile communication systems up to now, with optimized minimal-bandwidth modulation schemes, is the **coherence bandwidth** B_c, a description of the multipath channel in the frequency domain. It is a statistical measure of the range of frequencies over which the channel can be considered as "flat". This means, all spectral components within this bandwidth pass the channel with approximately equal gain and linear phase. Spectral components within B_c mutually are correlated in amplitude and phase and thus in fading.

Fleury [60] gives an inequality for B_c:

$$B_c \geq \frac{\arccos(\chi)}{2\pi \cdot \sigma_\tau}. \tag{A1. 8}$$

The factor χ describes the correlation of the fading of the spectral power density within the bandwidth. It has to be considered in the design of radio communication systems and modulation schemes.

The time variant radio channel with moving transmitter, reflectors, scatterers and receiver is characterized by **Doppler spread** and **coherence time**. The Doppler spread B_D is a measure for the spectral broadening due to the movement. The coherence time T_C is a measure of the interval length within the impulse response of the channel is approximately constant. If the channel changes during the transmission of a message, e.g. if the reciprocal bandwidth (or data bit length) is larger than the coherence time, a further degradation of transmission occurs.

Apart from some simple short range applications discussed above, radio sensor interrogation channels are subject to multipath propagation too. To ensure a reliable operation, here also the channel properties have to be measured and considered for the system design.

As an example, in Figure 57 the transmission function $S_{21}(f)$ is drawn for an industrial radio channel for a SAW sensor application. The distance range approx. is 15 m. The measurements have been performed utilizing a HP8753 NWA with a center frequency of 850 MHz and a measurement bandwidth of 200 MHz. A FFT yields the channel impulse response plotted in Figure 58.

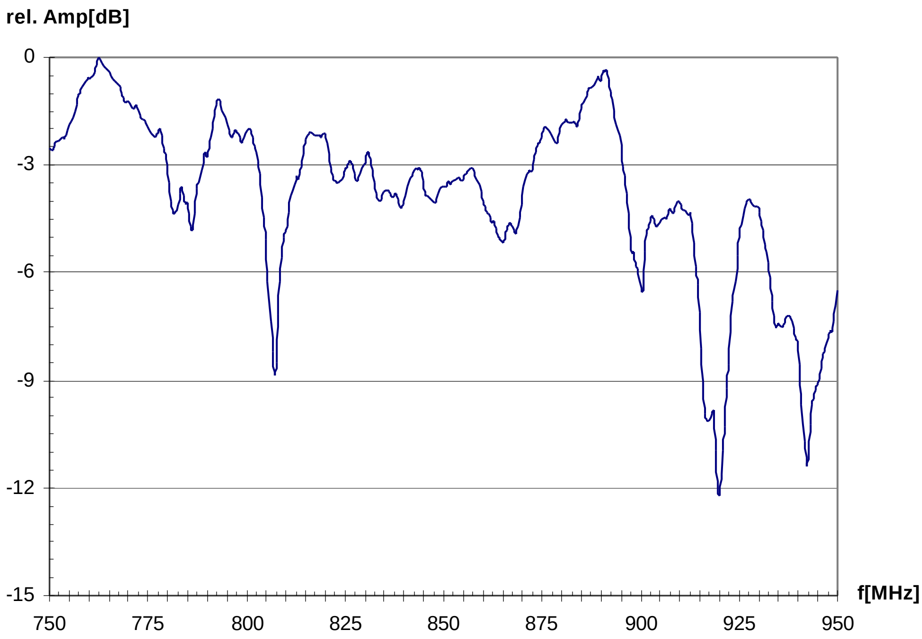

Figure 57: Transmission function $S_{21}(\omega)$ of an industrial radio channel for SAW sensor application

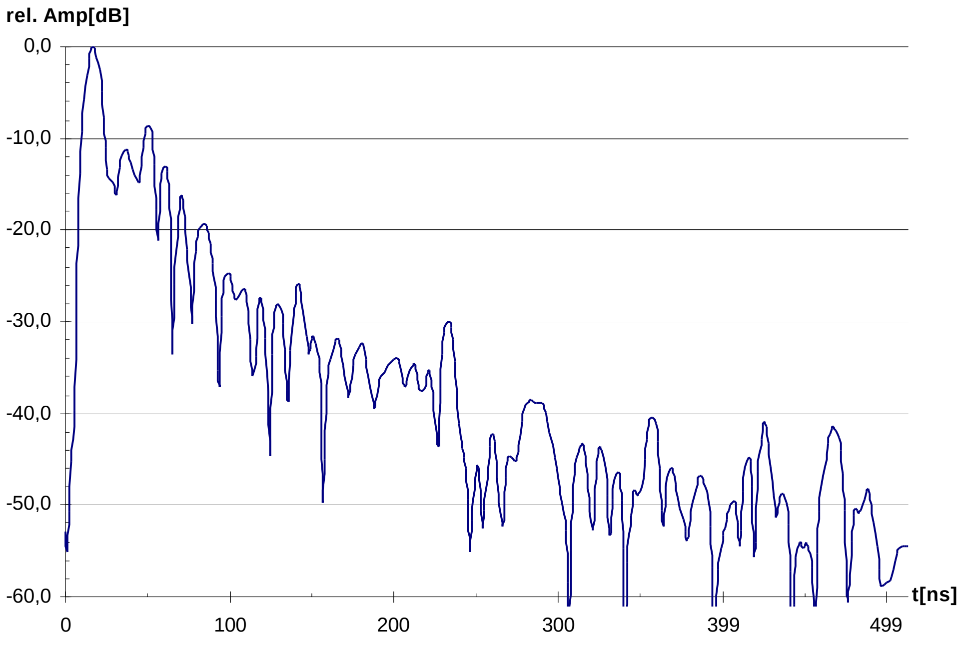

Figure 58: Impulse response of an indoor industrial radio channel at 850 MHz (B=200 MHz)

To find the statistical parameters for the channel description and for the sensor design, the measurement is performed for a (large) number of locations within the area of interest.

For our sensor channel (Figure 57, Figure 58) we found a mean excess delay of 19.3 ns (with a standard deviation of 3.8 ns), an rms delay spread of 17.8 ns (std. dev. 3.9 ns) and an {eds -20 dB} of 76.4 ns (std. dev. 16.9 ns).

The parameter x=20 dB for the excess delay spread was chosen to find the width of the time slots for TDMA (the minimum delay between two reflected signals) mutually causing an additional error of less than 1 %.

With the estimation given above, the coherence bandwidth B_c is larger than 4 MHz for $\chi = 0.9$. If the bandwidth covered by the radio signal is larger than this B_c, the multipath echoes cause multiple impulses in the receiver. For narrow band radio request, e.g. resonator systems, this multipath scenario yields amplitude fading, similar to the Rayleigh fading occurring in mobile communication systems.

Installing a radio sensor system, the properties of the individual radio channel are affected by the positioning of the antennas. To exploit this for an optimization of the system, an information about the reflections in time and space is necessary. A very powerful method of depicting the characteristic of a measured multipath channel's power profile is the **scattering function**, yielding an information about division of the multiple paths in time and space [58].

As described above, for (short: <1 m and medium range: <30 m) channel measurements, a network analyzer (NWA) is employed usually. The output information provided, is the transmission function $S_{21}(f)$ versus frequency.

To gain information about scatterers, the receiver antenna is moved linearly for approx. $\lambda/3$ and the measurement is repeated. This is done e.g. 16 times (at antenna positions 1, 2, 3, ... in Figure 59). In this way, the radio channel is sampled in frequency (by the NWA) and space (due to the antenna shift). The set of results is the time variant, or, for the moving antenna, the position variant transmission function $S_{21}(f,t)$. The space domain in minimum has to be sampled twice per wavelength. A shift of $\lambda/3$ means a moderate oversampling.

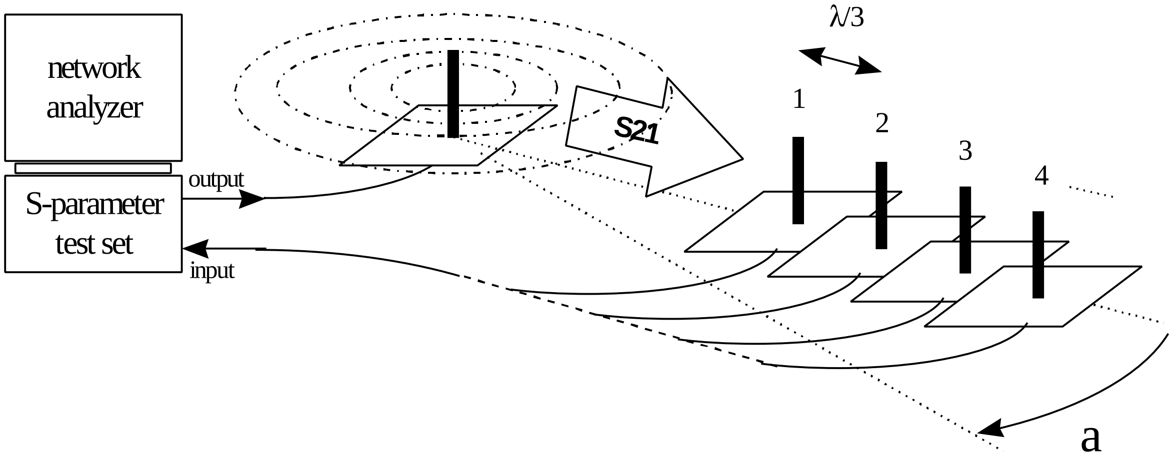

Figure 59: Channel Measurement with a vector network analyzer including space domain sampling

Parson [59] shows the relationship between the set of measurement results and the scattering function. This scattering function P_s is a function of time τ and space coordinate υ. It is calculated squaring the magnitude of the Doppler variant impulse response $S(\tau,\nu)$.

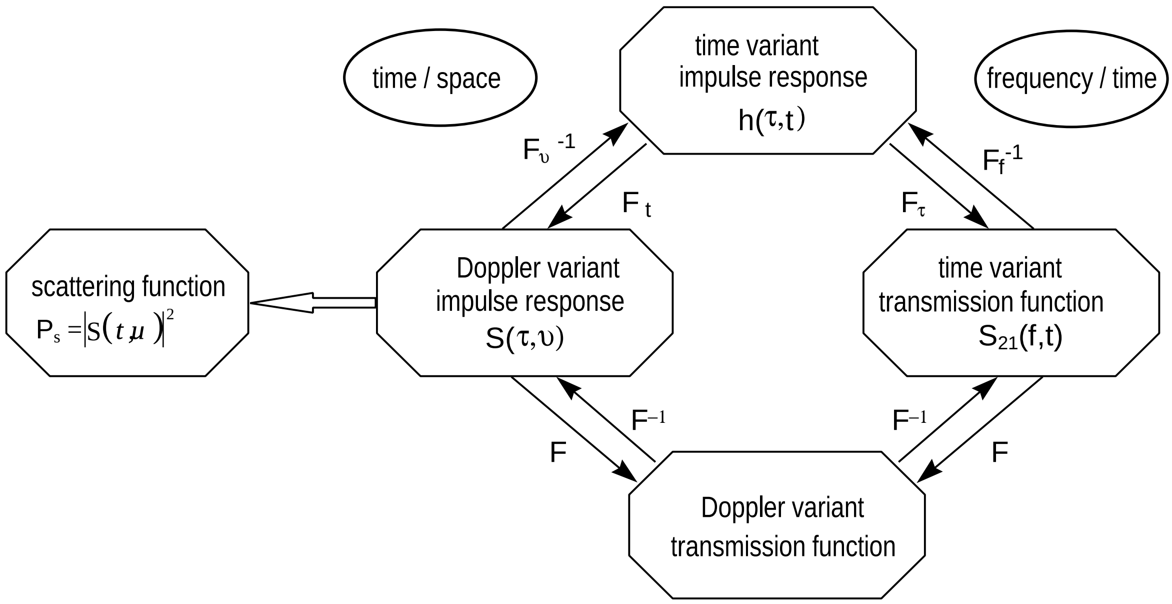

Figure 60: Relationship between the time, frequency and space variant functions of the radio channel, [59]

The scattering function P_S originally was defined for moving transmitters or receivers. For the quasistationary radio interrogation channel, the scattering function can be used to evaluate the direction of the echoes and to minimize their effect by appropriate positioning of the interrogation antennas and choosing their polarization. For measurement the method of the linearly shifted measurement points, discussed above, is employed. The graphical description of the scattering function yields the information of signal power versus time and angle of receipt. From this, the location of scatterers is evaluated (it has to be kept in mind, that the radio channel was assumed to be stationary).

A discrete Fourier transform F_s of the function $f(k \cdot \Delta s)$, (with k=1,2,3 ... and e.g. $\Delta s = \lambda/3$), is performed in space with N (e.g. N=16) samples spaced by Δs:

$$F_S\{f(k \cdot \Delta s)\} = \sum_{k=1}^{N} f(k \cdot \Delta s) \cdot e^{j\frac{2\pi}{\lambda} \cdot k \cdot \Delta s \cdot \cos\alpha} \quad . \qquad \text{(A1. 9)}$$

This calculation yields a significant result for α and τ, if the partial wave is received at τ from the direction with the azimuth angle α. In Figure 61 the scattering function the industrial radio channel mentioned above (Figure 57, Figure 58) is drawn:

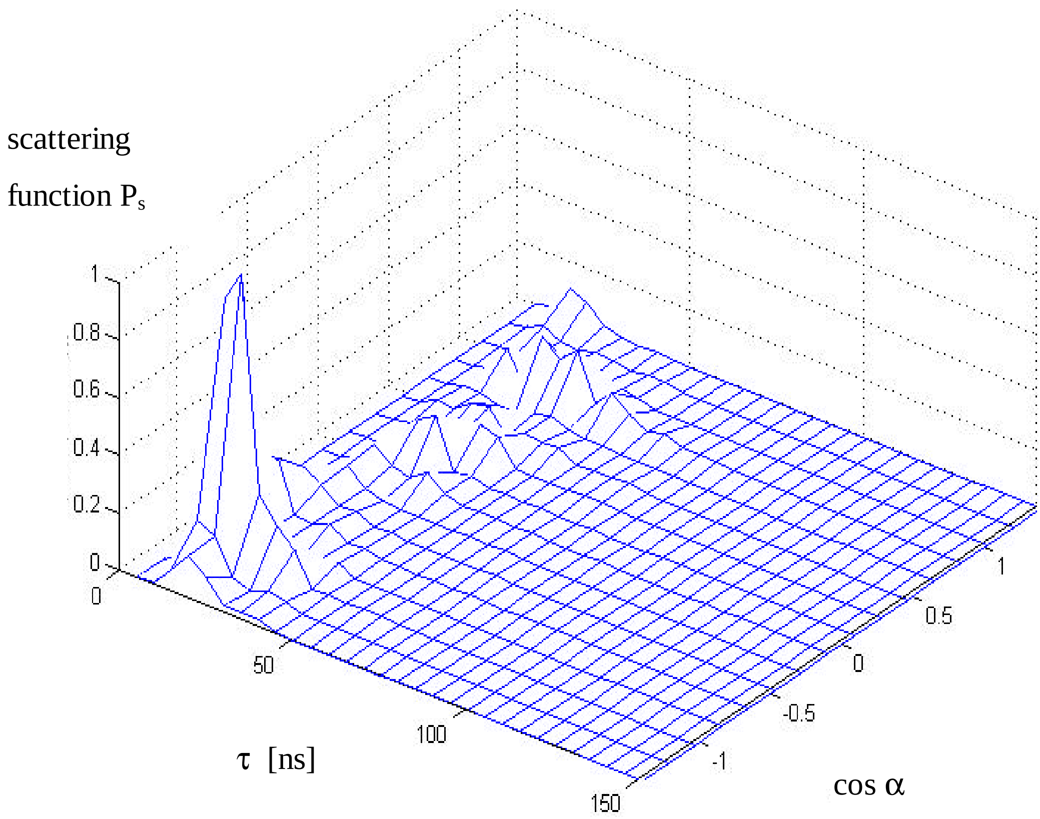

Figure 61: Scattering function for the radio channel for one of our SAW radio sensor applications in an industrial environment (steel plant)

In Figure 61 a powerful line of sight signal at 20 ns and at cos α = -1 can be observed. With a delay of a few tens of nanoseconds, lateral reflections arrive, with an amplitude ratio to the LOS signal of approx. -20 dB.

Obeying Carson's theorem, radio transmission via the same linear time invariant passive radio channel at the same frequency is reciprocal [56]. Radio interrogation signals (request and response) pass the same channel at the same frequency within a time interval of some microseconds. Even for fast moving sensors the radio channel can assumed to be stationary within this short time slot. Request (downlink)- and response (uplink)- channels are identical, all propagation effects occur twice. Therefore, the path loss is squared, i.e. doubled in dB, and the unidirectional transfer function of the channel versus frequency, as shown in Figure 57, has to be squared to give the sensor radio channel. Thus the total sensor interrogation impulse response is calculated from the auto convolution of the unidirectional channel impulse response. To estimate the total delay and delay spread, as an example we assumed a unidirectional channel impulse response consisting of two components with equal magnitude 1, spaced in time by ΔT:

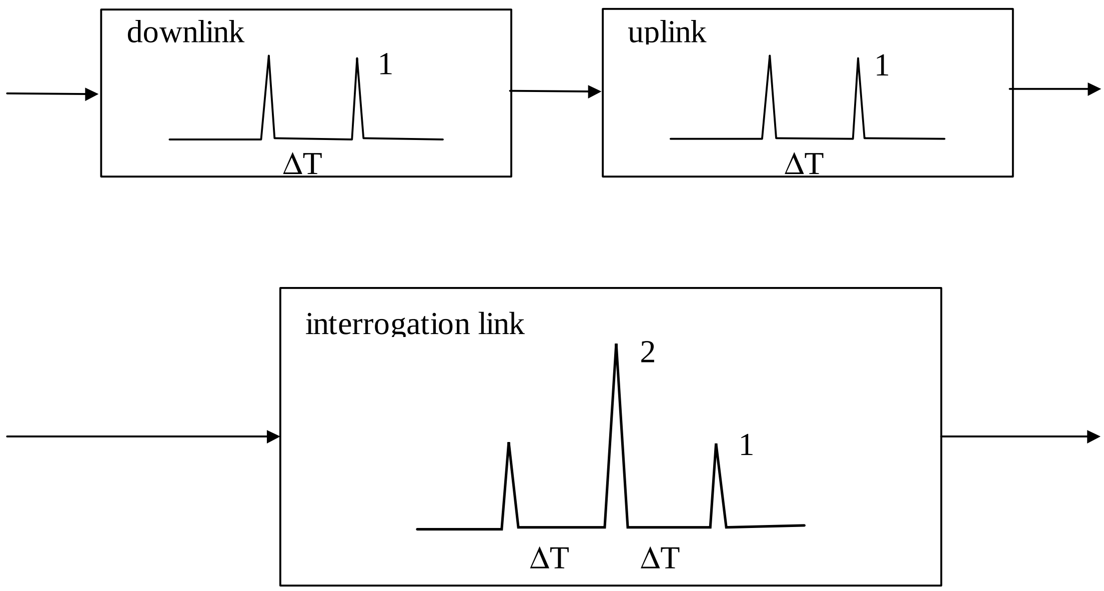

Figure 62: Impulse response of the interrogation link composed of two equal unidirectional radio links

From the sketch above, and with (A1.5) and (A1.6), the mean excess delay can be calculated to be $\Delta T/2$ for the down- and the uplink channel. The rms delay spread is $\Delta T/2$ for each of these paths. For the whole interrogation channel, the mean excess delay is calculated to be ΔT, it is doubled. The total rms delay spread for down and uplink is $\Delta T/\sqrt{3}$.

To find the timing parameter for a reliable sensor system we apply a worst case estimation: the delay and the delay spread is assumed to be doubled for the bi-directional transmission, the coherence bandwidth is halved.

A1.2 Sensor design with respect to the radio channel's properties

From the averaged parameters of the radio channel, the basic design rules for the timing and the bandwidth of the radio sensors and the radio interrogation system can be derived:

Investigating delay line devices, the doubled delay spread of the channel has to be the minimum spacing of the response signals in time. Therefore, the number of reflectors on one (SAW) sensor and the number of different sensors for multiple access is limited with a given maximum substrate length: Allowing for the temperature coefficient TK, the maximal operation temperature $\Delta\vartheta_{max}$, the excess delay spread eds{-x dB} for interference of an adjacent response decreased by x dB and the RF bandwidth B_{RF}, the earliest time position of the n-th reflector $t(x_n)$ to avoid interference from adjacent reflectors is

$$t(x_n) = (1 + TK \cdot \Delta\vartheta_{max}) \cdot t(x_{n-1}) + \left(2 \cdot \mathrm{eds}\{x\,dB\} + \frac{2}{B_{RF}}\right), \qquad \text{(A1. 10)}$$

considering the temperature range, the doubled excess delay spread and the pulse width $2/B_{RF}$ have to be added to the position of the (n-1)-th reflector.

Mathematical conversion yields

$$t(x_n) = (1 + TK \cdot \Delta\vartheta_{max})^n \cdot t(x_0) - \frac{1-(1+TK \cdot \Delta\vartheta_{max})^n}{TK \cdot \Delta\vartheta_{max}} \cdot \left(2 \cdot \mathrm{eds}\{x\,dB\} + \frac{2}{B_{RF}}\right). \qquad \text{(A1. 11)}$$

In Figure 63, the position of the n-th reflector in time is plotted for RF bandwidths of 1.7 and 10 MHz and a temperature range of 50 K and 500 K. A Lithiumniobate SAW sensor substrate, a basic delay t(x0) = 2 µs and an excess delay spread {eds -20 dB} of the radio channel of 200 ns is assumed. From Figure 63, the maximum substrate length, the number of sensors interrogated simultaneously, the RF bandwidth required, or the temperature range allowed for operation can be extracted. The estimation also applies to the number of on/off switched bits of an identification sensor: A $LiNbO_3$ ID tag with a total delay of 10 µs, for a temperature range of 50 K and interrogated by a radio signal with B_{RF}= 1.7 MHz can employ up to 6 bits. A 10 MHz bandwidth, e.g. in the 2.45 GHz ISM band allows 14 bits for ID or sensor applications with a 10 µs SAW delay line (2x15 mm SAW propagation length, approx. 20 mm substrate length). On the other hand, applying TDMA with two bit DLs and interleaved pairs of reflectors (Figure 54), up to 7 SAW sensors can be requested simultaneously.

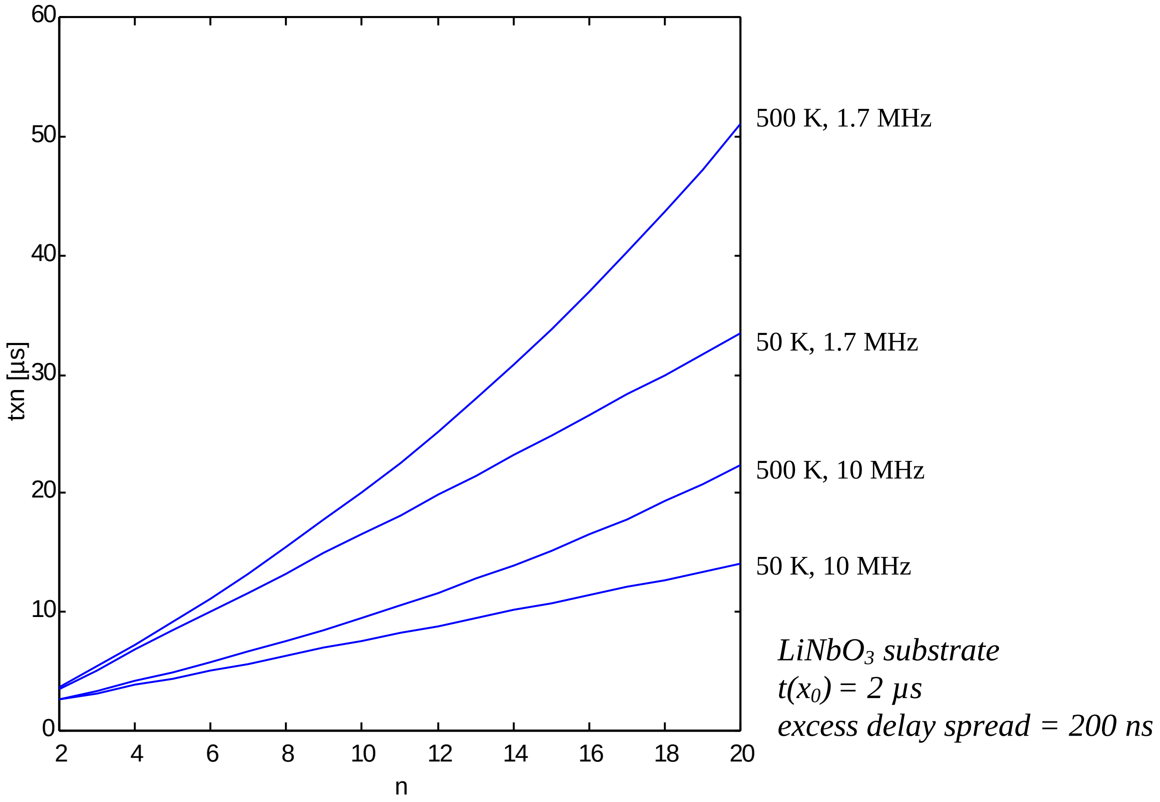

Figure 63: Allowed position of the n-th reflector on a $LiNbO_3$ DL in time with max. 1% interference for an RF bandwidth of 1.7 and 10 MHz and a temperature range of 50 and 500K.

The higher the bandwidth of the sensor system, the higher the insertion loss of the SAW sensor will be. A higher bandwidth of the SAW device means fewer finger pairs in all IDTs and therefore a poor total electroacoustic coupling. The insertion loss of today's 433 MHz (6 bit) ID tag type SAW sensors with a 5 MHz bandwidth and a 10 µs impulse response on a $LiNbO_3$ substrate is about 20 dB.

Appendix 2 - Measurement uncertainty

The uncertainty of the measurement is discussed in the main part [1], chapter 5, of this thesis. Starting with a definition and a brief discussion of sensitivity, resolution and accuracy, the errors occurring during the measurement with passive radio sensors are discussed in detail here. In this appendix, the supplementary information to the estimations in [1] is given.

A2.1 Uncertainty due to bandwidth limitation

In Figure 64 the measurement system is sketched as a chain of sub systems with the measurand as input and the readout as the output signal. The transfer function is the product of the transfer functions of the sub systems. The total bandwidth is affected by all sub systems. In Figure 64 the effect of SAW sensor (SAWS) properties to the chain is sketched. As also discussed in [1], 5.2.2, the directly affected SAWS belong to the sensor group and only the sensor environment, mechanical resonance, etc. are relevant for these. On the other hand, the indirectly affected SAW transponders mainly belong to the radio transmission.

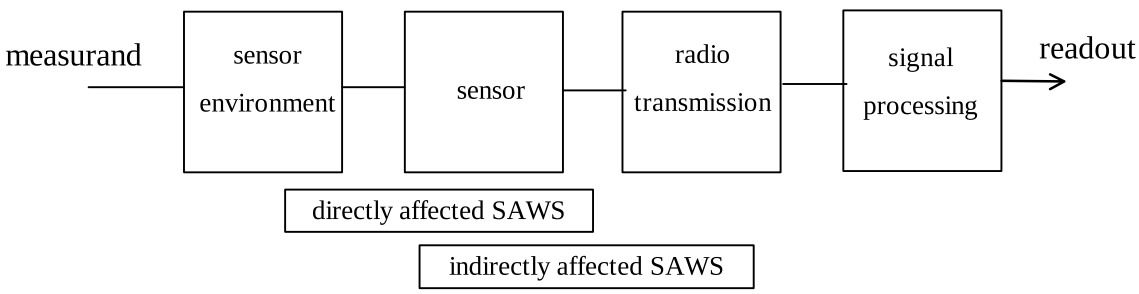

Figure 64: Measurement system

The radio transmission includes the antennas, the radio channel and the RF circuits in the interrogation system. This block can easily be designed in compliance with the demands and the governmental regulations, it is the most uncritical in the bandwidth discussion for passive radio sensor systems.

The signal processing block contains the electronic units in the interrogation system, employed for signal detection, coherent demodulation and for measurement of time, frequency and / or amplitude.

An error, originating from this processing block is the error due to a finite measurement interval: Usually, the measurand is evaluated from a time delay ΔT or by a frequency measurement, lasting a time interval ΔT. Within this time, an averaged value of the measurand is collected.

The effective scaling ε_{eff} of the response, the measurand is calculated from, is derived from the dynamic scaling $\varepsilon(t)$ [61]:

$$\varepsilon_{eff} = \frac{1}{\Delta T}\int_{\Delta T} \varepsilon(t)\ dt \qquad \text{(A2. 1)}$$

The timing of the radio interrogation for directly affected SAW delay line sensors is shown in Figure 65.

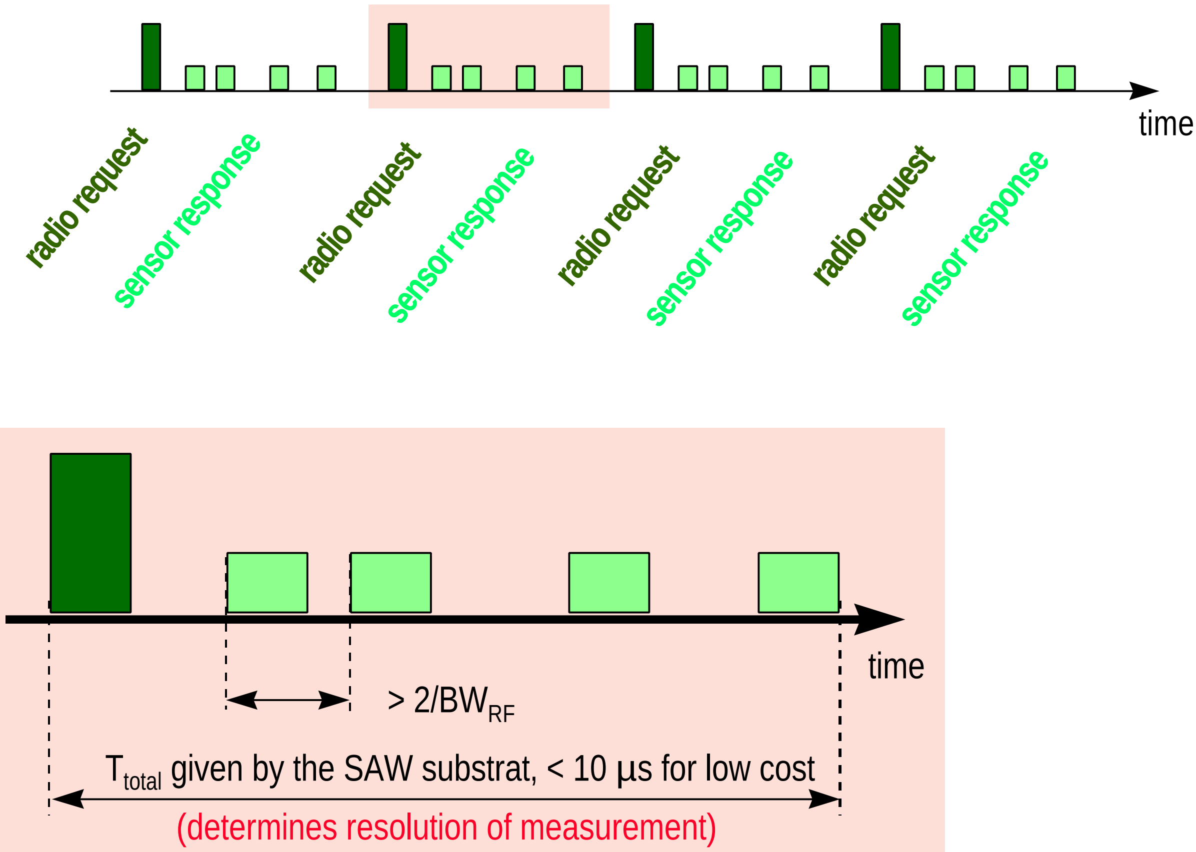

Figure 65: Timing of radio interrogation of directly affected SAW delay line sensors

As discussed in chapter 4.2, the measurand is evaluated from a delay measurement between the response signals. The duration of the response signal determines the number of ID codes as well as the resolution of measurement. To achieve high resolution, the integration time has to be high, reducing the bandwidth [1].

The timing for radio interrogation of the indirectly affected SAW transponder devices is sketched in Figure 66. The sensor information is encoded in the ratio of amplitude and phase difference between the "reference bit" and the "measurement bit". For a stationary radio transmission, the total integration time limiting the bandwidth, is the duration of the "measurement bit" [1].

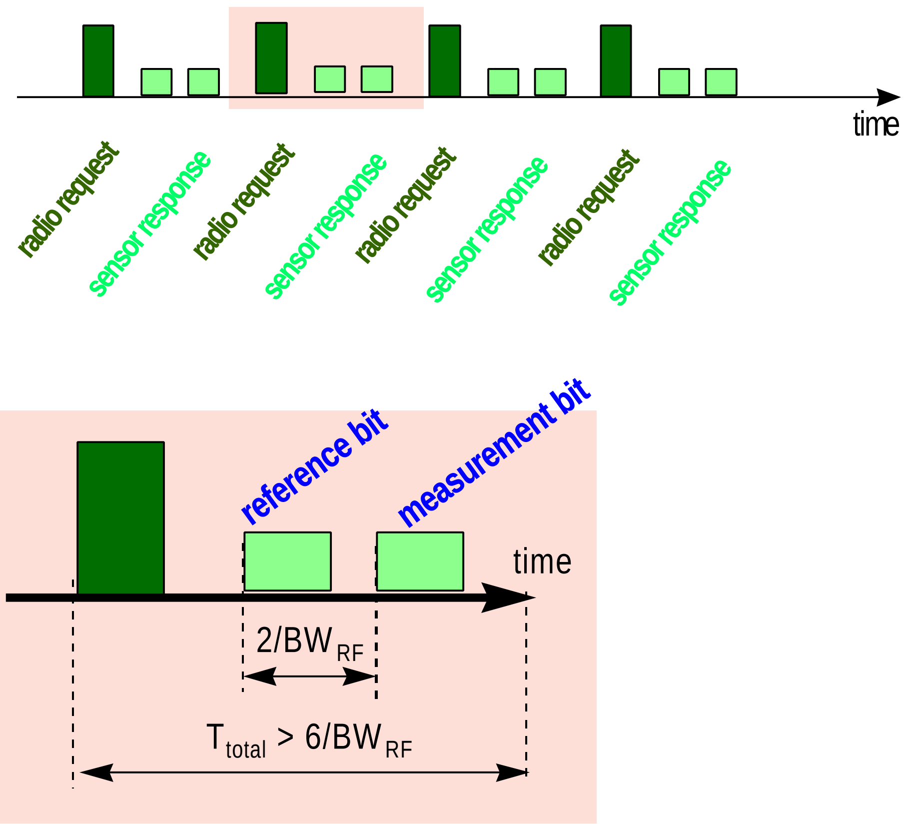

Figure 66: Timing of radio interrogation of indirectly affected SAW transponder sensors

As discussed in [1], employing the SAW transponder sensors, measurands with a bandwidth of several MHz can be recorded.

A2.2 Errors caused by poor adjustment of the baseband subunit of the interrogation system

The estimations discussed in this chapter mainly apply to coherent receiver concepts with inphase and quadrature signals, the signal's magnitude is calculated by $|r(t)| = \sqrt{I(t)^2 + Q(t)^2}$, the phase from $\varphi_{r(t)}(t) = \arctan\{Q(t)/I(t)\}$. The inphase and the quadrature component are sampled and digitized, I(t) $\rightarrow$ I[n], Q(t) $\rightarrow$ Q[n]. For estimation below we consider the time discrete components at sample n = i and substitute for the calculations in the vector space: I[i] $\rightarrow$ I, Q[i] $\rightarrow$ Q.

Different signal strength of the local oscillators in the quadrature demodulator, different gain in the I and Q channel (I'=I·a, Q'=Q·b) and e.g. a difference of reference voltage in the dual analog to digital conversion unit yield a phase error $\Delta\varphi$. The tan function is stretched (b>a) or compressed (a>b).

With $\tan(\varphi + \Delta\varphi) = \frac{b \cdot Q}{a \cdot I}$, due to Figure 67, the phase error $\Delta\varphi$ due to baseband gain difference can be calculated from

$$\Delta\varphi_{gain} = \arctan\left\{\frac{b \cdot Q}{a \cdot I}\right\} - \arctan\left\{\frac{Q}{I}\right\}. \qquad \text{(A2. 2)}$$

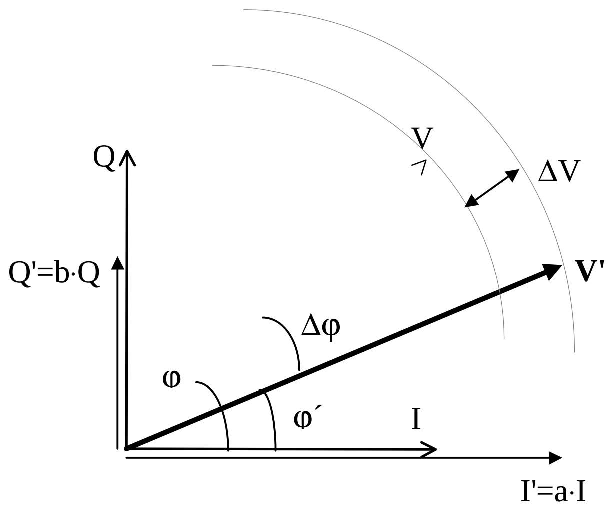

Figure 67: Calculation of phase and amplitude error due to gain difference in base band channels

The phase error versus the absolute phase of the received signal vector with parameter b/a is drawn in [1], fig. 8. A difference of 10 % between a and b (a ratio of b/a = 0.1) yields an additional error up to 3 degree if the phase of the response signal is approx. 40 degree in the receiver reference system of I and Q vectors.

The effects distorting the measured phase also yield an error in amplitude measurement:

With the received signal amplitude V=1 and a=1, from Figure 67 the ratio of detected amplitude V´ and actual amplitude can be calculated from:

$$\left.{V'}/{V}\right|_{b/a} = \sqrt{\left(\frac{b}{a}\right)^2 \cdot \sin^2 \varphi + \cos \ \varphi}\,. \qquad \text{(A2. 3)}$$

The detected relative amplitude (the relative amplitude error) versus the absolute phase with parameter b/a is drawn in [1], fig. 9. The factor a is assumed to be 1, the maximum error b/a occurs at φ=90°.

Quadrature detection in coherent receivers utilizes local oscillator signals shifted by 90 degree by PLL, delay lines, etc. An error of orthogonality, a phase deviation ε between the actual base system I_0' and Q_0' and the theoretical base vectors I_0 and Q_0 yields errors in phase and amplitude measurement. The errors can be found from the geometrical relations in Figure 68. A received signal vector V with the actual orthogonal components I and Q is depicted to I and Q´. Calculations of phase φ´=arctan(Q´/I) and amplitude $V' = \sqrt{I^2 + Q'^2}$ are afflicted with errors.

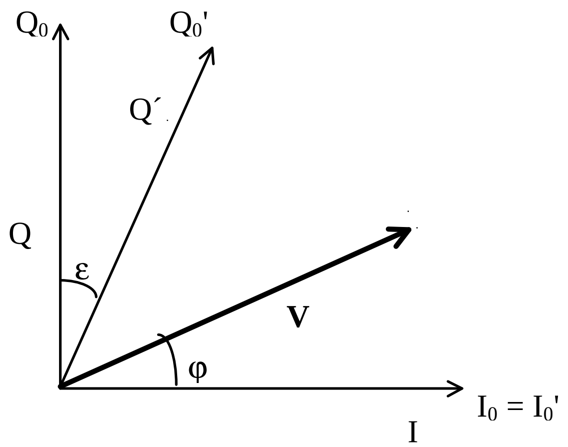

Figure 68: Estimation of errors due to non orthogonal reference with phase deviation ε.

This deviation also may occur, if electromagnetic feed through of the reference oscillator is present due to poor shielding, etc., and the phase of the resulting base signals is distorted.

According to Figure 68, with I = cos φ and |V| = 1, the phase error due to non orthogonal base vectors

$\Delta\varphi_\varepsilon = \varphi' - \varphi = \arctan(Q'/I) - \arctan(Q/I)$

can be calculated from

$$\Delta\varphi_\varepsilon = \arctan\left\{\frac{\cos(\pi/2 - \varphi - \varepsilon)}{\cos(\varphi)}\right\} - \varphi \,. \qquad \text{(A2. 4)}$$

The amplitude error $(V'/V)|_\varepsilon$ is

$$\left. {V'}\!\middle/\!{V} \right|_\varepsilon = \frac{\sqrt{I^2 + Q'^2}}{\sqrt{I^2 + Q^2}} = \sqrt{\cos^2(\varphi) + \cos^2(\pi/2 - \varphi - \varepsilon)} \,. \qquad \text{(A2. 5)}$$

Phase and amplitude error, caused by the deviation ε of the reference base system from orthogonality are drawn in [1], fig. 10 and fig. 11.

An ε = 5 degree phase deviation yields a phase error of up to approx. 5 degree but an amplitude error of up to 5 %, usually too much for a measurement system.

Further errors in magnitude and phase occur from poor performance, e.g. linearity, of the sampling and digitizing circuits. The maximum errors can be found from the specifications in the data sheets.

A2.3 Uncertainty caused by misadjustment of the RF unit - frequency offset

Most radio interrogation systems are built similar to coherent radar systems. The frequencies used for phase detection in the receiver section are generated from the same sources as the radio request signals previously have been traced from. Therefore, a phase error due to a frequency offset between transmitter and receiver does not occur if a stable source and no Doppler shift is present.

In the case of a sensor assembly mounted to a rotating shaft, or for a sensor fitted to a vehicle, and a readout from a motionless station, Doppler shift will occur and disturb the response signals. For a passive reflective system, the narrowband Doppler shift f_d is

$$f_d = 2 \cdot v_r \cdot \frac{f_c}{c}. \qquad (A2.\ 6)$$

A narrowband signal with center frequency f_c is shifted by f_d, proportional to the ratio of the doubled (since the shift applies to down- and uplink) relative velocity to the propagation velocity of the wave. For a sensor requested with a 1 GHz burst signal, mounted on a fast moving train with a speed of 100 m/s (approx. 360 km/h), the Doppler shift is approx. 667 Hz. A SAW delay line sensor with a number of reflectors is a linear device, each of the impulses of the response signal will start with the same initial phase. For a Doppler shift of 667 Hz, the phase error for consecutive impulses will become 2π after a (long) time of 1.5 ms. The duration of one impulse (e.g. burst) in the sensor response is determined by the duration of the request signal and the length of the impulse response of the SAW reflector. In practical ID tags, the impulses are shorter than 1 µs. Therefore, even a fast moving sensor will suffer a phase error smaller than 1° which degrades the resolution of the system negligibly.

A2.4 Measurement errors due to noise terms

Up to now in publications, sensitivity, accuracy and resolution usually are given simultaneously with a maximum distance range for radio request. No errors due to a signal to noise ratio decreasing with distance and other noise contributions are considered.

Although it is trivial, the basics of noise will be discussed here too:

During radio transmission and signal processing, all components generate noise. Passive resistive components generate thermal noise and most active devices shot noise, white stochastic processes.

The power density of a white process is the autocorrelation function for zero time shift ACF(0). For a Gaussian process, like thermal noise, this double side noise power density can be calculated from the probability density function:

It is equal to the variance σ^2 [62], [63]

$$\sigma^2 = N_0 / 2. \qquad (A2.\ 7)$$

The noise density N_0 of a noisy resistor R expressed as the occurring mean-square voltage density is $4 \cdot k \cdot T \cdot R$, with the Boltzmann constant $k = 1.38 \cdot 10^{-23}$ Ws/K and the absolute temperature T. The noise power N can be calculated from the product of power density and the two-sided bandwidth B.

$N = N_0/2 \cdot B$.

In semiconductors and active components, shot noise occurs. The noise power density is given by the mean square noise current $\overline{i^2_{n,shot}} = 2eI$, with the current I flowing through the device and the electron charge e. Further, due to surface effects within the semiconductors, a flicker noise term is added, its noise power density is decreasing with 1/f.

The SNR is the ratio of the signal to the noise power within the system's bandwidth. The self generated noise of two port circuits is described by the noise figure, the degradation of the SNR of a signal passing the circuit.

In radio reception, additional noise is added. Usually, this is assumed to be the thermal noise $N_0 = k \cdot T \cdot B$ of a matched resistor at the temperature of the background, the antenna is facing to.

Finally, for radio transmission systems a man made noise term has to be considered as an excess noise factor $F_{man\text{-}made}$ to the thermal noise at the antenna, originated by sparks, radio transmission etc. It depends on the frequency of operation. With a variance of approx. 6 dB it can be estimated from [64]:

$$F_{man\text{-}made} = 67.2 - 27.2 \cdot \log\{f/MHz\} \quad [dB] \qquad \text{(A2. 8)}$$

(it may be up to 10 dB larger in urban surroundings).

All noise power terms can be added, if they are statistically independent. Considering all noise contributions, the SNR at the detector, where the signal's amplitude and its phase is detected, can be calculated. Here, the noise vector, added to the received signal yields errors in phase and amplitude.

In radio communication science, extensive investigations have been performed to calculate or estimate the effects of errors due to noise. Many investigations have been reported in the literature, the basics, the methods of calculation and further results can be found there, e.g. [63]. Here, for the purposes of passive radio sensor interrogation it is tried to use these methods and these results as much as possible and convert them to fit our demands. For the sake of completeness the basics are mentioned also.

A2.4.1 AWGN amplitude error

We assume a burst signal (a response of a SAW radio sensor), received by the radio interrogation unit. A white noise with Gaussian probability density of the noise amplitude is added (AWGN). This single received response signal at center frequency f_c can be written as

$$r(t) = A_r \cdot g_T(t) \cdot \cos\{2\pi f_c t\} + n(t) \qquad \text{(A2. 9)}$$

with amplitude A_r and envelope function $g_T(t)$ normalized to one. Here, n(t) is a bandpass noise process with components inphase and in quadrature to the response signal r(t).

$$n(t) = n_I(t) \cdot \cos\{2\pi f_c t\} - n_Q(t) \cdot \sin\{2\pi f_c t\} \qquad \text{(A2. 10)}$$

Applying coherent demodulation, the noise $n_I(t)$ is converted to the base band. The probability density function (pdf) is still Gaussian, centered around the signal amplitude A_r.
If non coherent demodulation is performed, e.g. an envelope detector is employed, the pdf of the noise becomes Rice'ean. (Then, if no signal r(t) is present, the Rice pdf becomes a Rayleigh pdf). For a large SNR, the Rice pdf again can be estimated by a Gauss pdf.
For a Gauss pdf, the probability for error $P_{amplitude\_error}$, when the noise exceeds an admissible deviation $w \cdot A_r$ either up- or down side, is

$$P_{amplitude\_error} = 2 \cdot Q\left\{\frac{w \cdot A_r}{\sigma}\right\}. \qquad \text{(A2. 11)}$$

where σ is the standard deviation of the noise and Q{..} is the well known function derived from the error function *erf* and its complementary function *erfc* with

$$Q(z) = \frac{1}{2}\left[1 - \mathrm{erf}\left(\frac{z}{\sqrt{2}}\right)\right] = \frac{1}{2} \cdot \mathrm{erfc}\left(\frac{z}{\sqrt{2}}\right) = \int_z^\infty \frac{1}{\sqrt{2\pi}} \cdot e^{-\frac{y^2}{2}} dy\,. \qquad \text{(A2. 12)}$$

It is the probability of a Gaussian process to exceed a single sided deviation z from its average value. Since the power density of noise is $N_0/2 = \sigma_n^2$, the SNR can be inserted, the error probability can be written as

$$P_{amplitude\_error} = 2 \cdot Q\{w \cdot \sqrt{SNR}\} \text{ for } w \geq 0. \qquad \text{(A2. 13)}$$

In [1], figure 13, the probability that the amplitude error due to the AWGN exceeds $w \cdot A_r$ is shown versus the SNR at the detector with the parameter w.

A2.4.2 AWGN phase error

For sensor interrogation, the relative phase shift between components (separated in time) of the response signal is measured. AWGN is added during radio transmission. In signal vector space, the noise overlays the response signal vectors. The amplitude and the original phase is disturbed depending on the SNR. To characterize the effect of noise to the measurement error, the phase deviation due to the noise has to be investigated. The phase error is a major problem in digital radio transmission applying phase modulation (e.g. n- PSK, n = 8, 16, 32, 64, etc.). Since it also applies to radio sensor interrogation, the error estimation published for radio communication systems [63] can be adapted for our application.

Assuming an ID tag type sensor, the retransmitted response signal consists of RF bursts with a shape $g_T(t)$ modulating the carrier at a center frequency f_c. The m-th response impulse $u_m(t)$ (without noise) is written as

$$u_m(t) = g_T(t) \cdot \cos(2\pi f_c t + \Phi_m) \qquad \text{(A2. 14)}$$

with the ambiguous total phase $\Phi = e^{jwT}$, due to the delay T >> $1/f_c$.

The energy of these impulses can be calculated from

$$E_m = \int_{-\infty}^{\infty} u_m^2(t)dt \,. \qquad \text{(A2. 15)}$$

During transmission, AWGN n(t) is added. The received signal r(t) is

$$r(t) = u_m(t) + n(t) \,. \qquad \text{(A2. 16)}$$

As discussed above, during coherent detection, r(t) is correlated (multiplied and integrated) with the two base signals of the orthogonal reference system.

The outputs of these two correlators yield two components of the noise corrupted signal vector

$$\mathbf{r} = \mathbf{u}_m + \mathbf{n} \text{ , or} \qquad \text{(A2. 17)}$$

$$\mathbf{r} = (r_I, r_Q) = \left(\sqrt{E_m}\cos(2\pi\varphi) + n_I, \sqrt{E_m}\sin(2\pi\varphi) + n_Q\right). \qquad \text{(A2. 18)}$$

The noise term are, by definition [63]

$$n_I = \frac{1}{\sqrt{4E_m}} \int_{-\infty}^{\infty} g_T(t) \cdot n_I(t) dt, \text{ and} \tag{A2. 19}$$

$$n_Q = \frac{1}{\sqrt{4E_m}} \int_{-\infty}^{\infty} g_T(t) \cdot n_Q(t) dt\,. \tag{A2. 20}$$

Since the quadrature noise components $n_I(t)$ and $n_Q(t)$ have a zero average value and are uncorrelated, the expectation values $E[n_I]$, $E[n_Q]$ and the expectation value of the product $E[n_I n_Q]$ are zero. The variances of noise at the correlator output are

$$E\left[n_I^2\right] = E\left[n_Q^2\right] = \frac{N_0}{2}\,. \tag{A2. 21}$$

To evaluate the effect of the noise to the discriminated phase, we assume a single RF pulse response vector $\mathbf{u}_0$ retransmitted from the sensor in phase with the cosine of the orthogonal basis,

$$\mathbf{u}_0 = \left(\sqrt{E_m}, 0\right). \tag{A2. 22}$$

This yields a received signal vector

$$\mathbf{r} = (r_1, r_2) = \left(\sqrt{E_m} + n_I, n_Q\right), \tag{A2. 23}$$

$$\text{and } E[r_1] = \sqrt{E_m}\ ,\ E[r_2] = 0\ ,\ \sigma_{r1}^2 = \sigma_{r2}^2 = {}^{N_0}\!/_{2} = \sigma_r^2. \tag{A2. 24}$$

In rectangular coordinates, the pdf is given by

$$f_r(r_1, r_2) = \frac{1}{2\pi \cdot \sigma_r^2} \cdot e^{-\left[\left(r_1 - \sqrt{E_m}\right)^2 + r_2^2\right]/2\sigma_r^2} \tag{A2. 25}$$

After the transform $V = \sqrt{r_1^2 + r_2^2}$ and $\Theta_r = \arctan(r_2/r_1)$ of rectangular to polar coordinates in magnitude v and phase θ_r, the two dimensional pdf is

$$f_{V,\Theta_r}(v, \theta_r) = \frac{v}{2\pi \cdot \sigma_r^2} \cdot e^{-\left[v^2 + E_m - 2\sqrt{E_m} \cdot v \cdot \cos\theta\right]/2\sigma_r^2}\,. \tag{A2. 26}$$

Since we want to find the phase error independently from amplitude, we have to integrate this function for all amplitudes v:

$$f_{\Theta_r}(\theta_r) = \int_0^{\infty} f_{V,\Theta_r}(v,\theta_r)dv = \frac{1}{2\pi} \cdot e^{-2\frac{E_m}{N_0}\cdot\sin^2(\theta_r)} \cdot \int_0^{\infty} v \cdot e^{-\frac{1}{2}\cdot\left(v-\sqrt{4\frac{E_m}{N_0}}\cdot\cos(\theta_r)\right)^2} dv\,. \tag{A2. 27}$$

The ratio E_m/N_0 characterizes the SNR of the received burst signal.

From this equation, the probability for the deviation $\Delta\varphi$ of the actual phase φ, to be $\Delta\varphi < \Theta_r$ can be calculated by solving the integral of this function between the boundaries $-\Theta_r$ and Θ_r. In other words, the probability that the phase error exceeds the admissible deviation Θ_r due to the AWGN and therefore the probability P_e of measurement error is

$P_e = P\{\Delta\varphi > \Theta_r)$

$$P_e = 1 - \int_{-\Theta_r}^{\Theta_r} f_{\Theta_r}(\theta)\, d\theta\,. \tag{A2. 28}$$

This integral have to be evaluated numerically.

In [63], for small phase deviations due to a large SNR, the approximation

$$f_{\Theta_r}(\theta_r) \approx \sqrt{\frac{2}{\pi}\cdot\frac{E_m}{N_0}} \cdot \cos\theta_r \cdot e^{-2\frac{E_m}{N_0}\cdot\sin^2\theta_r} \tag{A2. 29}$$

yields

$$P_e \approx 2\cdot Q\left\{\sqrt{2\frac{E_m}{N_0}}\cdot\sin\Theta\right\}. \tag{A2. 30}$$

In [1] (figure 14), the probability of phase error ($\Delta\varphi > \Theta_r$) is drawn versus the SNR (assumed to be equal E_m/N_0 for non spread spectrum signals and no integration over multiple interrogation events is applied at all), with the parameter Θ_r. From this graph it can be found, that a maximum phase error of 3 degree in at least 99.9 % of measurements requires an SNR of better than 33 dB at the detector.

Looking for the SNR needed for a phase error smaller than ε, the equation above has to be rearranged. The inverse Q function can be approximated by $\arcsin\left(a/\sqrt{SNR}\right)$ with a constant "a" depending on the actual probability to be investigated.

The inverse relation is plotted in Figure 69 for the phase error ε versus SNR with the probability as parameter.

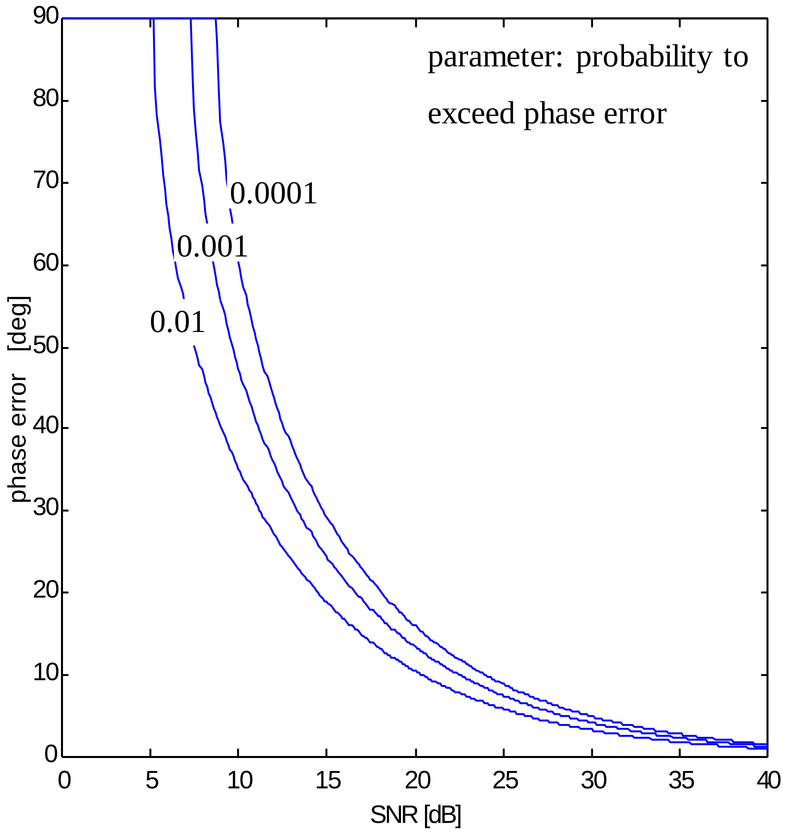

Figure 69: Phase error ε versus SNR with the probability to be exceeded by AWGN as parameter.

A2.4.3 Phase noise errors

Radio interrogation systems apply local oscillators (LOs) to generate the radio request signal, to convert the received response signals into an IF and for coherent demodulation. In [1], chapter 5.2.4, the phase noise error degrading the measurement, is investigated and in [1], fig. 14, a phase noise limit is given for the local oscillators (LO) in interrogation systems. Since it is usually used to specify phase noise characteristics of oscillators in frequency domain [65] and it can be measured easily, the single sideband phase noise density is applied here.

Phase noise is a stochastic process, yielding phase and amplitude fluctuations of the output signal of an oscillator due to a finite quality factor of the resonant device and due to fluctuations in the oscillator amplifier. For worst case approximation, the contributions of the oscillators in transmitter and receiver are assumed to be statistically independent, the total effect can be calculated considering the sum of the noise power contributions, shifting the graphs e.g. for 3 dB if the same types of oscillators are applied.

In Figure 70 the phase noise of an oscillator, stabilized by a SAW resonator and usually employed in our interrogation units, is plotted. For comparison, the phase noise limit from [1], fig. 12 is sketched dotted in the semi logarithmic plot.

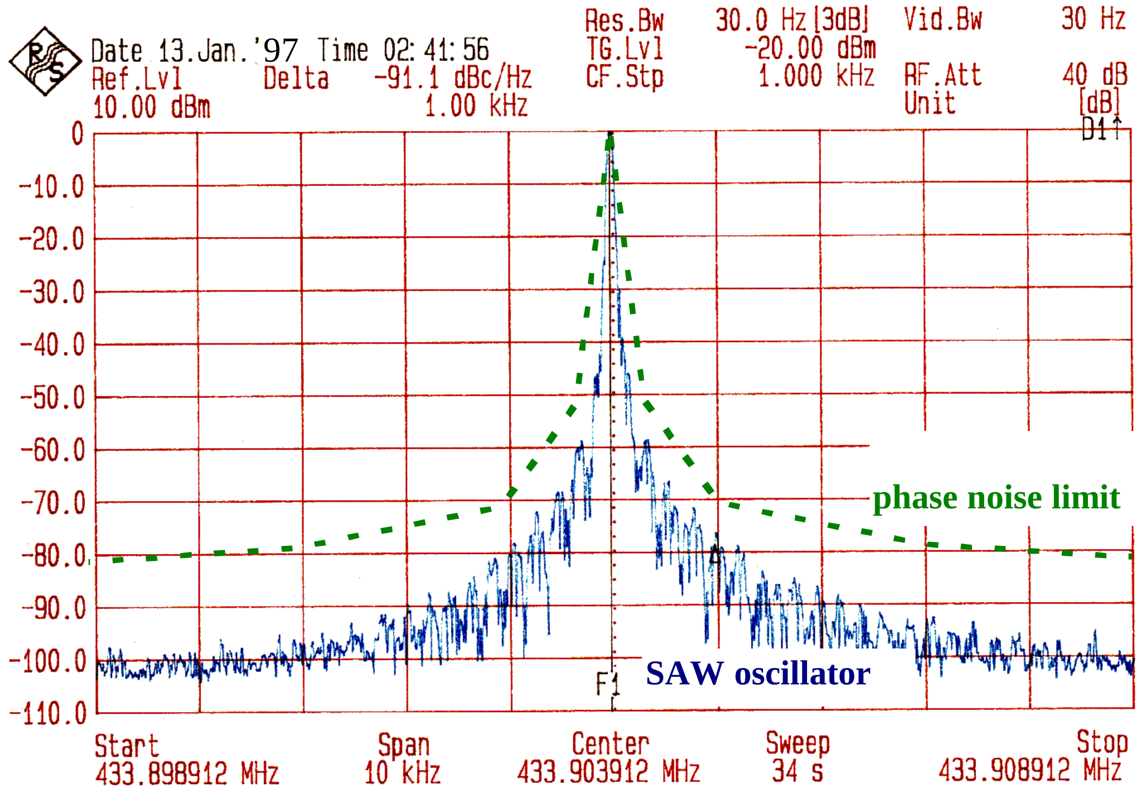

Figure 70: Spectrum of a SAW resonator stabilized oscillator at 433.9 MHz and phase noise limit for a total additional phase measurement error of less than 1 degree.

As seen in Figure 70 the phase noise of the actual SAW resonator stabilized oscillator is more than 10 dB better than the estimated specification for a total phase error of 1°. Usage of this oscillator type will provide no significant additional phase errors.

The amplitude errors due to phase noise of the local oscillators affect the system performance in a similar but reduced manner. Since in the mixers and frequency converter circuits, the LO signal is used to switch diodes etc., a fluctuation in amplitude does not cause considerable errors.

A2.5 Errors due to RF interference

In radio transmission systems, radio interference may occur as a source of errors. Here, coherent interference, usually caused by feed through of LOs etc., and incoherent co-channel interference mainly caused by other ISM band users can be distinguished. An estimation of the effects of coherent and incoherent interference is given in [1], chapter 5.2.5 and fig. 15.

A2.6 Digitization error

Digitization in an analog to digital converter (ADC) yields an error of up to ½ of the least significant bit (LSB). This yields an RMS noise voltage of $U_{LSB}/12$. The well known estimation for the signal dynamic and the SNR of digital systems gives an enhancement of SNR by 6 dB per Bit. The effect to passive sensor systems is discussed in [1], chapter 5.2.6.

A2.7 Integration error

Coherent integration yields an enhanced SNR for signal detection at the expense of measurement duration. A non stationary measurand with a shift of γ for each sample
yields a phase error of $\gamma.N/2$ and an amplitude error $E_{a,N}$ ([1], chapter 3.4) of:

$$E_{a,N} = \frac{N - 2 \cdot \sin\left[\left(\frac{1}{2} + N\right) \cdot \frac{\gamma}{2}\right]}{N \cdot \sin\left(\frac{\gamma}{4}\right)} \qquad \text{(A2. 31)}$$

It is obvious that there is an upper limit for the integration time when a dynamic process is monitored. The errors due to the changing measurand limit the number of integrated cycles.

A2.8 Total error

Since the physical reasons are totally different, the effects discussed above and causing errors during signal detection, are assumed to be statistically independent. To get the total error power the individual power contributions, the variances, have to be summed up.

References

[1] A. Pohl, "A Review of Wireless SAW Sensors", IEEE Transactions on Ultrasonics Ferroelectrics and Frequency Control, Vol. 47, No. 2, March 2000, pp. 317-332.

[2] Elektronikschau 12/1998.

[3] A. Pohl, M. Brandl, "A reliable SAW based low cost chirp spread spectrum system", part I, "Improvements of a SAW based chirp spread spectrum system", part II, " Further Comments on a SAW Based Chirp Spread Spectrum System ", part III, all submitted to Journal on Selected Areas of Communication, 1999.

[4] A. Pohl, R. Steindl, L. Reindl, F. Seifert, "Gated chirps for signal processing and communication engineering", Proceedings IEEE Ultrasonics Symposium 1998, Sendai, Japan, pp. 359-362.

[5] A. Pohl, R. Baechtiger, M. Loder, L. Reindl, "Verfahren und Vorrichtung zur Vermeidung von Störungen in nach der Pulskompressionstechnik arbeitenden Übertragungssystemen", Schweizer Patent CH 2288/97-30.9.97, Internationale Patentanmeldung CH98/00419-30.9.98

[6] A. Pohl, R. Bächtiger, Verfahren und Vorrichtung zur Expansion breitbandiger Pulse, Schweizer Patentanmeldung CH1452/98, 8. Juli 1998.

[7] A. Pohl, C. Posch, L. Reindl, F. Seifert, "Digitally Controlled Compressive Receiver", Proc. IEEE International Symposium on Spread Spectrum Techniques and Applications 1996, Mainz, Germany, pp. 409-413

[8] A. Pohl, G. Ostermayer, C. Ruppel, F. Seifert, "A New Adaptive SAW Compressive Receiver Applied to Measurements of the Electromagnetic Radiation Spectrum of a Microwave Oven", submitted for publication in IEEE Transactions on Instrumentation and Measurements, 1999.

[9] TELEFUNKEN Microsystems, Product Information, RDKS, Germany 1997.

[10] K. Finkenzeller, "RF ID Handbuch", Hanser, München, 1998.

[11] L. Reindl et al., "Hybrid SAW-ID-Tag for an European Train Control System",

Proceedings IEEE Ultrasonics Symposium 1994, Cannes, France, pp. 175-179.

[12] K. Slavic, "Dieelektrische Resonatoren als Sensoren", diploma thesis, TU Wien, 1997.

[13] C. Tyren, "Method for Excitation and Detection of Magnetic Elements by a Mechanical Resonance", US Patent 5,760,580 (June, 2, 1998) and "Method of Remote Sensing of Objects", US Patent 5,001,458 (March, 19, 1991).

[14] Bartels, Mangold Co. Germany, Product Information, www.iq-mobil.de.

[15] A. Pohl, L. Reindl, F. Seifert, W.E. Bulst, "Sensorsystem und Verfahren für Überwachung / Messung des Kraftschlusses von Reifen mit Funksensoren", Deutsche Patentanmeldung 198 07 004.7, Europäisches Patent 99102173.4-2213.

[16] A. Pohl, R. Steindl, F. Seifert, W.E. Bulst, "Profilelemente in Kraftfahrzeugreifen zur drahtlosen Überwachung von Reifenabnützung und Aquaplaning", Deutsche Patentanmeldung, 03/2000.

[17] R. Steindl, A. Pohl, F. Seifert, "Impedance Loaded SAW Sensors Offer a Wide Range of Measurement Opportunities", IEEE Transactions on Microwave Theory and Technology, Vol. 47, No. 12, December 1999, pp. 2625-2629.

[18] A. Pohl, Ch. Hausleitner, R. Steindl, H. Hauser, J. Nicolics, "Giant Magneto Impedance Effect Magnetic Field Sensor with Surface Acoustic Wave Technology", Proceedings IEEE Eurosensors 1999, Delft, The Netherlands, in print;
+ accepted for publication in the Special Eurosensor 99 Issue of Sensors and Actuators.

[19] A. Pohl, F. Seifert, P. Steinrück, W. Zeppelzauer, "Verschleißmonitor für Kolben-kompressoren".Österr. Patent AT 1322/98 (31.7.98), PCT Patent 99890200.1-2302.

[20] A. Pohl, F. Seifert, 'Wirelessly Interrogable SAW Sensors for Vehicular Applications", Proceedings IEEE Instrumentation and Measurement Conference 1996, pp. 1465-1468

[21] A. Pohl, "Measurements of Vibration and Acceleration utilizing SAW sensors", Tagungsband SENSOR 99, Nürnberg, Germany, pp. 53-58.

[22] A. Pohl, G. Ostermayer, L. Reindl, F. Seifert, "Monitoring the Tire Pressure at Cars Using Passive SAW Sensors", Proceedings. IEEE Ultrasonics Symposium 1997, Toronto, Canada, pp. 471-474.

[23] A. Pohl, A. Springer, L. Reindl, F. Seifert, R. Weigel, "New Applications of Wirelessly Interrogable Passive SAW Sensors", Proceedings IEEE Symposium on Microwave Theory and

Technology (MTT-S) 1998, Baltimore, USA, pp. 503-506.

[24] A. Pohl, R. Steindl, "Measurement of mechanical parameters utilizing passive sensors", Proceedings Mechatronics '98, Sweden, Elsevier, ISBN 0-08-043339-1, pp. 571-576.

[25] A. Pohl, R. Steindl, L. Reindl, F. Seifert, "Wirelessly interrogable sensors for different purposes in industrial radio channel", Proceedings IEEE Ultrasonics Symposium 1998, Sendai, Japan, pp. 347-350.

[26] R.M. White, T.M. Voltmer, "Direct Piezoelectric Coupling to Surface Acoustic Waves", Appl. Physics Letters, Vol. 7, pp. 314-316, 1965.

[27] D.P. Morgan, "Surface Acoustic Wave Devices for Signal Processing", Elsevier 1985.

[28] A. Pohl, "Akustische Oberflächenwellenbauelemente und -Sensoren", Skriptum zur Vorlesung 383.024, TU Wien, 1999.

[29] K. Yamanouchi, "GHz-Range SAW Device Using Nano Meter Electrode Fabrication Technology", Proceedings IEEE Ultrasonics Symposium 1994, Cannes, France, pp. 421-428.

[30] Siemens Matsushita, databook, SAW components, 1996.

[31] L. Reindl, G. Scholl, T. Ostertag, C. Seisenberger, J. Hornsteiner, A. Pohl, "Berührungslose Messung der Temperatur mit passiven OFW Sensoren", Tagungsband VDI/GMA Temperatur 98, VDI-Berichte Nr. 1379, pp. 93-98.

[32] personal information, Dr. Ruile, Siemens

[33] J. Hornsteiner, "Oberflächenwellen Bauelemente für Hochtemperaturanwendungen", Ph.D. thesis, TU Munich, Germany, 1999.

[34] U. Rösler, W. Ruile, C.C.W. Ruppel, "RF SAW Filters for Mobile Communications", Proceedings 137th ASA Meeting, Berlin, Germany, 1999.

[35] personal information, Dr. Reindl, Siemens

[36] W. Buff, "SAW Sensors", Sensors and Actuators A42 (1992), pp. 117-121

[37] T. Nomura, K. Oofuchi, T. Yasuda, S. Furukawa, "SAW Humidity Sensor Using Dielectric Hygroscopic Polymer Film", Proceedings IEEE Ultrasonics Symposium 1994, Cannes, France, pp. 503-506.

[38] C. Di Natale, F. Davide, A. D´Amico, G. Saggio, P. Verardi, E. Verona,

"Multicomponent Analysis of a Tri-axial Accelerometer Based on Surface Acoustic Wave Sensors", Proceedings IEEE Ultrasonisc Symposium 1994, Cannes, France, pp. 495-498.

[39] M.J. Vellekoop, G.W. Lubking, A. Venema, "Acoustic-Wave Based Monolithic Microsensors", Proceedings IEEE Ultrasonisc Symposium 1994, Cannes, France, pp. 565-574.

[40] F. Seifert, W.E. Bulst, C.C.W. Ruppel, "Mechanical Sensors Based on Surface Acoustic Waves", Sensors and Actuators, A44 (1994), pp. 231-239.

[41] W.E. Bulst, C.C.W. Ruppel, "Akustische Oberflächenwellentechnologie für Innovation", Siemens Review, Spring 1994, pp. 38-41.

[42] P.A. Nysen, H. Skeie and D. Armstrong, "System for interrogating a passive transponder carrying phase-encoded information", US Patent Nos. 4725841; 4 625 207; 4 625 208 (1983-1986).

[43] L.Reindl and W. Ruile, "Programmable reflectors for SAW-ID-tags", Proceedings IEEE Ultrasonics Symposium 1993, pp. 125-130.

[44] F. Seifert, A. Pohl, G. Ostermayer, G. Berger, "Wireless Sensors and Data Links Based on SAW Devices", (invited), Proceedings IEEE MTT/AP and UFFC Chapter Workshop 1997, Germany, pp. 27-34.

[45] A. Pohl, G. Ostermayer, F. Seifert, "Wireless Sensing Using Oscillator Circuits Locked to Remote High-Q SAW Resonators", IEEE Transactions on Ultrasonics, Ferroelectrics and Frequency Control, Special issue on sensors and actuators, Vol. 45, No. 5, September 1998, pp. 1161-1168.

[46] G. Ostermayer, A. Pohl, R. Steindl, F. Seifert, "SAW sensors and correlative signal processing – a method providing multiple access capability", Proceedings International Symposium on Spread Spectrum Techniques and Applications 1998, Sun City, South Africa, pp. 902-906.

[47] A. Pohl, "A Low Cost High Definition Wireless Sensor System Utilizing Intersymbol Interference", IEEE Transactions on Ultrasonics, Ferroelectrics and Frequency Control, Special issue on sensors and actuators, Vol. 45, No. 5, September 1998, pp. 1355-1362.

[48] H.D. Lüke, "Signalübertragung", Springer, Heidelberg, New York, Tokyo, 1985.

[49] ACAM GmbH., Product Information: Time to Digital Converter - TDC, www.acam.de

[50] W. Baldauf, "Oberflächenwellen-Resonatoren zur Drehmomentmessung", Berichtsband

zum Kolloquium "Integrierte Drehmomentmessung", TH Darmstadt 1992, pp. 57-63.

[51] A. Pohl, G. Ostermayer, F. Seifert, "Messung der Frequenz eines ausschwingenden Resonators mit Hilfe einer PLL", Deutsches Patent 195 39 506.9, US- Patent US1996000736371, Feb. 1999.

[52] Ch. Hausleitner, R. Steindl, A. Pohl, M. Brandl, F. Seifert, "State of the Art Radio Interrogation System for Passive Surface Acoustic Wave Sensors", accepted for publication at the Eurocom 2000, Munich, Germany.

[53] G.R. Cooper, C.D.McGillem, "Modern Communications and Spread Spectrum", Mc Graw Hill, New York, 1986.

[54] G. Ostermayer, A. Pohl, L. Reindl, F. Seifert, "Multiple Access to SAW Sensors Using Matched Filter Properties", Proceedings IEEE Ultrasonics Symposium 1997, Toronto, Canada, pp. 339-342.

[55] G. Ostermayer, A. Pohl, C. Hausleitner, L. Reindl, F. Seifert, "CDMA for Wireless SAW Sensor Applications", Proceedings IEEE International Symposium on Spread Spectrum Techniques and Applications 1996, Mainz, Germany, pp. 795-799.

[56] E. Bonek, G. Magerl, "Wellenausbreitung 2", Skriptum zur Vorlesung, Institut für Nachrichtentechnik, TU Wien, März 1999.

[57] T.S. Rappaport, "Wireless Communications - Principles & Practice", IEEE Press, Piscataway, NJ, ISBN 0-7803-1167-1.

[58] P.A. Bello, "Characterization of randomly time variant linear channels", IEEE Transactions CS-11, pp. 360-393 (1963)

[59] J.D. Parson, "The mobile radio propagation channel", Pentech Press, London (1992)

[60] B.H. Fleury, "An Uncertainty Relation for WSS Processes and Its Application to WSSUS Systems", IEEE Transactions on Communications, Vol. 44, No. 12, December 1996, pp. 1632-1634.

[61] A. Pohl, F. Seifert, "New Applications of Wirelessly Interrogable Passive SAW Sensors", IEEE Transactions on Microwave Theory and Techniques, Vol.46 part II, No.12, Dec. 1998, pp. 2208-2212.

[62] H. Weinrichter, F. Hlawatsch, "Stochastische Grundlagen nachrichtentechnischer Signale", Springer, New York, 1991.

[63] J.G. Proakis, M. Salehi, "Communication Systems Engineering", Prentice Hall International, 1994.

[64] CCIR Rec., 1990, Vol. VI (Propagation in ionized media), Genf, ITU 1990, Rep. 258-4 (Man-made radio noise).

[65] J.K. Holmes, "Coherent Spread Spectrum Systems", Krieger Publishing Co., Malabar, Florida, 1990.

Figures

Tables

Selected Publications on Radio Sensor Technology

1. A. Pohl, "A Review of Wireless SAW Sensors", IEEE Transactions on Ultrasonics Ferroelectrics and Frequency Control, Vol. 47, No. 2, March 2000, pp. 317-332.
2. A. Pohl, "State of the art in signal processing for the interrogation of passive wireless sensors", *invited to IEEE UFFC International Frequency Control Symposium 99*, Besancon, France, Proceedings pp. 1031-1036.
3. A. Pohl, F. Seifert, "Wirelessly Interrogable SAW Sensors for Vehicular Applications", IEEE Transactions on Instrumentation and Measurements, Vol. 46 (1997), No. 4, pp. 1031-1038.
4. A. Pohl, G. Ostermayer, F. Seifert, "Wireless Sensing Using Oscillator Circuits Locked to Remote High-Q SAW Resonators", IEEE Transactions on Ultrasonics, Ferroelectrics and Frequency Control, Special issue on sensors and actuators, Vol. 45, No. 5, September 1998, pp. 1161-1168.
5. A. Pohl, "A Low Cost High Definition Wireless Sensor System Utilizing Intersymbol Interference", IEEE Transactions on Ultrasonics, Ferroelectrics and Frequency Control, Special issue on sensors and actuators, Vol. 45, No. 5, September 1998, pp. 1355-1362.
6. A. Pohl, L. Reindl, F. Seifert, "New Applications of Wirelessly Interrogable Passive SAW Sensors", Special Issue IEEE Transactions on Microwave Theory and Techniques, Vol. 46, No. 12, December 1998, pp. 2208-2212.
7. A. Pohl, R. Steindl, L. Reindl, "The 'Intelligent Tire' Utilizing Passive SAW Sensors - Measurement of Tire Friction", IEEE Transactions on Instrumentation and Measurement, Vol. 48, No. 6, December 1999, pp. 1041-1046.

"Further" attached publications

1. A. Pohl, L. Reindl, F. Seifert, R. Weigel, "Chirp gating enhances performance of chirp spread spectrum systems", Proc. IEEE MTT/AP Workshop on Commercial radio sensor and communication techniques, International Radar Symposium, September 1998, Munich, Germany, pp. 139-146.
2. A. Pohl, G. Ostermayer, C. Hausleitner, F. Seifert, L. Reindl, "Wavelet Transform with a SAW Convolver for Sensor Application", Proceedings IEEE Ultrasonics Symposium 1995, Seattle, WA, USA, pp. 143-146.
3. A. Pohl, C. Posch, F. Seifert, L. Reindl, "Wideband Compressive Receiver with SAW Convolver", Proceedings IEEE Ultrasonics Symposium 1995, Seattle, WA, USA, pp. 155-158.
4. A. Pohl, C. Posch, L. Reindl, F. Seifert, "Digitally Controlled Compressive Receiver", Proceedings IEEE International Symposium on Spread Spectrum Techniques and Applications, 1996, Mainz, Germany, pp. 409-413.
5. A. Pohl, G. Ostermayer, R. Steindl, F. Seifert, R. Weigel, "Fine tuning of data rate enhances performance of a chirp spread spectrum system", Proceedings IEEE International Symposium on Spread Spectrum Techniques and Applications 1998, Sun City, South Africa, pp. 78-81.
6. A. Pohl G. Ostermayer, R. Steindl, L. Reindl, F. Seifert, R. Weigel, "Fast adaptive interference cancellation in low cost SAW based chirp spread spectrum systems", Proceedings IEEE International Symposium on Spread Spectrum Techniques and Applications 1998, Sun City, South Africa, pp. 883-887.
7. A. Pohl, M. Brandl, R. Steindl, L. Reindl, F. Seifert, "Gated Chirps for Signal Processing and Communication Engineering", Proceedings IEEE Ultrasonics Symposium 1998, Sendai, Japan, pp. 359-362.
8. M. Brandl, A. Pohl, F. Seifert, L. Reindl, "Fast Adaptive Interference Cancellation in Chirp Spread Spectrum Systems", Proceedings IEEE Globecom 1999, Rio de Janeiro, Brazil, pp. 2218-2222.